FLIGHT SIMULATION AND CONTROL OF A HELICOPTER

A THESIS SUBMITTED TO
THE GRADUATE SCHOOL OF NATURAL AND APPLIED SCIENCES
OF
MIDDLE EAST TECHNICAL UNIVERSITY

BY

GÜLSÜM HİLAL ERÇİN

IN PARTIAL FULFILLMENT OF THE REQUIREMENTS
FOR
THE DEGREE OF MASTER OF SCIENCE
IN
AEROSPACE ENGINEERING

DECEMBER 2008

Approval of the thesis:

FLIGHT SIMULATION AND CONTROL OF A HELICOPTER

submitted by **GÜLSÜM HİLAL ERÇİN** in partial fulfillment of the requirements for the degree of **Master of Science in Aerospace Engineering Department, Middle East Technical University** by,

Prof. Dr. Canan Özgen
Dean, Gradute School of **Natural and Applied Sciences** _____

Prof. Dr. İsmail H. Tuncer
Head of Department, **Aerospace Engineering** _____

Prof. Dr. Ozan Tekinalp
Supervisor, **Aerospace Engineering Department, METU** _____

Dr. İlkay Yavrucuk
Co-Supervisor, **Aerospace Engineering Department, METU** _____

Examining Committee Members:

Prof. Dr. Cahit Çıray
Aerospace Engineering Dept., METU _____

Prof. Dr. Ozan Tekinalp
Aerospace Engineering Dept., METU _____

Prof. Dr. Kemal Özgören
Mechanical Engineering Dept., METU _____

Dr. Volkan Nalbantoğlu
ASELSAN, MGEO _____

Dr. D. Funda Kurtuluş
Aerospace Engineering Dept., METU _____

Date: _____

I hereby declare that all information in this document has been obtained and presented in accordance with academic rules and ethical conduct. I also declare that, as required by these rules and conduct, I have fully cited and referenced all material and results that are not original to this work.

Name, Last Name: Gülsüm Hilal Erçin

Signature :

ABSTRACT

FLIGHT SIMULATION AND CONTROL OF A HELICOPTER

Erçin, Gülsüm Hilal
M.S., Department of Aerospace Engineering
Supervisor : Prof. Dr. Ozan Tekinalp
Co-Supervisor : Dr. İlkay Yavrucuk

December 2008, 106 pages

In this thesis the development of a nonlinear simulation model of a utility helicopter and the design of its automatic flight control system is addressed. In the first part of this thesis, the nonlinear dynamic model for a full size helicopter is developed using the MATLAB/SIMULINK environment. The main rotor (composed of inflow and flapping dynamics parts), tail rotor, fuselage, vertical stabilizer, horizontal stabilizer of the helicopter are modeled in order to obtain the total forces and moments needed for the flight simulation of the helicopter. Total forces and moments are used in 6 degrees of freedom equations of motion model and helicopter states are calculated for the specified flight conditions such as hover and forward flight. Trim and linearization programs are developed. The linearized models of hover and forward flight conditions are used for the automatic flight control system design. Automatic flight control system model consists of necessary systems in order to ease the pilot control of the helicopter. A classical inner stability loop and outer flight directory mode approach is taken to design the automatic flight control system. For the inner stability loop both classical rate feedback and truncated system state feedback control approaches are used. The outer loop modes implemented are heading hold, attitude hold (pitch, roll), altitude acquire and hold mode for hover condition and heading hold, attitude hold (pitch, roll), altitude

acquire and hold mode and airspeed hold for forward flight condition. Finally, the success of the controllers are demonstrated through nonlinear simulations for different flight directory modes in hover and forward flight conditions.

Keywords: Helicopter, Simulation, Kontrol, Linearization, Trim

ÖZ

HELİKOPTER UÇUŞ SİMULASYONU VE KONTROLÜ

Erçin, Gülsüm Hilal
Yüksek Lisans, Havacılık ve Uzay Mühendisliği Bölümü
Tez Yöneticisi : Prof. Dr. Ozan Tekinalp
Ortak Tez Yöneticisi : Dr. İlkay Yavrucuk

Aralık 2008, 106 sayfa

Bu tezin amacı, uçuş mekaniği matematiksel benzetim modeli ve otomatik kontrol sistemi algoritması geliştirmektir. Tezin birinci bölümünde, doğrusal olmayan dinamik bir benzetim modeli MATLAB/SIMULINK kodlama arkayüzü kullanılarak geliştirilmiştir. Helikopterin ana rotor (akış ve flaplama dinamiği dahil olmak üzere), kuyruk rotoru, gövde, dik kuyruk, yatay kuyruk bölümleri, uçuş benzetim modeli için gerekli olan helikopter üzerindeki toplam kuvvet ve momentleri hesaplamak üzere modellenmiştir. Helikopter üzerindeki kuvvet ve momentler, 6 serbestlik dereceli hareket denlemleri modelinde kullanılmakta ve helikopterin askı durumu ve ileri uçuş durumu gibi belirlenmiş uçuşlardaki durum değerleri hesaplanmaktadır. Uçuş mekaniği matematiksel modelinin denge durumu değerlerini hesaplayan ve doğrusallaştıran programlar geliştirilmiştir. Helikopter doğrusal otomatik kontrol modelleri, klasik kontrol yöntemleri kullanılarak askı durumu ve ileri uçuş durumu olmak üzere her iki uçuş durumu için de tasarlanmaktadır. Otomatik uçuş kontrol modeli pilota yardımcı sistemlerden oluşmaktadır. Helikopter açısal hız değerlerini kontrol ederek helikopterin denge durumunu korumasını sağlayan uçuş kontrol modeli ile helikopteri hedeflenen yükseklik, hız ve yönelim durumuna getirip bu durumu koruyarak uçmasını sağlayacak uçuş kontrol algoritmaları klasik kontrol metodları kullanılarak tasarlanmıştır. İç kararlılık döngü modeli

için hız geri besleme metodu ve model evirimi metodu kullanılarak iki ayrı kontrol sistemi tasarlanmış, hız geri besleme yöntemi kullanılarak tasarım tamamlanmıştır. Askı uçuş durumu dış kararlılık döngüsü için helikopteri hedeflenen yükseklik ve yönelim durumuna getirip bu durumu koruyarak uçmasını sağlayacak uçuş kontrol algoritması ile ileri uçuş durumu dış kararlılık döngüsü için helikopteri hedeflenen yükseklik, hız ve yönelim durumuna getirip bu durumu koruyarak uçmasını sağlayacak uçuş kontrol algoritması tasarlanmıştır. Sonuç olarak tasarlanan tüm benzetim ve kontrol modelleri helikopterin askı durumu ve ileri uçuş durumu için incelenmiş ve model performansları ilgili grafiklerle gösterilmiş ve tartışılmıştır.

Anahtar Kelimeler: Helikopter, Simülasyon, Kontrol , Doğrusallaştırma, Denge

To my family

ACKNOWLEDGMENTS

I would like to express my sincere gratitude to my thesis supervisor Prof Dr. Ozan Tekinalp and co-supervisor Dr. İlkay Yavrucuk for their support and guidance. I appreciate for useful discussions we had with Deniz Yılmaz and Onur Tarımcı. I would like to thank to my family for their trust and support.

TABLE OF CONTENTS

LIST OF TABLES

TABLES

LIST OF FIGURES

FIGURES

LIST OF ABBREVIATIONS

a	Lift slope
A	Main rotor disk area
$\dot{a_1}$	Longitudinal tip path plane angular rate
a_1	Pitch axis flapping angle
$AFCS$	Automatic flight control system
$a\sigma$	Product of lift curve slope and solidity
b	Number of blades
b_1	Roll axis flapping angle
$\dot{b_1}$	Lateral tip path plane angular rate
c	Blade chord
C_{Do}	Effective profile drag for the main rotor blade cross section
CG	Center of gravity
C_T	Thrust coefficient
d_{fus}	Distance of fuselage aerodynamic center from center of gravity
d_{hub}	Distance of fuselage hub from center of gravity
dfw_{emp}	Empirical correction for fuselage aerodynamic center shift magnification
da_1/du	Tip path plane pitch up with speed
db_1/dv	Tip path plane dihedral effect
dL/dB_1	Primary flapping stiffness
dL_1/dA_1	Cross flapping stiffness
e	Effective hinge offset
fs_{hub}	Fuselage reference system location of the main rotor hub measured aft of the zero fuselage station
fs_{cg}	Location of the center of gravity in the fuselage reference system in inches from the zero fuselage station
fs_{fus}	Fuselage station corresponding to the effective center of pressure in the vertical axis
fs_{vt}	Fuselage station for the effective aerodynamic center of the vertical fin
g	Gravity
h	Altitude
h_{fus}	Height of fuselage aerodynamic center from center of gravity
h_{hub}	Height of hub relative to center of gravity
itb	Flapping primary response
I_{b1}	Blade flapping inertia
i_s	Forward tilt of rotor shaft w.r.t. fuselage
I_{XX}	Inertia in body x-axis
I_{YY}	Inertia in body y-axis
I_{ZZ}	Inertia in body z-axis
I_{XZ}	Inertia on body x-z plane
I_{XY}	Inertia on body x-y plane
I_{YZ}	Inertia on body y-z plane
K_1	Blade pitch-flap coupling proportion
K_C	Flapping aerodynamic coupling proportion
L_{MR}	Main rotor z-force
L^{fus}	Fuselage rolling moment
L	Rolling moment
M	Pitching moment
m	Mass
M^{fus}	Fuselage pitching moment
N	Yawing moment
NED	North-East-Down axis
N_{MR}	Main rotor yawing moment

$\dot{p}$	Roll angular rate
p	Body roll rate
$P^{mr}_{accessories}$	Power loss due to main rotor accessories
P^{climb}	Power loss due to change in potential energy
P^{fus}	Power loss from fuselage aerodynamic drag
$P^{mr}_{induced}$	Power loss due to main rotor induced velocity
$P^{tr}_{induced}$	Power loss due to tail rotor induced velocity
P^{mr}	Power loss from main rotor and fuselage
$P^{mr}_{profile}$	Power loss due to main rotor profile drag
P_{total}	Total power
P^{tr}	Power loss from tail rotor
$\dot{q}$	Pitch angular rate
q	Body pitch rate
$\dot{r}$	Yaw angular rate
r	Body yaw rate
R	Main rotor radius
SAS	Stability augmentation system
TPP	Tip path plane
T^{tr}	Tail rotor thrust
$Torque_{MR}$	Main rotor torque
$\dot{u}$	x-axis body acceleration
u	Velocity in body x-body axis
u_g	Ground axis longitudinal velocity
$\dot{v}$	y-axis body acceleration
v	Velocity in body y-body axis
v^{ht}_a	Horizontal tail local lateral velocity
v^{vt}_a	Vertical tail local lateral velocity
v_g	Ground axis lateral velocity
v_i	Main rotor induced velocity
v^{tr}_i	Tail rotor induced velocity
V_T	Total velocity
V_{tip}	Tip velocity
V_{trans}	Transition velocity
V_{Ttrim}	Total velocity trim value
$\dot{w}$	z-axis body acceleration
w	Velocity in body z-body axis
W	Helicopter gross weight
$wake_{func}$	Wake function
w^{fus}_a	Apparent vertical velocity on fuselage
w^{ht}_a	Horizontal tail local vertical velocity
w_b	Net vertical velocity relative to rotor blade
w_g	Ground axis vertical velocity
w_n	Natural frequency
w_r	Net vertical velocity through actuator disk
X^{fus}_{aero}	Fuselage drag component
X_{CG}	Center of gravity in x-axis
X_{fus}	Drag force
X_G	Ground axis x-position
X_{MR}	Main rotor x-axis force
X_{TR}	Tail rotor x-axis force
X_{fus}	Fuselage x-axis force
X^{fus}_{uu}	Effective flat plate drag in x-axis
Y^{fus}_{aero}	Fuselage side force component
Y^{vt}_{aero}	Vertical tail normal force
Y_{CG}	Center of gravity in y-axis
Y_G	Ground axis y-position
Y_{fus}	Side force
Y^{vt}_{min}	Stall effect
Y_{MR}	Main rotor y-axis force
Y^{tr}	Tail rotor y-axis force
Y^{vt}_{uu}	Aerodynamic camber effect
Y^{fus}_{vv}	Effective flat plate drag in y-axis
Y^{vt}_{uv}	Lift slope effect
Z^{fus}_{aero}	Fuselage downwash component
Z^{ht}_{aero}	Horizontal tail normal force

Z_{fus}	Fuselage z-axis aerodynamic force
Z_G	Ground axis z-position
Z^{ht}	Horizontal tail z-axis force
Z^{ht}_{min}	Stall effect
Z_{MR}	Main rotor z-axis force
Z^{ht}_{uu}	Aerodynamic camber effect
Z^{ht}_{uw}	Lift slope effect
Z^{fus}_{ww}	Effective flat plate drag in z-axis
ω	Main rotor angular rate
α	Angle of attack
β	Sideslip angle
ξ	Damping ratio
δ_a	Lateral cyclic control
δ_c	Collective control
δ_e	Longitudinal cyclic control
δ_p	Pedal control
θ	Pitch angle
θ_{twist}	Main rotor twist angle
ρ	Air density
τ	Pressure coefficient
ϕ	Roll angle
ψ	Yaw angle
$6-DOF$	Six degrees of freedom

CHAPTER 1

INTRODUCTION

Helicopters are widely used in both military and civilian operations. Helicopters, in general, are more difficult to fly than airplanes. Consequently pilot training becomes an important issue. Simulation of air vehicles has an important role in pilot training by decreasing the cost of training and increasing capability of pilots in all flight missions including the emergency conditions. Simulator training systems develops with new technologies and supports pilot requirements in many different subjective training missions. Nonlinear flight models are used to model the flight for several flight conditions like take off, forward flight, hover, cruise, autorotation and landing. Especially for helicopters, complex nonlinear flight models are used to simulate the unstable characteristics of helicopter aerodynamics, structure and coupled flight dynamics.

For the piloted aerospace vehicles automatic flight control systems are used to alleviate the pilot workload. This becomes even more important for vehicles that are inherently very lightly damped or even unstable such as helicopter. Automatic flight control system design always requires nonlinear simulation codes to test the success of the control system.

Development of flight simulators and design of automatic flight control systems are being investigated under a number of ongoing research projects in the Simulation, Control and Avionics Laboratory of METU Aerospace Engineering Department. This thesis work addresses the development of helicopter flight simulation model as well as the design of automatic flight control system for a helicopter. In defence industry, simulator related projects has a big role. However, necessary models and designs required for simulation are usually gained partially from different foreign companies. The aim of this thesis is developing a simulation and AFCS model together with a trim and a linearization algorithm that will supply the full requirements

of a dynamic simulation and control algorithm of a helicopter simulator.

A non-linear mathematical model of the UH-60A BLACK HAWK helicopter was developed and published previously [39]. This mathematical model, which is based on the Sikorsky General Helicopter (Gen Hel) Flight Dynamics Simulation, provides the Army with an engineering simulation for Performance and Handling Qualities evaluations. The model is a total force, large angle representation in six rigid body degrees of freedom. Rotor blade flapping, lagging and hub rotational degrees of freedom are also represented. In addition to the basic helicopter modules, supportive modules have been defined for the landing interface, power unit, ground effects and gust penetration. In the light of this UH-60 Gen Hel model [39], a minimum complexity math model was developed by Heffley and Mnich [37]. Simulation codes given in this study are based on the minimal complexity helicopter math model. Motivating factors behind this study were the computational delays, cost, and inflexibility of the very sophisticated math models now in common use. A helicopter model form is given which addresses each of these factors and provides better engineering understanding of the specific handling qualities features which are apparent to the simulator pilot. The technical approach begins with specification of features which are to be modelled followed by a build-up of individual vehicle components and definition of equations. In this study Bell AH-IS Cobra, UH-1H and Agusta 109 helicopters are examined as specified models. Agusta 109 helicopter parameters are selected to develop it's nonlinear mathematical model. To convert control stick input into rotor inputs, flight controls are fed through a so-called mixing-unit. It combines the collective, cyclic and pedal inputs applied by the pilot to proportional output to the main and tail rotor controls. There are some additional coupling between the longitudinal and lateral motions of the aircraft [2]. Nonlinear helicopter model includes a subsystem for mixing unit of the control inputs. After completing the simulation process, nonlinear mathematical model requires to be validated by flight tests. However, the trim based procedure allows to supplement data for those parts of the flight envelope for which no flight test values are available. Well-defined steady-state reference conditions also serve as basis for model linearization, enabling linear system analysis required for stability and control considerations, handling qualities issues or control design tasks.

Determination of trim data for steady-state flight conditions is the primary importance in different engineering studies. Trim state and control input values are combined in order to zero total forces and moments acting on helicopter and satisfy given flight condition at that time.

Trim defines conditions for both design and analysis based on aircraft models. In simulations, these analysis points establish initial conditions comparable to flight conditions. Based on aerodynamic and propulsion systems models of an aircraft, trim analysis can be used to provide the data needed to define the operating envelope or the performance characteristics. Linearization is performed around trim points. Automatic flight control systems are designed and evaluated at trim conditions. By using trim conditions of the aircraft different models of the aircraft are compared and also models are compared with original flight data. In order to analyse the stability characteristics of the generated mathematical model trim data is required. In reference [3] a general solution to the aircraft trim problem is considered.This paper describes the development and implementation of a MATLAB based object oriented computational tool that allows numerical trimming of complex high fidelity simulation models implemented in SIMULINK. Equilibrium points for the simulation model are determined numerically by an optimization tool. The nonlinear trim equations to be solved are defined by so called trim templates, which are built around the simulation model, enforcing the desired flight condition by superimposing numerical constraints to the model. The object oriented implementation and the trim algorithm are applied to a complex simulation model featuring a high system order as many subsystem states (e.g. those of the propulsion system, actuators or sensors) augment the original rigid body states. The aircraft rigid body trim template allows to specify different flight maneuvers, e.g. steady-state straight horizontal flight, climbing and turning flight with the implementation of several constraints or more complex cases like steady heading sideslips as well as failure cases or quasi-steady maneuvers, e.g. the determination of the maximum achievable steady-state roll rate or acceleration.

In the light of these references a trim model is implemented to the nonlinear mathematical model in order to validate the model and serve a basis for model linearization and enabling linear system analysis. Perturbation method is used as linearization method. For the helicopter model a mean motion around trim conditions and a dynamic motion obtained by giving small perturbations to the trim states around the mean motion. Then stability derivatives are calculated and then state and control matrices are obtained [36].

Designing a controller for a physical system presents several challenges. Typically, the optimum balance between model fidelity and simplicity of the mathematical model of a system is difficult to achieve. In addition, there are usually unexpected errors or variations in the model of a system, and in the model of the environment in which it operates. The main goal of a

control system is thus to maintain correct system operation in the presence of all modeling errors and changes in operating conditions. For systems that have known bounds on the uncertainties, it is possible to design a controller that can be tuned a-priori to compensate for these errors [10]. Level 1 models (i.e. rigid body models) are among the most common because of their manageable complexity. A typical rigid body model is nonlinear and has the position, orientation, linear and angular velocities as states, resulting in a 12th order system model. Depending on the application, researchers have either simplified or enhanced this basic model by adjusting the model order. Other alternatives in simplifying the system dynamics include using only the roll angle, pitch angle, the linear and the angular rates as the states (8th order); using the linear and angular rates together with the orientation as the states (9th order); and using the simplified 8th or 9th order model in combination with the rotor dynamics (10th or 11th order). Because of their complexity, Level 2 and Level 3 models are rarely used for design of automatic control systems. They are primarily used in the area of system (mechanical) design and simulation analysis (e.g. training flight simulator), where effects such as rotor airflow and blade vibrations are significant. In contrast, for a typical control application operating with slow, simple maneuvers such as hover, these higher order effects are less significant. [1]. For the purpose of this thesis, a Level 1 rigid body model will be derived.

The main objective of this thesis is building a flight simulation mathematical helicopter model which will be applicable for a full size helicopter and designing an automatic flight control system by using classical control methods. Automatic flight control system model will include an inner loop control part for stability augmentation systems for the longitudinal and lateral states. Inner loop control is important for pilots in order to solve the instability problems in helicopter dynamics and also ease pilot controls by smoothing the collective, cyclic and pedal control inputs using state feedback inputs. After inner loop control design, an outer loop control model is designed in order to model helicopter flight directory modes. Flight directory modes are selected by pilots considering their actual flight missions. Most preferable flight directory modes are altitude hold, attitude hold and heading hold modes concerning the search and rescue operations.

In chapter 2 models used for nonlinear helicopter simulation are presented. Chapter 3 gives the details of the trim code as well as the approach taken to design stability augmentation systems and flight directory modes of the helicopter. Chapter 4 presents simulation results of the automatic flight control system. Finally conclusions are given.

CHAPTER 2

NONLINEAR MODEL

In this chapter nonlinear dynamic model of a full size helicopter is presented. The nonlinear model is based on the minimum complexity math modeling idea [37]. The nonlinear model is composed of main rotor inflow model, main rotor flapping dynamics model, fuselage model, vertical stabilizer, horizontal stabilizer and tail rotor models. Also, an atmosphere model and 6-DOF equations of motion model is designed in order to calculate body and inertial states of the helicopter. 6-DOF equations of motion model containing translational and rotational dynamics and navigation units are also employed.

2.1 Nonlinear Helicopter Model

Nonlinear model is based on the idea of a minimum complexity helicopter simulation model from [37]. First the helicopter main rotor, fuselage, tail rotor, horizontal tail and vertical tail parts are modeled in order to obtain the forces and moments applied to the helicopter. Then, 6-DOF equations of motion model are implemented. An atmosphere model is also included in the simulation.

2.1.1 Mixing Unit Model

To convert control stick input into rotor inputs, flight controls are fed through a mixing-unit. It combines the collective, cyclic and pedal inputs applied by the pilot to proportional output to the main and tail rotor controls [2]. This mixing unit provides control mixing functions in order to minimize inherent control coupling. There are four types of mechanical mixing with

following functions:

- Collective to Pitch - Compensates for the effects of changes in rotor downwash on the stabilizer caused by collective pitch changes. The mixing unit provides forward input to the main rotor as collective is increased and aft input as collective is decreased.
- Collective to Yaw - Compensates for changes in torque effect caused by changes in collective position. The mixing unit increases tail rotor pitch as collective is increased and decreases tail rotor pitch as collective is decreased.
- Collective to Roll - Compensates for the rolling moments and translating tendency caused by changes in tail rotor thrust. The mixing unit provides left lateral input to the main rotor system as collective is increased and right lateral input as collective is decreased.
- Yaw to Pitch - Compensates for changes in the vertical thrust component of the canted tail rotor as tail rotor pitch is changed. The mixing unit provides aft input to the main rotor system as tail rotor pitch is increased and forward input as tail rotor pitch is decreased.

By the help of the mixing unit the control coupling is reduced and this effect helps to stabilize the system. Effects of the mixing unit model may be observed from the linearized model.

2.1.2 Main Rotor Model

The main rotor modeling is the most critical part of helicopter simulation. There are some common approaches for modeling of main rotor: the Classical Momentum Theory [37] and Blade Element Rotor Model [39] and [5] are some of them. ”Traditional approaches for blade-element rotor models usually consist of an integrated description of rotor blade kinematics, local per-blade-element aerodynamic force and moment generation, blade dynamics subject to kinematic constraints, and global inflow field model. The treatment of blade dynamics leads to ordinary differential equations that describe the movement of each physical blade and its blade elements with respect to time. Traditional blade-element rotor models usually simulate the evolution of each rotor physical blade as it turns around the rotor axis. Each blade is treated as a solid whose movement through the local air mass (including local wind

and induced flow) generates aerodynamic forces and moments at each blade element; the blade equations of motion are solved taking into account these forces and moments, other external forces and moments and kinematic restrictions. The induced flow is hard to treat locally, since it is hard to maintain local inflow velocity from one blade sweep to the next, so a global induced flow model is used. With traditional approaches, total blade forces and moments are computed and applied to each blade, and blade motion is determined by solving numerically the classical dynamics ordinary differential equations, taking into account the constraints of blade kinematics" [5]. Howlett [39] uses the similar approach for main rotor. The main rotor model is based on a blade element analysis in which total rotor forces and moments are developed from a combination of aerodynamic, mass and inertia loads acting on each simulated blade. The blade segment set up option defined for this Black Hawk model is that of equal annuli area swept by the segment. This technique allows the number of segments to be minimized and distributes the segments towards the higher dynamic pressure areas. The total forces acting on the blade are derived from the total acceleration and velocity components at the blade together with control inputs. Accelerations develop from body motion and blade motion. Velocity components are made up of body velocities, gust velocities, the rotor's own downwash and blade motion. Hefley and Mnich [37] uses classical momentum theory for main rotor model. The primary component of this model is the main rotor. Key features of the main rotor model are generation of a vertical thrust vector and an induced-velocity field; calculation of rotor torque; flapping stiffness and flapping dynamics. Thrust and induced velocity are computed assuming a uniform flow distribution. The tip-path-plane dynamics is modeled as simple first order lags giving the main rotor the qualities of a force actuator with a lag. "It is suggested that two major components of cross coupling will be avoided until the detailed model matching process is underway. One of these is the off-axis hub moments due to flapping and the second is the off-axis coupling in the tip path plane dynamics. It has been found that including these higher order effects in a simple model does not automatically produce a high quality match to flight data."[37] This is the approach taken in this study. Physical features of main rotor model are [37]:

- Thrust
- Torque
- Induced Velocity

- Tip path plane lag
- Induced power
- Profile power
- No off-axis flapping stiffness
- Decoupled TPP dynamics
- Constant RPM

Response features of the main rotor model are [37]:

- 1st order flapping
- Power required
- Trim
- Phugoid
- Short period
- Dihedral
- Pitch mode
- Roll mode
- Min x-coupling
- Power off glide

Next, the model details are provided. In the first section the main rotor flapping dynamics is given followed by the main rotor inflow dynamics to calculate thrust and induced velocity. In the third section power requirements for main rotor are established.

2.1.2.1 Main Rotor Flapping Dynamics Model

Rotor flapping is modeled with a first order flapping equation in the pitch and roll axis. The most important feature of the flapping is the apparent control lag following cyclic input which effects the time required to process the tip path plane to a new orientation. Equations are given below [37]:

$$itb = \frac{I_{bl}}{16\rho acR^4}\Omega\left(1 + \frac{8}{3}\frac{e}{R}\right) \tag{2.1}$$

$$\frac{itb^2}{\Omega} = 0 \tag{2.2}$$

$$K1 = 0 \tag{2.3}$$

$$KC = \left(0.75\frac{\Omega e}{Ritb}\right) + K1 \tag{2.4}$$

$$V_{tip} = R\Omega \tag{2.5}$$

$$C_T = \frac{W}{\rho\pi R^2 V_{tip}^2} \tag{2.6}$$

$$a\sigma = \frac{abc}{\pi R} \tag{2.7}$$

$$\frac{db_1}{dv} = \frac{da_1}{du} = \frac{2}{\Omega R}\left(\frac{8C_T}{a\sigma} + \sqrt{\frac{C_T}{2}}\right) \tag{2.8}$$

$$u < V_{trans} \Longrightarrow wake_{func} = 1 \tag{2.9}$$

$$u \geq V_{trans} \Longrightarrow wake_{func} = 0 \tag{2.10}$$

$$\dot{a}_1 = -itb\left(a_1 + B_1 - (KC * b_1) + \frac{da_1}{du}u\left(1 + 2wake_{fun}\right)\right)$$

$$-\frac{itb^2}{\Omega}\left(b_1 - A_1 + (KCa_1) + \frac{da_1}{du}u\left(1 + 2wake_{fun}\right)\right) - q \tag{2.11}$$

$$\dot{b}_1 = -itb\left(b_1 - A_1 + (KCa_1) + \frac{da_1}{du}u\left(1 + 2wake_{fun}\right)\right)$$

$$+\frac{itb^2}{\Omega}\left(a_1 + B_1 - (KC * b_1) + \frac{da_1}{du}u\left(1 + 2wake_{fun}\right)\right) - p \tag{2.12}$$

2.1.2.2 Main Rotor Inflow Dynamics Model

Induced velocity of air passing through the rotor disc creates a relationship among thrust, power and induced velocity. Therefore thrust and induced velocity has an interaction in an aerodynamic feedback loop. Induced velocity effects on main rotor aerodynamics is modeled with classical momentum theory. By iterating the thrust and induced velocity in a feedback aerodynamic loop, induced velocity will be iterated until it reaches the final induced velocity value in order to obtain necessary thrust. Equations are given below [37]:

$$T = (w_b - v_i)\frac{\rho\Omega RabcR}{4} \tag{2.13}$$

$$v_i^2 = \sqrt{\left(\frac{(\hat{v})^2}{2}\right)^2 + \left(\frac{T}{2\rho A}\right)^2} - \frac{(\hat{v})^2}{2} \tag{2.14}$$

$$w_r = w_a + (a_1 + i_s)\, u_a - b_1 v_a \tag{2.15}$$

$$w_b = w_r + \frac{2}{3}R\left[\theta_{col} + \frac{3}{4}\theta_{twist}\right] \tag{2.16}$$

$$\hat{v}^2 = u_a^2 + v_a^2 + w_r\,(w_r - 2v_i) \tag{2.17}$$

$$A = \pi R^2 \tag{2.18}$$

2.1.2.3 Main Rotor Power Required Model

After modeling the main rotor inflow, power requirements of the main rotor are calculated in order to obtain the necessary main rotor torque which will be used to calculate main rotor forces and moments. The equations are given below [37]:

$$P_{total} = P^{mr} + P^{tr} + P^{fus} + P^{climb} \tag{2.19}$$

$$P^{mr} = P^{mr}_{induced} + P^{mr}_{profile} + P^{mr}_{accessories} \tag{2.20}$$

$$P^{mr}_{induced} = T + v_i \tag{2.21}$$

$$P^{mr}_{profile} = \frac{\rho}{2}\frac{C_{D_0} bcR}{4}\Omega R\left[(\Omega R)^2 + 4.6\left(u_a^2 + v_a^2\right)\right] \tag{2.22}$$

$$P^{tr} = P^{tr}_{induced} = T^{tr} v_i^{tr} \tag{2.23}$$

$$P^{fus} = -X_{fus} u_a - Y_{fus} v_a + Z_{fus}\left(w_a - v_i\right) h \tag{2.24}$$

$$P^{climb} = mg\dot{h} \tag{2.25}$$

$$Torque_{MR} = \frac{P^{MR}}{\Omega} \tag{2.26}$$

$$X_{MR} = -T\left(a_1 - i_s\right) \tag{2.27}$$

$$Y_{MR} = Tb_1 \tag{2.28}$$

$$Z_{MR} = -T \tag{2.29}$$

$$L_{MR} = (Y_{MR}h_{hub}) + \left(\frac{dL}{dB_1}b_1\right) + \left(\frac{dL}{dA_1}(-a_1 + B_1 - (K_1b_1))\right) \tag{2.30}$$

$$N_{MR} = Torque_{MR} \tag{2.31}$$

2.1.3 Fuselage Aerodynamics Model

Fuselage drag model is based on a quadratic aerodynamic form. [37] Forces are expressed as a summation of terms formed by the product of translational velocity components in each axis. The constants in each term are the effective flat plane drag. This form can be easily extended to account for fuselage asymmetries, lifting effects and lift gradients. There are three effects of fuselage aerodynamic form related to power losses. First effect is the drag in forward flight which limits maximum airspeed, second effect is drag in sideward flight and third effect is rotor downwash impinging on the fuselage.

Profile drag forces can constitute a significant portion of the overall power required and therefore computed prior to main rotor torque. They are computed at the center of pressure located at the point relative to the center of mass in the x, y and z axes.

Physical features of fuselage model are [37]:

- Mass at C.G.
- Moments of inertia
- Parasite power
- Cross products of inertia are zero

Response features of the fuselage model are [37]:

- Trim
- Power required
- Minimum cross coupling
- Power off glide

Fuselage model equations are given below [37]:

$$d_{hub} = \frac{\left(fs_{hub} - fs_{cg}\right)}{12} \tag{2.32}$$

$$d_{fus} = \frac{\left(fs_{fus} - fs_{cg}\right)}{12} \tag{2.33}$$

$$w_a^{fus} = w - v_i \tag{2.34}$$

$$dfw = \left(\frac{u}{-w_a^{fus}} \left(h_{hub} - h_{fus}\right) - \left(d_{fus} - d_{hub}\right) \right) \tag{2.35}$$

$$dfw_{emp} = 3dfw \tag{2.36}$$

$$X_{aero}^{fus} = \frac{\rho}{2} X_{uu}^{fus} u_a u_a \tag{2.37}$$

$$Y_{aero}^{fus} = \frac{\rho}{2} Y_{vv}^{fus} v_a v_a \tag{2.38}$$

$$Z_{aero}^{fus} = \frac{\rho}{2} Z_{ww}^{fus} w_a w_a \tag{2.39}$$

$$M^{fus} = Y_{aero}^{fus} h_{fus} \tag{2.40}$$

$$L^{fus} = \left(Z^{fus}_{aero} df w_{emp}\right) - \left(X^{fus}_{aero} h_{fus}\right) \tag{2.41}$$

2.1.4 Tail Rotor Model

Thrust and induced velocity for the tail rotor is computed in the same manner as for the main rotor except that no flapping effects are included [37]. Physical outputs of tail rotor model are [37]:

- Thrust
- Torque
- Induced velocity
- Induced power
- Profile power

Response features of the fuselage model are [37]:

- Trim
- Power required
- Roll mode

2.1.5 Horizontal Tail Model

The horizontal tail is modeled in quadratic aerodynamic form of airfoils. In order to determine whether the horizontal tail surface is immersed in the rotorwash field, first its lift is computed. Because the horizontal tail is assumed to be primarily a lift producer. This will influence local vertical velocity. Then, the force computed above is compared with the maximum achievable at that same airspeed. Pitching moment is computed based on the location of the aerodynamic center relative to the center of gravity. The geometric location of the horizontal tail in the rotor flow field is used to obtain the local apparent wind component. The location of the horizontal tail provides effective static stability. Physical features of horizontal tail model are [37]:

- Lift/Stall
- Exposure to main rotor induced velocity

Response features of the horizontal tail model are [37]:

- Short period
- Trim
- Pitch mode
- Power required

Equations of the horizontal tail model are given below:

$$w_a^{ht} = w_a + v_i \tag{2.42}$$

normal force:

$$Z_{aero}^{ht} = \frac{\rho}{2}\left(Z_{uu}^{ht} u_a u_a + Z_{uw}^{ht} u_a w_a^{ht}\right) \tag{2.43}$$

2.1.6 Vertical Tail Model

Vertical tail is modeled in the same manner with horizontal tail. The only difference is the effect of the flow field on the vertical tail, produced by tail rotor. It is calculated out of the tail rotor downwash. Physical features of vertical tail model are [37]:

- Lift/Stall

Response features of the vertical tail model are [37]:

- Dutch Roll
- Roll mode

Equations of vertical tail are given below:

$$v_a^{ht} = v_a + v_i^{tr} \tag{2.44}$$

Normal force:

$$Y_{aero}^{vt} = \frac{\rho}{2}\left(Y_{uu}^{vt} u_a u_a + Y_{uv}^{vt} u_a v_a^{vt}\right) \tag{2.45}$$

2.1.7 Gravitational Force Model

In this model forces due to gravity rotated through pitch and roll angles are calculated. Equations of gravitational force model are given below:

$$X_G = -mgsin\theta \tag{2.46}$$

$$Y_G = mgsin\theta cos\phi \tag{2.47}$$

$$Z_G = mgcos\theta cos\phi \tag{2.48}$$

2.1.8 Equations of Motion Model

2.1.8.1 Coordinate Axis Definition

Inertial Axis System: (Oxi yi zi) is fixed with respect to distant stars and is located at the center of the Earth.

Earth-Fixed Axis system: (OxE yE zE) is an axis system rotating with the Earth and it is fixed at the center of the Earth.

Navigation System (NED axis system): Flat earth assumption is considered. (Oxe ye ze) is located on the surface of the Earth such that the Oze axis is directed towards the center of the

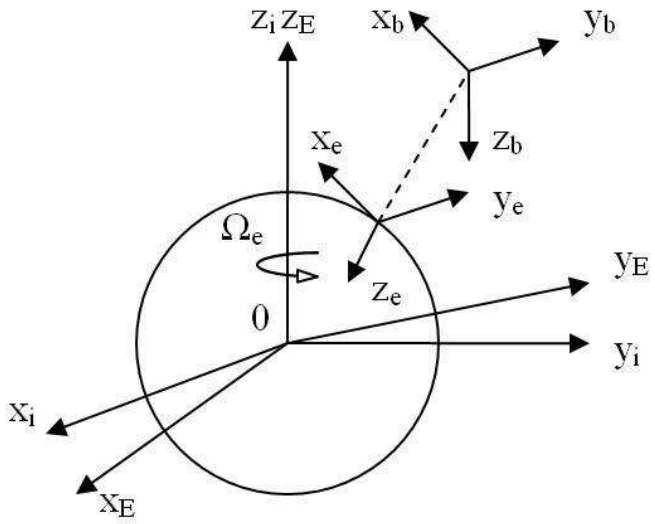

Figure 2.1: Coordinate Systems

spherical Earth. The Oxe axis usually points towards the local north and Oye points the local east to form a right-hand system.

Body axis system: (Oxb yb zb) is an axis system fixed to the vehicle and moving with it. The origin of the body axis system is the mass center of gravity.

2.1.8.2 Total Force and Moment at CG Model

In this model the first order effects of all components are summed in three force equations and three moments equations. Equations are given below:

$$X_{CG} = X_G + X^{mr} + X^{fus} \tag{2.49}$$

$$Y_{CG} = Y_G + Y^{mr} + Y^{tr} + Y^{vt} \tag{2.50}$$

$$Z_{CG} = Z_G + Z^{mr} + Z^{fus} + Z^{ht} \tag{2.51}$$

2.1.8.3 Linear Velocity Calculation Model

In this model body axis accelerations are calculated. They are directly integrated to body axes velocities.

$$\dot{u} = \frac{X_{CG}}{m} - gsin\theta - qw + rv \tag{2.52}$$

$$\dot{v} = \frac{Y}{m} + gcos\theta sin\phi - ru + pw \tag{2.53}$$

$$\dot{w} = \frac{Z}{m} + gcos\theta cos\phi - ru + qu \tag{2.54}$$

2.1.8.4 Rotational Dynamics Model

In this model angular accelerations are calculated. Angular velocities are calculated by directly integrating angular accelerations.

$$\dot{p} = \frac{1}{\left(I_{xz}^2 - I_{xx}I_{zz}\right)}\left(qr\left(I_{zz}^2 - I_{zz}I_{yy} + I_{xz}^2\right) - qpI_{xz}\left(I_{zz} - I_{yy} + I_{xx}\right) - (I_{zz}L + I_{xz}N)\right) \tag{2.55}$$

$$\dot{q} = \frac{1}{I_{yy}}\left(M + pr\left(I_{zz} - I_{xx}\right) - \left(p^2 - r^2\right)I_{xz}\right) \tag{2.56}$$

$$\dot{r} = \frac{1}{\left(I_{xz}^2 - I_{xx}I_{zz}\right)}\left(qrI_{xz}\left(I_{zz} - I_{yy} + I_{xx}\right) - qp\left(I_{xz}^2 - I_{yy}I_{xx} + I_{xx}^2\right) - (I_{xz}L + I_{xx}N)\right) \tag{2.57}$$

where;

$$Ixy = 0 \tag{2.58}$$

$$Iyz = 0 \tag{2.59}$$

Assumptions:

- X_B, Y_B and Z_B are zero
- PQ, QR and $P^2 - R^2$ are zero
- R^2 and P^2 are zero

Then the equation becomes:

$$\dot{p} = \frac{L}{I_{xx}} \tag{2.60}$$

$$\dot{q} = \frac{1}{I_{yy}} \left(M - pr \left(I_{xx} - I_{zz} \right) - I_{xz} \left(p^2 - r^2 \right) \right) \tag{2.61}$$

$$\dot{r} = \frac{N}{I_{zz}} + \dot{p} \frac{I_{xz}}{I_{zz}} \tag{2.62}$$

2.1.8.5 Ground Axis Position Model

In this model, body axis velocities are converted to earth relative velocities using a common Euler angle direction cosine transformation. Assuming that this is NED axis frame, these earth relative velocities are directly integrated in order to obtain NED axis positions.

$$u_g = (ucos\theta + wsin\theta)\, cos\phi cos\psi \tag{2.63}$$

$$v_g = vcos\psi + usin\psi \tag{2.64}$$

$$w_g = (usin\theta - wcos\theta)\, cos\phi \tag{2.65}$$

2.1.8.6 Attitude Dynamics Model

In order to obtain Euler angles , the relationship between the body-fixed angular velocity vector and the rate of change of the Euler angles are used by resolving the Euler rates into the body-fixed coordinate frame.

$$\dot{\phi} = p + (qsin(\phi) + rcos(\phi))tan(\theta) \tag{2.66}$$

$$\dot{\theta} = qcos(\phi) - rsin(\phi) \tag{2.67}$$

$$\dot{\psi} = (rcos(\phi) + qsin(\phi))/cos(\theta) \tag{2.68}$$

2.1.9 Atmosphere Model

In this model total body axis velocity, angle of attack and sideslip angle are calculated.

Total body axis velocity:

$$V_t = \sqrt[2]{u^2 + v^2 + w^2} \tag{2.69}$$

Angle of attack:

$$\alpha = tan^{-1}\left(\frac{w}{u}\right) \tag{2.70}$$

Sideslip angle:

$$\beta = sin^{-1}\left(\frac{v}{V_t}\right) \tag{2.71}$$

CHAPTER 3

LINEAR CONTROLLER DESIGN

In this chapter a linear controller design algorithm for the nonlinear helicopter model is presented. In the first part trim condition generation algorithm is explained. In the second part the linearization algorithm is given. In the third part controller system design approach is explained.

3.1 Trim Condition Generation

In order to design a linear controller, the nonlinear model must be linearized around a trim point. Therefore the trim or equilibrium conditions must be known. Therefore a trim tool is developed.

”Determining aircraft steady-state flight conditions is of primary importance in a variety of engineering studies. Trim defines conditions for both design and analysis based on aircraft models. In simulations, these analysis points establish initial conditions comparable to flight conditions. Based on aerodynamic and propulsion systems models of an aircraft, trim analysis can be used to provide the data needed to define the operating envelope or the performance characteristics. Linear models are typically derived at trim points. Control systems are designed and evaluated at points defined by trim conditions. And these trim conditions provide a starting point for comparing one model against another, one implementation of a model against another implementation of the same model, and the model to flight-derived data” [3].

”The term simulation-based optimization is currently applied to the methodology in which complex physical systems are designed, analyzed, and controlled by optimizing the results of computer simulations. In the simulation-based optimization setting, a computer simulation

must be run, repeatedly, in order to compute the various quantities needed by the optimization algorithm. Furthermore, the resulting simulation output must then be post processed to arrive finally at values of the objective and constraint functions. These complications can make obtaining derivatives for gradient-based methods at the very least difficult, even when the underlying objective and constraint functions are smooth (i.e., continuously differentiable)" [3].

"The aircraft trim problem falls right into the context of simulation-based optimization, where the term optimization equals to determine the combination of flight control settings and other state variables that make the steady-state flight possible" [3].

Trim model is composed of three main parts:

- Trim Constraint Model: Nonlinear equality and inequality constraints are defined.
- Trim Cost Model: Minimization of the cost function is performed.
- Trimmer Model: Simulation-based optimization is performed.

3.1.1 Trim Constraint Model

In this model trim constraint equations are defined for the hover and forward flight conditions. The same approach will be used for both flight condition. Trim constraint nonlinear equality is defined as given below:

Constraint equation for total velocity:

$$V_T - V_{Ttrim} = 0 \tag{3.1}$$

3.1.2 Trim Cost Model

In this model, the states and the control inputs of the helicopter such as attitude angles, aerodynamic surface deflections and thrust direction for the desired trim condition is obtained numerically by minimizing a conveniently defined cost function. Parameters used in order to calculate cost function are:

- Angular velocities

- Linear accelerations
- Angular accelerations
- Main rotor flapping angles

In trim condition total forces and moments should be zero. Therefore the angular and linear accelerations will be zero to hold the vehicle in the specified trim condition. A quadratic cost function is obtained by summing up the weighted squared values of the angular parameters given above and the aim is to minimize the cost function.

$$\begin{aligned} cost = &\left(weight_p * p^2\right) + \left(weight_q * q^2\right) + \left(weight_r * r^2\right) + \left(weight_{\dot{u}} * \dot{u}^2\right) + \\ &\left(weight_{\dot{v}} * \dot{v}^2\right) + \left(weight_{\dot{w}} * \dot{w}^2\right) + \left(weight_{\dot{p}} * \dot{p}^2\right) + \left(weight_{\dot{q}} * \dot{q}^2\right) + \\ &\left(weight_{\dot{r}} * \dot{r}^2\right) + \left(weight_{\dot{a}_1} * \dot{a}_1^2\right) + \left(weight_{\dot{b}_1} * \dot{b}_1^2\right) \end{aligned} \tag{3.2}$$

3.1.3 Trimmer Model

In this model, simulation based optimization is performed by using an algorithm in order to find a minimum of constrained nonlinear multi variable function. First lower and upper bounds of the specified trim parameters are defined. Then the velocity and position values are entered in order to define the trimmed flight condition.

$$\min_x f(x) \tag{3.3}$$

subject to

$$c(x) \leq 0 \tag{3.4}$$

$$c_{eq}(x) = 0 \tag{3.5}$$

$$Ax \leq b \tag{3.6}$$

$$A_{eq}x = b_{eq} \tag{3.7}$$

$$l_b \leq x \leq u_b \tag{3.8}$$

where, x , b, b_{eq}, l_b, u_b are vectors; A, A_{eq} are matrices; $c(x)$, $c_{eq}(x)$ are functions that return vectors and $f(x)$ is a function that returns a scalar. $f(x)$,$c(x)$, $c_{eq}(x)$ can be nonlinear functions.

By the help of the optimization tool algorithm constrained minimum of the predefined states are calculated. Control input parameters and state values are obtained. In the results and discussion part trimmer solutions will be given and discussed.

3.2 Linearization Model

Well-defined steady-state reference conditions serve as basis for model linearization, enabling linear system analysis required for stability and control considerations, handling qualities issues or control design tasks. Linearization of the nonlinear helicopter model is performed around some given sensible trim points within the considered flight envelope. By giving small perturbations to the state variables around equilibrium points, an interpolation is performed and elements of the system and input matrices are obtained. By the help of these system and input matrices state space representation are obtained.The stability of the system for the specified flight condition are examined from the eigenvalues of the system matrix. Then, these parameters will be used to design a linear control system.

Linearization is defined around the $\bar{X}_e$ and $\bar{u}_e$are hover and forward flight equilibrium points through a Taylor series expansion:

$$\dot{\tilde{x}} \triangleq \bar{A}\bar{x} + \bar{B}\bar{u} \tag{3.9}$$

where $\tilde{x} = x - x_e$

$$\bar{A} = \begin{bmatrix} \left.\frac{\partial \bar{F}_1}{\partial \bar{x}_1}\right|_{\bar{x}_e,\bar{u}_e} & \left.\frac{\partial \bar{F}_1}{\partial \bar{x}_2}\right|_{\bar{x}_e,\bar{u}} & \cdots & \left.\frac{\partial \bar{F}_1}{\partial \bar{x}_n}\right|_{\bar{x}_e,\bar{u}} \\ \left.\frac{\partial \bar{F}_2}{\partial \bar{x}_1}\right|_{\bar{x}_e,\bar{u}} & \left.\frac{\partial \bar{F}_2}{\partial \bar{x}_2}\right|_{\bar{x}_e,\bar{u}} & \cdots & \left.\frac{\partial \bar{F}_2}{\partial \bar{x}_n}\right|_{\bar{x}_e,\bar{u}} \\ \vdots & \vdots & \vdots & \vdots \\ \left.\frac{\partial \bar{F}_n}{\partial \bar{x}_1}\right|_{\bar{x}_e,\bar{u}} & \left.\frac{\partial \bar{F}_n}{\partial \bar{x}_2}\right|_{\bar{x}_e,\bar{u}} & \cdots & \left.\frac{\partial \bar{F}_n}{\partial \bar{x}_n}\right|_{\bar{x}_e,\bar{u}} \end{bmatrix} \tag{3.10}$$

$$\bar{B} = \begin{bmatrix} \left.\frac{\partial \bar{F}_1}{\partial \bar{u}_1}\right|_{\bar{x}_e,\bar{u}} & \cdots & \left.\frac{\partial \bar{F}_1}{\partial \bar{u}_n}\right|_{\bar{x}_e,\bar{u}} \\ \left.\frac{\partial \bar{F}_2}{\partial \bar{u}_1}\right|_{\bar{x}_e,\bar{u}} & \cdots & \left.\frac{\partial \bar{F}_2}{\partial \bar{u}_n}\right|_{\bar{x}_e,\bar{u}} \\ \vdots & \vdots & \vdots \\ \left.\frac{\partial \bar{F}_n}{\partial \bar{u}_1}\right|_{\bar{x}_e,\bar{u}} & \cdots & \left.\frac{\partial \bar{F}_n}{\partial \bar{u}_n}\right|_{\bar{x}_e,\bar{u}} \end{bmatrix} \tag{3.11}$$

For a rigid aerospace vehicle we have twelve states for positions, Euler angles, linear and angular velocities. For the control vector collective, longitudinal cyclic, lateral cyclic, pedal control inputs are considered. State and input matrices' order may be reduced by neglecting the positions and the heading angle.

3.3 Design of the Automatic Flight Control System

Automatic flight control system will be designed using classical control theory. Sequential loop closing method will be used. In this method an inner loop linear control model is designed for the stability augmentation system to ease the pilot's control. After the implementation of the inner loop controllers, outer loop controllers will be desined. These outer loop modes are usually called flight directory modes or upper automatic flight control system modes of the helicopter such as altitude acquire and hold, velocity acquire and hold, pitch attitude hold, roll attitude hold and heading hold modes.

In the following section , inner loop and outer loop automatic flight control system design approaches are described.

3.3.1 Inner loop linear controller design

First, the nonlinear flight simulation model is linearized around the desired equilibrium (trim) point and necessary state and control matrices are obtained using umerical linearization code. Longitudinal and lateral states will be assumed to be uncoupled and treated separately. The

longitudinal state vector is:

$$x_{longitudinal} = \begin{bmatrix} u \\ w \\ q \\ \theta \end{bmatrix} \tag{3.12}$$

Longitudinal control vector is:

$$u_{longitudinal} = \begin{bmatrix} \delta_c \\ \delta_e \end{bmatrix} \tag{3.13}$$

Lateral state vector is:

$$x_{lateral} = \begin{bmatrix} \phi \\ v \\ p \\ r \end{bmatrix} \tag{3.14}$$

$$u_{lateral} = \begin{bmatrix} \delta_a \\ \delta_p \end{bmatrix} \tag{3.15}$$

The inner loop control model is usually achieved by feeding back body angular rates. Pitch angular rate feedback is used in the longitudinal part where roll and yaw angular rate feedbacks are used in the lateral part. In addition lead compensators may be used to improve the stability of the system. On the other hand a state variable feedback law may be given as:

$$\dot{x} = Ax + Bu \tag{3.16}$$

and measurement is,

$$y = Cx + Du \tag{3.17}$$

If,

$$u = -Kx$$

In this approach all loops are closed at once. The gain matrix K is selected such that the closed loop system has the desired dynamics.

Truncated system state feedback control method: in this method number of states should be equal to the number of controls. For this purpose all coupling terms are omitted. Thus it is the state feedback for the truncated system equations.

$$\dot{x} = Ax + Bu \tag{3.18}$$

$$y = Cx \tag{3.19}$$

where A=n*n, B=n*n, C=I(n)

$$u = -Ky \tag{3.20}$$

Desired state matrix is constructed by selecting proper, stable eigenvalues.

$$\dot{x} = A_d x \tag{3.21}$$

$$\Longrightarrow u = -KCx \tag{3.22}$$

$$\dot{x} = Ax - BKCx \approx A_d x \tag{3.23}$$

Then truncated system state feedback controller is:

$$K = B^{-1}(A - A_d)C^{-1} \tag{3.24}$$

In the approaches presented above the eigenvalues of the full system together with the feedbac controllers shall be examined for stability.

3.3.2 Outer loop controller design: Flight Directory Modes

Upper modes or flight directory modes of automatic flight control systems are important for different flight operations like search and rescue, hoist/sling operations, and fire extinguishing operations. The aim of designing an outer loop control systems is to keep the helicopter at the desired flight conditions. For hover flight four upper modes of helicopter flight may be considered. These are altitude acquire/hold, roll hold, pitch hold and heading hold modes. In addition to these upper modes, velocity acquire/hold is also designed for forward flight.

3.3.2.1 Altitude Acquire and Hold Mode

Altitude hold mode is considered in order to design a controller to keep the helicopter at a desired altitude. The main input for controlling altitude is the collective control input.

Inner loop control model is already implemented for the nonlinear model. Together with the inner loop controls the nonlinear simulation model is again linearized to obtain the new state space representation to account for the errors involved in uncoupling and truncating the full system equations during inner loop design. Then collective control input to vertical speed state transfer function is obtained and the root locus plot is analyzed to select the necessary gain and lead compensator. For hover flight a lead compensator is designed however for the forward flight proportional control gain is enough to control the system.

3.3.2.2 Roll Hold Mode

Roll hold mode is a necessary mode for the realization of other flight directory modes such as altitude hold. If it is left uncontrolled, this can cause instability. To control roll attitude, state feedback gain is calculated considering the related transfer function and root locus plot.

3.3.2.3 Pitch Hold Mode

Pitch hold mode is implemented in order to add damping to the longitudinal cyclic control in order and help the instability in the longitudinal axis. Desired pitch attitude is selected to be the pitch attitude of the desired altitude. Feedback gain is selected from the root locus plot of

pitch attitude versus longitudinal cyclic transfer function.

3.3.2.4 Heading Hold Mode

Heading hold mode is designed in order to control the heading angle through pedal input. For hover flight a lead compensator is designed however for the forward flight state feedback gain was enough to control the system.

3.3.2.5 Velocity Acquire and Hold Mode

Velocity hold mode is designed for forward flight condition. When the velocity hold mode is activated, earth axis longitudinal velocity increases to the desired velocity and after that desired velocity is conserved. This mode is implemented together with attitude hold (i.e. roll, heading, pitch) and altitude acquire and hold modes. Again a proportional control is used.

CHAPTER 4

RESULTS AND DISCUSSION

In this chapter trim solutions, mixing unit effect to the control inputs and simulation results of the various modes are presented and discussed. In the first section trim solutions will be given for different altitudes, in the second part mixing unit effects are examined for 100 ft hover trim condition, in the third part control system design and simulation results are considered for 100 ft hover condition and in the last part control system design and simulation results are considered for the 100 ft altitude 60 knot forward flight condition.

4.1 Trim solutions

In this part trim solutions for different altitudes will be given.

4.1.1 Trim solutions for sea level altitude

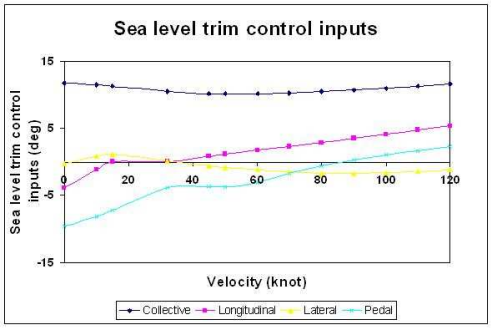

Figure 4.1: Sea level trimmed flight control input values versus forward velocity (in NED frame)

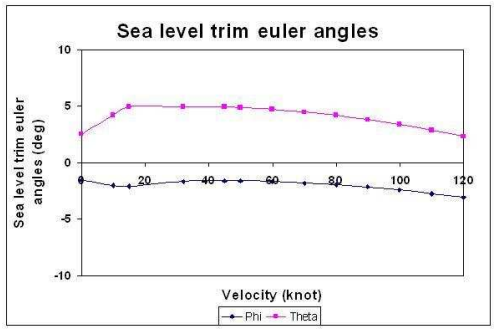

Figure 4.2: Sea level trimmed flight euler attitude values versus forward velocity (in NED frame)

Table 4.1: Sea level trimmed flight control input and attitude values versus forward velocity(in NED frame)

V_t(knot)	δ_c(deg)	δ_e(deg)	δ_a(deg)	δ_p(deg)	ϕ(deg)	θ(deg)
0	11.696	-3.924	-0.268	-9.558	-1.559	2.501
10	11.510	-1.196	0.855	-8.148	-1.985	4.232
20	11.294	0.012	1.203	-7.242	-2.071	4.900
30	10.485	0.015	0.149	-3.859	-1.697	4.957
40	10.211	0.830	-0.588	-3.691	-1.611	4.952
50	10.176	1.125	-0.866	-3.778	-1.611	4.900
60	10.193	1.708	-1.223	-3.124	-1.660	4.734
70	10.294	2.293	-1.522	-1.734	-1.768	4.495
80	10.460	2.886	-1.701	-0.660	-1.929	4.189
90	10.678	3.488	-1.754	0.296	-2.139	3.816
100	10.940	4.100	-1.675	1.015	-2.400	3.377
110	11.242	4.725	-1.449	1.630	-2.714	2.874
120	11.582	5.360	-1.202	2.268	-3.081	2.305

4.1.2 Trim solutions for 100 ft altitude

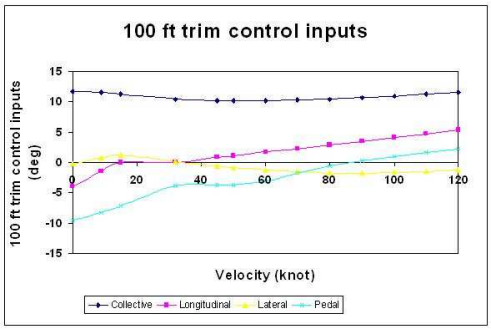

Figure 4.3: 100 ft altitude trimmed flight control input values versus forward velocity (in NED frame)

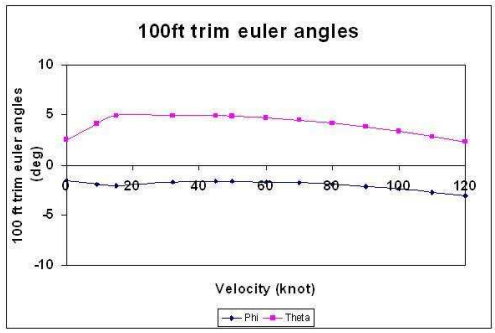

Figure 4.4: 100 ft altitude trimmed flight euler attitude values versus forward velocity (in NED frame)

Table 4.2: 100 ft altitude trimmed flight control input and attitude values versus forward velocity(in NED frame)

V_t(knot)	δ_c(deg)	δ_e(deg)	δ_a(deg)	δ_p(deg)	ϕ(deg)	θ(deg)
0	11.681	-3.928	-0.273	-9.551	-1.556	2.497
10	11.530	-1.455	0.766	-8.330	-1.956	4.080
20	11.279	0.017	1.202	-7.240	-2.073	4.908
30	10.470	0.014	0.148	-3.859	-1.697	4.956
40	10.197	0.828	-0.588	-3.691	-1.612	4.951
50	10.163	1.123	-0.865	-3.775	-1.613	4.898
60	10.180	1.706	-1.222	-3.120	-1.664	4.732
70	10.283	2.290	-1.521	-1.733	-1.771	4.492
80	10.449	2.883	-1.698	-0.660	-1.932	4.184
90	10.667	3.485	-1.752	0.300	-2.146	3.811
100	10.930	4.097	-1.672	1.015	-2.406	3.370
110	11.233	4.721	-1.446	1.628	-2.721	2.864
120	11.573	5.357	-1.200	2.265	-3.090	2.294

4.1.3 Trim solutions for 1000 ft altitude

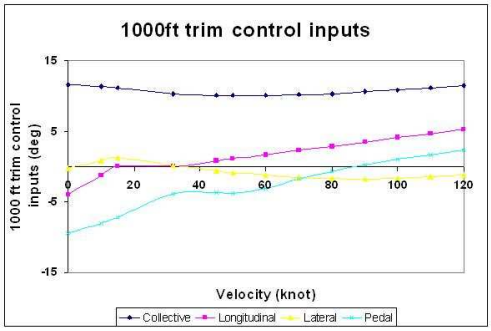

Figure 4.5: 1000 ft altitude trimmed flight control input values versus forward velocity (in NED frame)

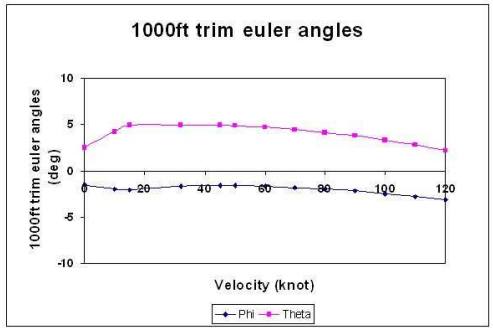

Figure 4.6: 1000 ft altitude trimmed flight Euler attitude values versus forward velocity (in NED frame)

Table 4.3: 1000 ft altitude trimmed flight control input and attitude values versus forward velocity(in NED frame)

V_t(knot)	δ_c(deg)	δ_e(deg)	δ_a(deg)	δ_p(deg)	ϕ(deg)	θ(deg)
0	11.546	-3.951	-0.316	-9.482	-1.529	2.473
10	11.358	-1.211	0.821	-8.099	-1.976	4.237
20	11.141	0.003	1.177	-7.212	-2.072	4.919
30	10.338	0.001	0.136	-3.866	-1.699	4.953
40	10.076	0.809	-0.587	-3.675	-1.623	4.940
50	10.046	1.102	-0.860	-3.753	-1.627	4.883
60	10.071	1.683	-1.210	-3.097	-1.686	4.711
70	10.179	2.265	-1.504	-1.719	-1.801	4.462
80	10.351	2.856	-1.678	-0.655	-1.971	4.144
90	10.574	3.458	-1.730	0.292	-2.192	3.758
100	10.843	4.070	-1.649	1.006	-2.465	3.306
110	11.151	4.694	-1.423	1.616	-2.792	2.785
120	11.498	5.331	-1.176	2.247	-3.175	2.199

4.2 Mixing unit

In this part mixing unit effect to the control input values will be analyzed by considering the trim control input values for the 100 ft hover trim condition. Mixing unit model is implemented to avoid the control coupling. Mixing unit does dot have a distinct effect on collective and longitudinal cyclic control inputs. However for the lateral cyclic and pedal control inputs mixing unit has an important role. In hover, there is a substantial coupling between the lateral cyclic and pedal controls.

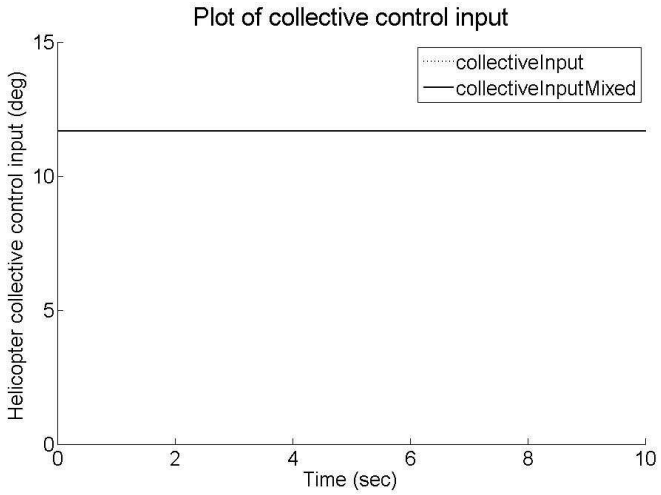

Figure 4.7: Helicopter collective control input with and without mixing unit for 100 ft hover trim flight condition

From the figure 4.7 it is observed that collective control input is not effected by the mixing unit.

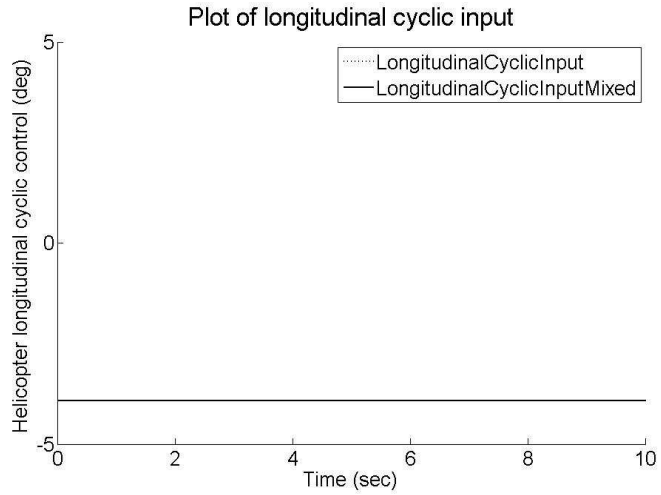

Figure 4.8: Helicopter longitudinal cyclic control input with and without mixing unit for 100 ft hover trim flight condition

From the figure 4.8 it is observed that longitudinal cyclic control input is also not effected by the mixing unit.

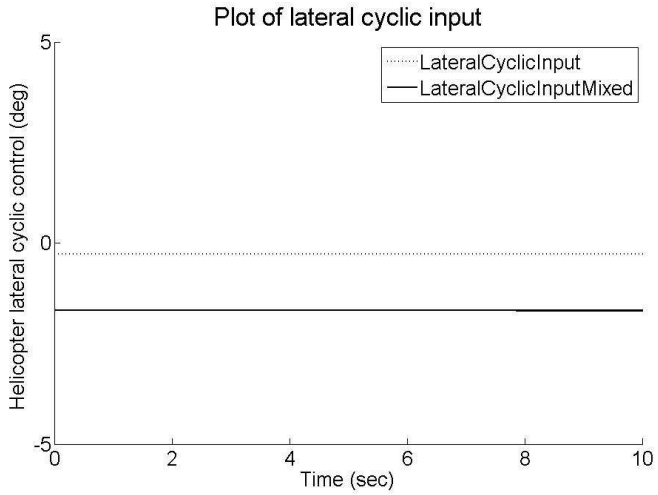

Figure 4.9: Helicopter lateral cyclic control input with and without mixing unit for 100 ft hover trim flight condition

From the figure 4.9 it is observed that lateral cyclic control input is effected by the mixing unit.

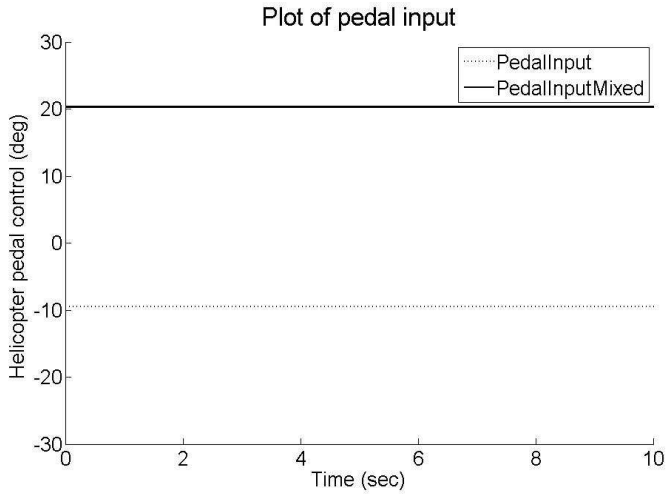

Figure 4.10: Helicopter pedal control input with and without mixing unit for 100 ft hover trim flight condition

From the figure 4.10 it is observed that pedal control input is effected by the mixing unit.

4.3 AFCS design for hover flight

In this section helicopter model will be considered in trim condition without any automatic flight control system implemented on it. Trim behavior of the helicopter states will be analyzed for this condition.

4.3.1 Helicopter simulation results for 100 ft hover flight condition in trim mode

The helicopter is brought to 100 ft hover trim condition and the simulation is started. Thus, all the inputs and initial states are taken from the trim calculations. Normally helicopter shall stay at this condition. However, due to the instability inherent in the system and slight differences in the exact trim values and calculated ones as well as the numerical inaccuracies, the simulation starts to diverge as may be observed in the following plots.

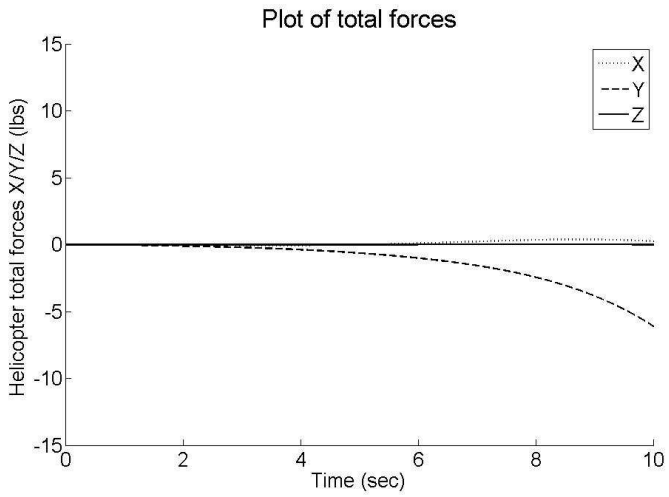

Figure 4.11: Total forces on helicopter for trim condition in 100 ft hover

In trim condition total forces and moments acting on the helicopter should be zero. As it may be observed from the graphs, total forces and moments in three axis are almost zero. However the Y axis force and yawing moment (N) starts to diverge after a while in a small amount. This divergence will cause instability if the helicopter stays in trim without any AFCS control for a longer time. By the help of AFCS model these instability problems shall be solved.

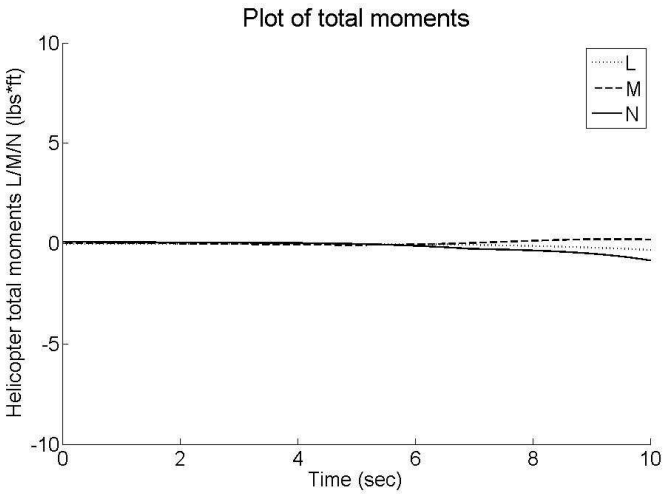

Figure 4.12: Total moments on helicopter for trim condition in 100 ft hover

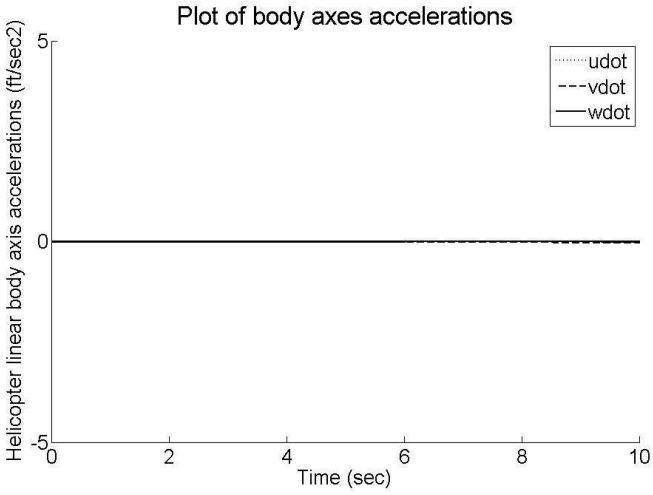

Figure 4.13: Body axis accelerations for trim condition in 100 ft hover

In trim condition body axes accelerations should be zero as it is observed from the 4.13.

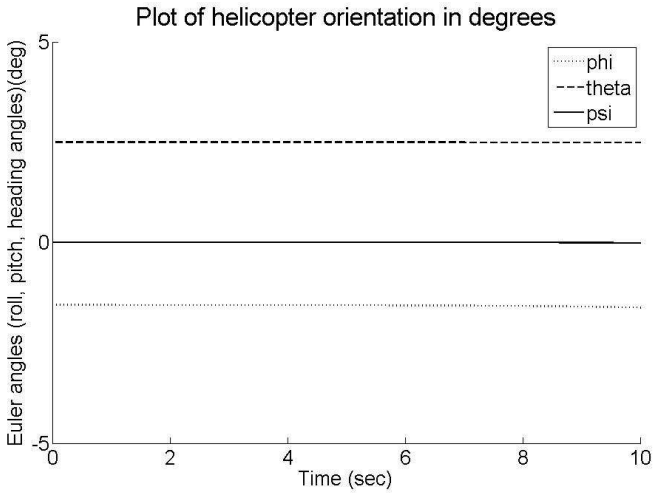

Figure 4.14: Euler angles for trim condition in 100 ft hover

In trim condition helicopter orientation and position should be conserved, because total forces and moments are zero and therefore helicopter should not tend to change it's orientation and position.

4.3.2 Helicopter inner loop control for 100 ft hover condition

In this section inner stability loop controller designs with classical control method and truncated system state feedback control method are given. First linearization results of uncontrolled model is presented. Then after each different design the new closed loop system is linearized to examine the stability and performance of the new system.

4.3.2.1 Uncontrolled linearized helicopter model

State matrix is obtained by considering positions, Euler angles, body axis velocities and body angular velocities. However position and heading angle are neglected since these are rigid body modes of the system. The states considered are:

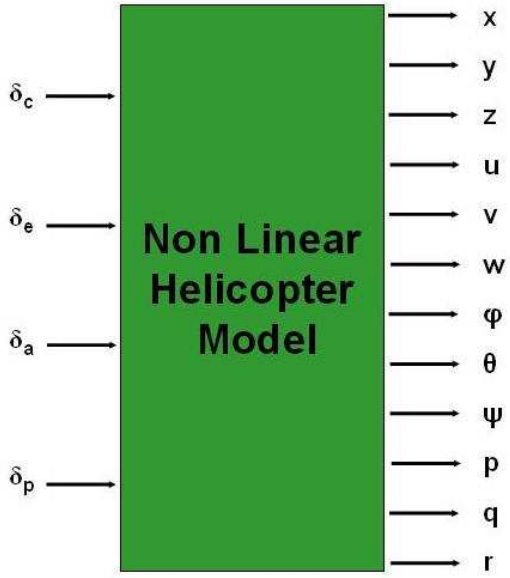

Figure 4.15: Helicopter model without AFCS

$$x = \begin{bmatrix} u & w & q & \theta & v & p & \phi & r \end{bmatrix}^T \tag{4.1}$$

where the control matrix is:

$$u = \begin{bmatrix} \delta_e & \delta_c & \delta_a & \delta_p \end{bmatrix}^T \tag{4.2}$$

$$A = \begin{bmatrix} -0.0008 & 0.0161 & -0.0289 & -32.1694 & 0.0005 & 0.0000 & 0.0000 & -0.0009 \\ 0.0149 & -0.3883 & -0.0014 & -1.4028 & -0.0111 & 0.0009 & 0.8726 & -0.0000 \\ 0.0077 & -0.0018 & -0.0008 & -0.0002 & -0.0000 & 0.0004 & -0.0000 & -0.0000 \\ 0.0000 & -0.0000 & 0.9996 & 0 & 0.0000 & 0.0000 & -0.0000 & 0.0271 \\ -0.0215 & -0.0120 & 0.0000 & 0.0382 & -0.0111 & 0.0008 & 32.1572 & 0.2319 \\ -0.0211 & -0.0077 & -0.0019 & 0.0001 & -0.0039 & -0.0138 & -0.0002 & 0.0781 \\ -0.0000 & -0.0000 & -0.0012 & 0.0000 & -0.0000 & 1.0000 & 0.0000 & 0.0437 \\ 0.0083 & 0.0216 & -0.0002 & -0.0000 & 0.0063 & 0.0141 & 0.0002 & -0.1201 \end{bmatrix} \tag{4.3}$$

$$B = \begin{bmatrix} 0.0691 & 15.5387 & -0.0000 & 0.0000 \\ 0.0000 & -356.0544 & -0.0001 & -0.0001 \\ 3.6569 & -1.6727 & -0.0077 & 0.0000 \\ 0.0037 & -0.0017 & -0.0000 & -0.0001 \\ 0.0000 & 13.1654 & 5.3711 & 9.6401 \\ -0.0402 & -1.3604 & 20.9928 & 3.2650 \\ -0.0000 & -0.0014 & 0.0210 & 0.0030 \\ -0.0050 & -1.9484 & -0.3666 & -5.0247 \end{bmatrix} \tag{4.4}$$

Eigenvalues of the linearized A matrix are:

$$\lambda_{1,2} = 0.3191 \pm 0.5614i \tag{4.5}$$

$$\lambda_{3,4} = 0.1771 \pm 0.3963i$$

$$\lambda_5 = -0.6507$$

$$\lambda_6 = -0.5746$$

$$\lambda_7 = 0.0054$$

$$\lambda_8 = -0.3075$$

These eigenvalues indicate 2 unstable complex conjugate pair and an unstable root. To apply separate designs, the system and input matrices are partitioned and separated to longitudinal and lateral dynamics.

Longitudinal state and control vectors are:

$$x = \begin{bmatrix} u & w & q & \theta \end{bmatrix}^T \tag{4.6}$$

$$u = \begin{bmatrix} \delta_c & \delta_e \end{bmatrix}^T \tag{4.7}$$

Eigenvalues of the longitudinal part then becomes:

$$\lambda_{1,2} = 0.3126 \pm 0.5422i \tag{4.8}$$

$$\lambda_3 = -0.6254$$

$$\lambda_4 = -0.3897$$

It may be observed that there is a relation between these eigenvalues and the eigenvalues of the full system matrix. The first two complex conjugate eigenvalues are close to the unstable complex conjugate pair of the eigenvalues of the full system matrix. Then the transfer function between the pitch rate and longitudinal cyclic input is,

$$\frac{q}{\delta_e} = \frac{3.657s^3 + 1.423s^2 - 0.000444s - 0.0003533}{s^4 + 0.3899s^3 + 0.000802s^2 + 0.2452s + 0.09545} \tag{4.9}$$

Associated root locus plot is given in the figure below. From the plot it may be observed that the pitch mode may not be stabilized by a p-control only:

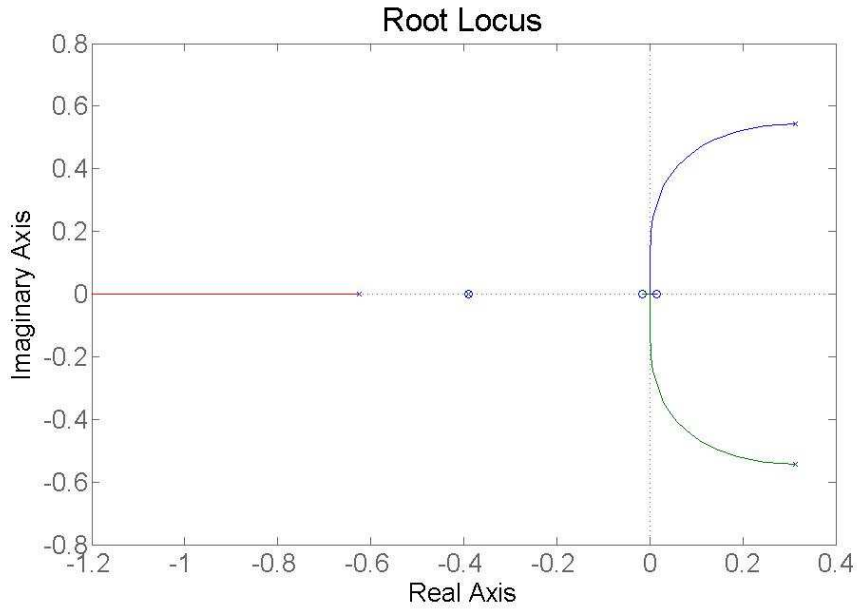

Figure 4.16: Pitch rate feedback root locus plot

Lateral state and control vectors are:

$$x = \begin{bmatrix} v & p & \phi & r \end{bmatrix}^T \tag{4.10}$$

$$u = \begin{bmatrix} \delta_a & \delta_p \end{bmatrix}^T \tag{4.11}$$

Eigenvalues of the lateral state matrix are:

$$\lambda_1 = -0.5434 \tag{4.12}$$

$$\lambda_{2,3} = 0.1957 \pm 0.4198i$$

$$\lambda_4 = 0.0069$$

Comparing these eigenvalues by the ones given for the full system matrix the unstable complex conjugate couple is close to the second unstable complex conjugate couple of the full system matrix. Unstable real root is close to the unstable root of the full system matrix.

The transfer function between the roll rate and lateral cyclic input becomes:

$$\frac{p}{\delta_a} = \frac{20.99s^3 + 2.705s^2 - 0.005358s - 0.1838}{s^4 + 0.145s^3 - 0.0007759s^2 + 0.1166s - 0.0008051} \tag{4.13}$$

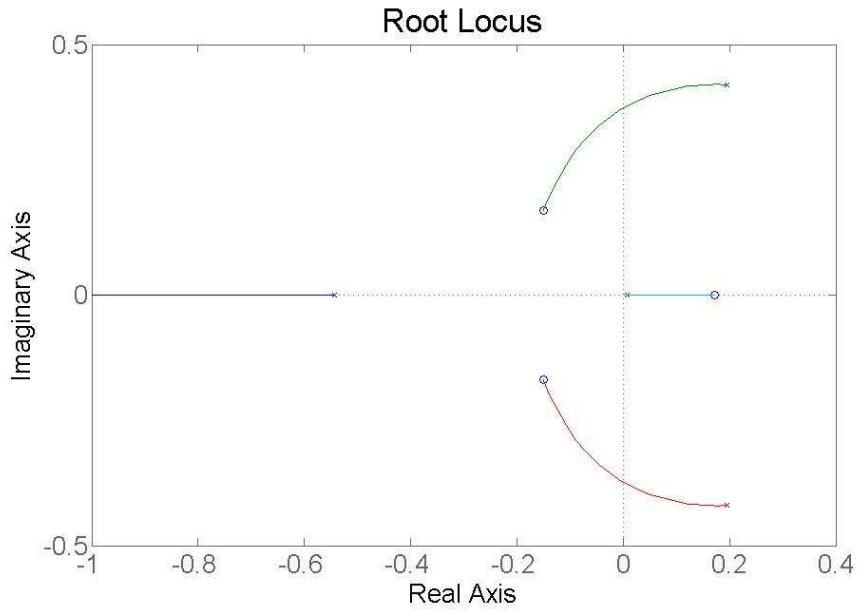

Figure 4.17: Roll rate feedback root locus plot

Similarly transfer function between yaw rate and pedal input becomes:

$$\frac{r}{\delta_p} = \frac{-5.025s^3 + 0.01835s^2 + 0.0003059s + 0.0313}{s^4 + 0.145s^3 - 0.0007759s^2 + 0.1166s - 0.0008051} \tag{4.14}$$

The root locus plots for roll and yaw rate indicate that these transfer functions can not be stabilized by p-control only.

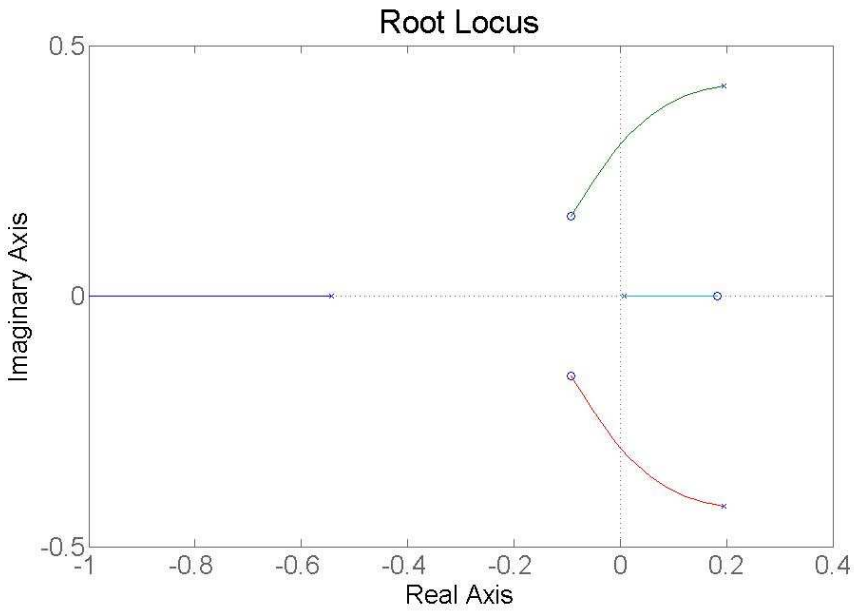

Figure 4.18: Yaw rate feedback complementary root locus plot

4.3.2.2 The inner loop controller designed using classical control method

Helicopter pitch, roll and yaw rate feedbacks required a lead compensator for stabilization. By considering the longitudinal and lateral eigenvalues together with root locus plots necessary gains and lead compensators are selected. The aim is moving the unstable roots to the left half s-plane and increase the stability of the system.

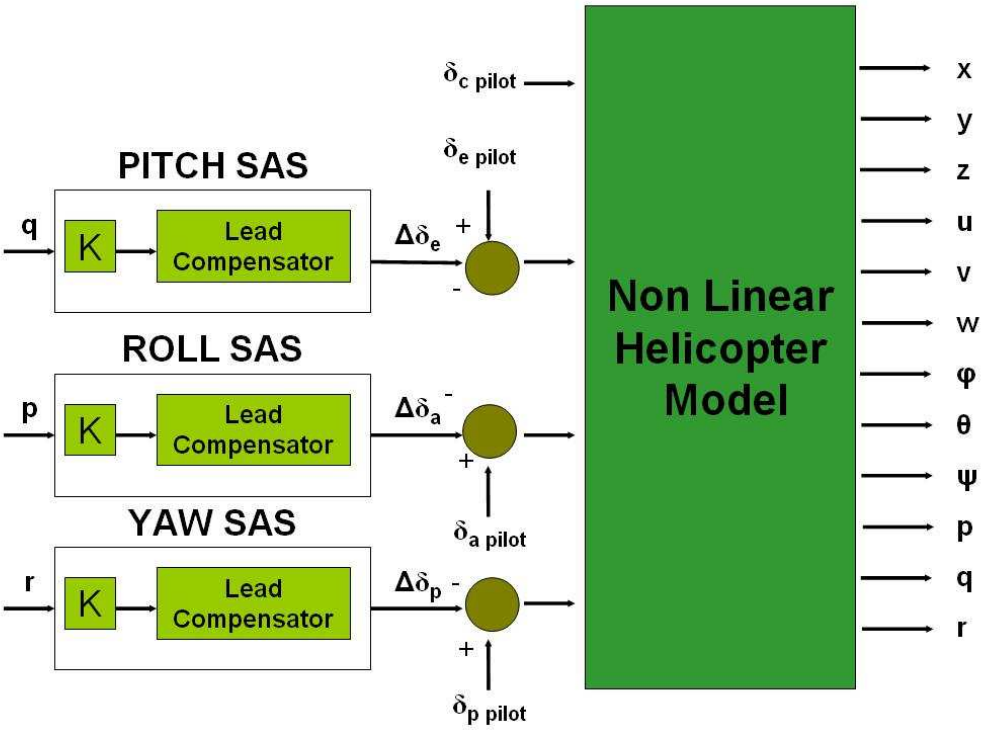

Figure 4.19: Helicopter model with inner loop controller

Figure 4.20: Pitch rate feedback

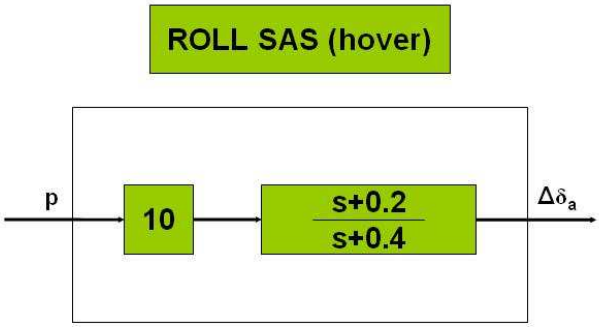

Figure 4.21: Roll rate feedback

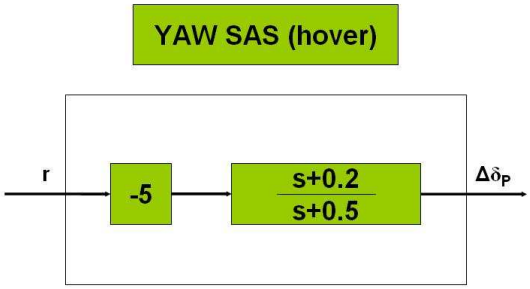

Figure 4.22: Yaw rate feedback

The system matrix considering q, p and r states is obtained by using nonlinear model with numerical linearization code. The system matrix considering q, p, r states is:

$$A = \begin{bmatrix} -7.2580 & 0.0624 & 0.0011 \\ 0.0632 & -170.0890 & 12.9246 \\ 0.0097 & 2.9018 & -24.5566 \end{bmatrix} \tag{4.15}$$

Eigenvalues belonging to q, p, r states become:

$$\lambda_1 = -7.2580 \tag{4.16}$$

$$\lambda_2 = -170.3463$$

$$\lambda_3 = -24.2994$$

The new system matrix is obtained using nonlinear model with numerical linearization code. The new system matrix is:

$$A = \begin{bmatrix} -0.0008 & 0.0161 & -0.1658 & -32.1694 & 0.0005 & 0.0000 & 0.0000 & -0.0008 \\ 0.0148 & -0.3883 & -0.0014 & -1.4028 & -0.0111 & 0.0013 & 0.8726 & -0.0005 \\ 0.0076 & -0.0018 & -7.2580 & -0.0002 & -0.0000 & 0.0624 & -0.0000 & 0.0011 \\ 0.0000 & -0.0000 & 0.9923 & -0.0000 & 0.0000 & 0.0002 & -0.0000 & 0.0265 \\ -0.0200 & -0.0106 & -0.0033 & 0.0382 & -0.0106 & -43.3709 & 32.1572 & 46.4328 \\ -0.0167 & -0.0059 & 0.0632 & 0.0001 & -0.0031 & -170.0890 & -0.0002 & 12.9246 \\ -0.0000 & -0.0000 & -0.0011 & 0.0000 & -0.0000 & 0.8107 & -0.0000 & 0.0571 \\ 0.0081 & 0.0211 & 0.0097 & -0.0000 & 0.0061 & 2.9018 & 0.0002 & -24.5566 \end{bmatrix} \tag{4.17}$$

Then the eigenvalues of the new system matrix are more stable than the uncontrolled system as given below:

$$\lambda_1 = -170.3472 \tag{4.18}$$

$$\lambda_2 = -24.3099$$

$$\lambda_3 = -7.2624$$

$$\lambda_4 = -0.3890$$

$$\lambda_{5,6} = 0.0021 \pm 0.1819i$$

$$\lambda_7 = 0.0222$$

$$\lambda_8 = -0.0213$$

There is a positive complex conjugate couple and a real positive root in the eigenvalues of the new system. These eigenvalues belong to the slower states of the helicopter such as linear velocities u, v, w.

4.3.2.3 Inner loop controller design using truncated system state feedback control method

In order to design a controller using truncated system state feedback control method number of states should be equal to number of controls. Therefore related to body angular rates are selected together with the associated input vector are selected.

$$x = \begin{bmatrix} w & q & p & r \end{bmatrix}^T \tag{4.19}$$

$$u = \begin{bmatrix} \delta_c & \delta_e & \delta_a & \delta_p \end{bmatrix}^T \tag{4.20}$$

Then the truncated system, input and output measurement matrices are:

$$A = \begin{bmatrix} -0.3883 & -0.0014 & 0.0009 & 0 \\ -0.0018 & -0.0008 & 0.0004 & 0 \\ -0.0077 & -0.0019 & -0.0138 & 0.0781 \\ 0.0216 & -0.0002 & 0.0141 & -0.1201 \end{bmatrix} \tag{4.21}$$

$$B = \begin{bmatrix} -356.0544 & 0 & -0.0001 & -0.0001 \\ -1.6727 & 3.6569 & -0.0077 & 0 \\ -1.3604 & -0.0402 & 20.9928 & 3.2650 \\ -1.9484 & -0.0050 & -0.3666 & -5.0247 \end{bmatrix} \tag{4.22}$$

$$C = \begin{bmatrix} 1 & 0 & 0 & 0 \\ 0 & 1 & 0 & 0 \\ 0 & 0 & 1 & 0 \\ 0 & 0 & 0 & 1 \end{bmatrix} \tag{4.23}$$

The truncated system has the following eigenvalues:

$$\lambda_1 = -0.3883 \tag{4.24}$$

$$\lambda_2 = -0.1297$$

$$\lambda_3 = -0.0040$$

$$\lambda_4 = -0.0010$$

Desired state matrix is selected such as:

$$A_{desired} = \begin{bmatrix} -15 & 3 & -3 & 3 \\ 3 & -8 & -3 & 1 \\ -3 & -3 & -12 & 0 \\ 3 & 1 & 0 & -3 \end{bmatrix} \tag{4.25}$$

Then the state feedback gain matrix is calculated as:

$$K = \begin{bmatrix} -0.0410 & 0.0084 & -0.0084 & 0.0084 \\ -0.8395 & 2.1915 & 0.8178 & -0.2694 \\ 0.0440 & 0.1188 & 0.5786 & 0.0944 \\ 0.6063 & 0.1849 & -0.0426 & -0.5830 \end{bmatrix} \tag{4.26}$$

The new eigenvalues of the truncated state matrix are obtained such as:

$$\lambda_1 = -17.4443 \tag{4.27}$$

$$\lambda_2 = -13.2479$$

$$\lambda_3 = -1.4757$$

$$\lambda_4 = -5.8321$$

The new eigenvalues of the full state matrix become:

$$\lambda_1 = -17.4766 \tag{4.28}$$

$$\lambda_2 = -13.2497$$

$$\lambda_3 = -5.7902$$

$$\lambda_4 = -1.4509$$

$$\lambda_{5,6} = -0.0270 \pm 0.4519i$$

$$\lambda_{7,8} = 0.0048 \pm 0.0244i$$

From the above eigenvalues, it may be observed that the system is still unstable because there is an unstable complex conjugate pair close to the origin. The unstable complex conjugate root observed in full state matrix belongs to the slower states of the helicopter like linear velocity. It should be dedicated that the helicopter with this feedback is much easier to fly than the original helicopter.

4.3.2.4 Simulation results with inner loop classical controller

As it is observed from the plots, helicopter total forces and moments are zero that is helicopter conserves it's trim condition. Before implementing inner loop control model, forces and moments started to diverge by a small amount after about five seconds. By the help of inner loop controller system stability is achieved and helicopter stays in trim condition.

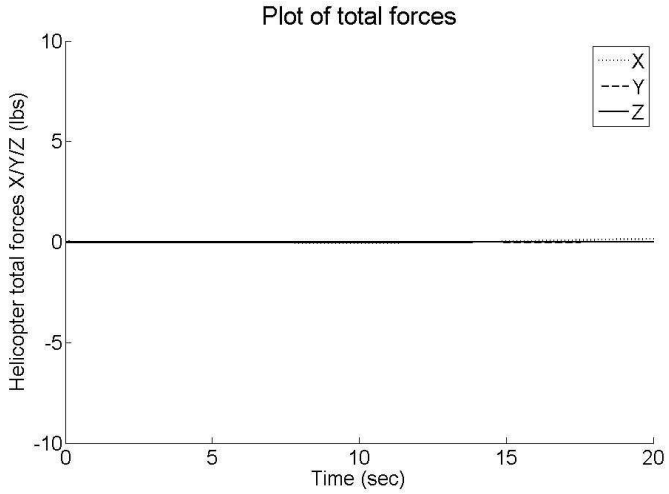

Figure 4.23: Forces during 100ft hover trim condition with inner loop controller

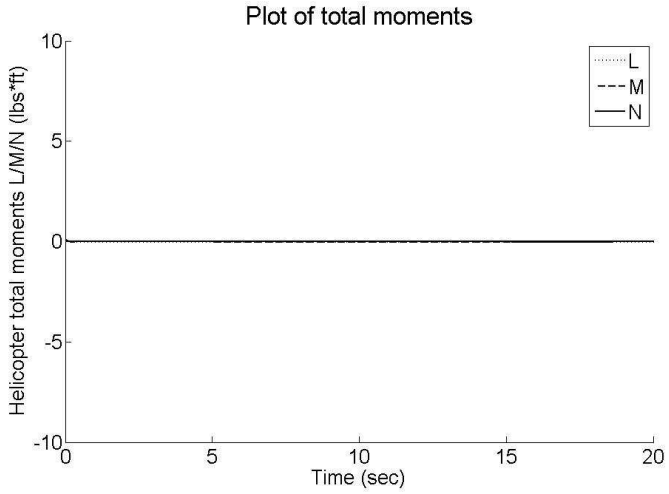

Figure 4.24: Moments during 100ft hover trim condition with inner loop controller

Because the total forces and moments on the helicopter are zero, accelerations are zero as expected.

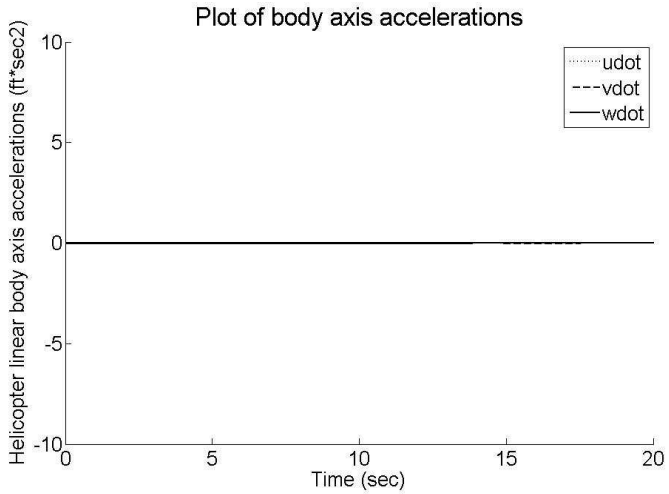

Figure 4.25: Body axis accelerations during 100ft hover trim condition with inner loop controller

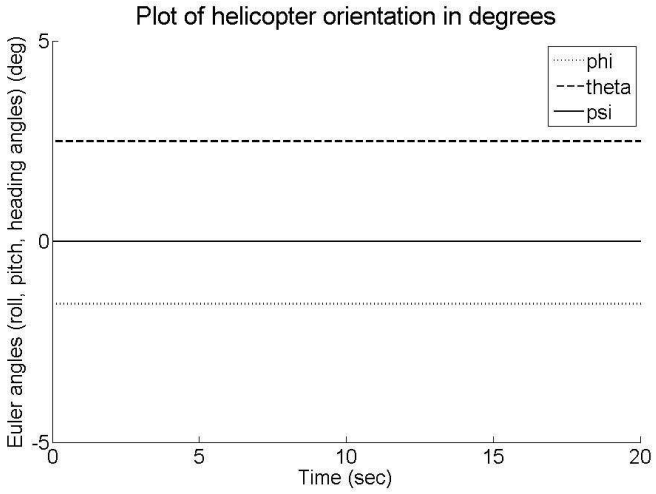

Figure 4.26: Euler angles during 100ft hover trim condition with inner loop controller

Helicopter orientation and positions with respect to the NED frame are fixed to the trim condition by the help of inner loop controller.

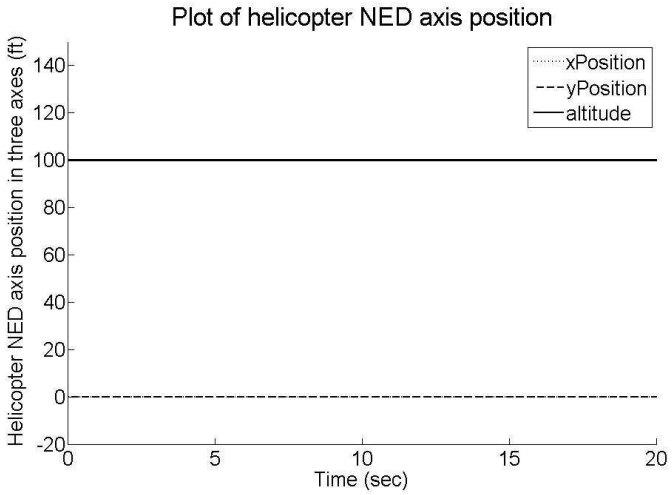

Figure 4.27: Positions with respect to the NED during 100ft hover trim condition with inner loop controller

4.3.3 Simulation results with disturbance to initial states to helicopter model with inner loop controller

In this part disturbance to body angular rates will be introduced to the helicopter originally at trim in order to examine the behavior of the helicopter.

4.3.3.1 Response to initial roll rate

In this section 0.01 rad/sec disturbance is given to the roll angular rate in 100 ft hover trim condition. Trim state plots for this condition are given below:

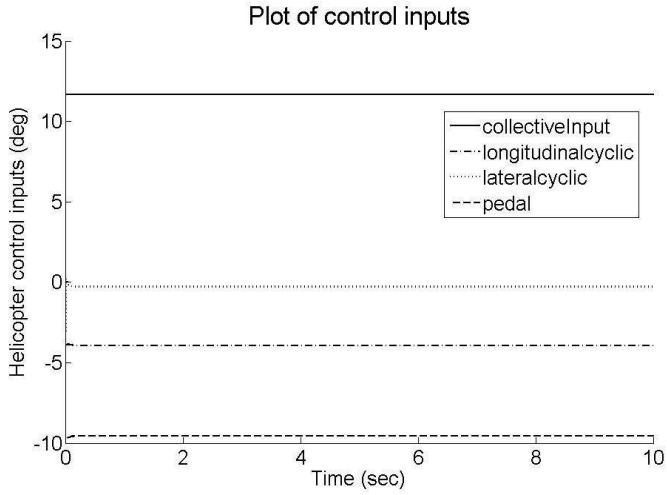

Figure 4.28: Control inputs for disturbed hover trim condition

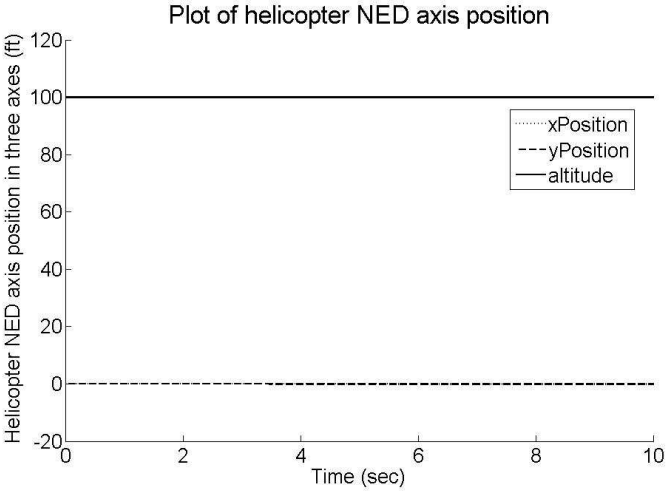

Figure 4.29: Positions during disturbed hover trim simulation

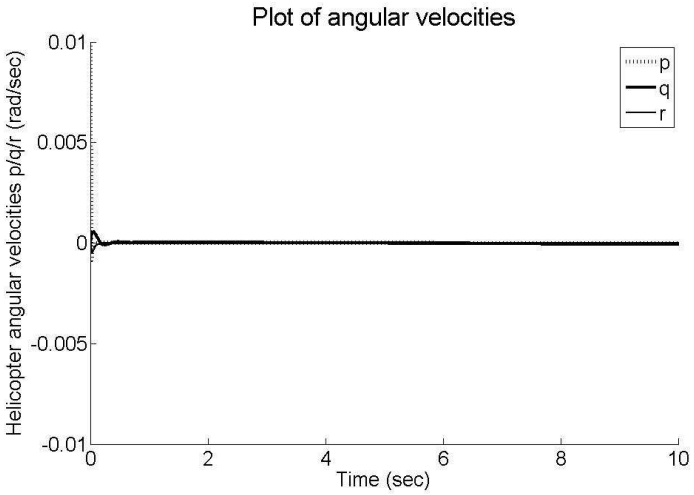

Figure 4.30: Angular rates for disturbed hover trim simulation

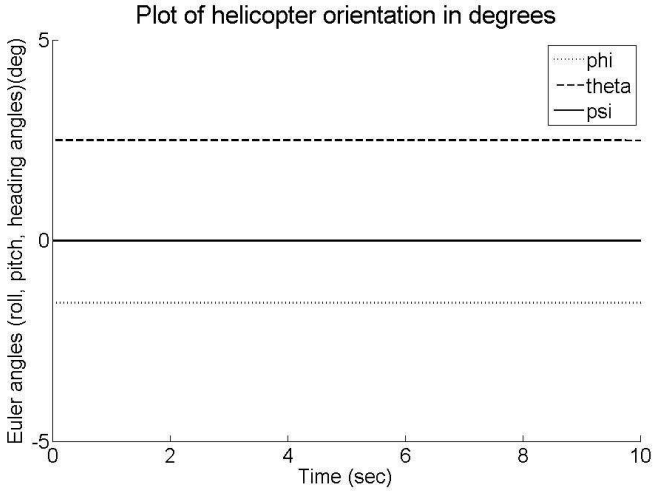

Figure 4.31: Helicopter orientation for disturbed hover trim simulation

As it is observed from the graphs by the help of inner loop control model helicopter model is stabilized although a disturbance is given to the helicopter trim states.

4.3.3.2 Response to initial pitch rate

In 100 ft hover trim condition an initial pitch angular rate of 0.01 rad/sec is introduced to the simulation. Trim state plots for this condition are given below:

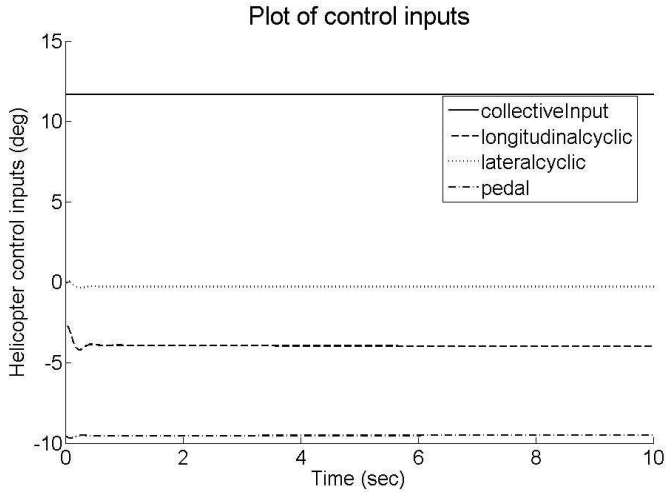

Figure 4.32: Control inputs for disturbed hover trim condition

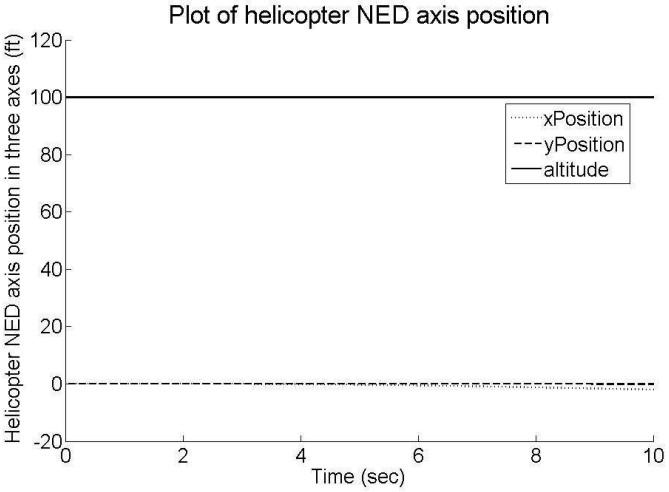

Figure 4.33: Control inputs for disturbed hover trim condition

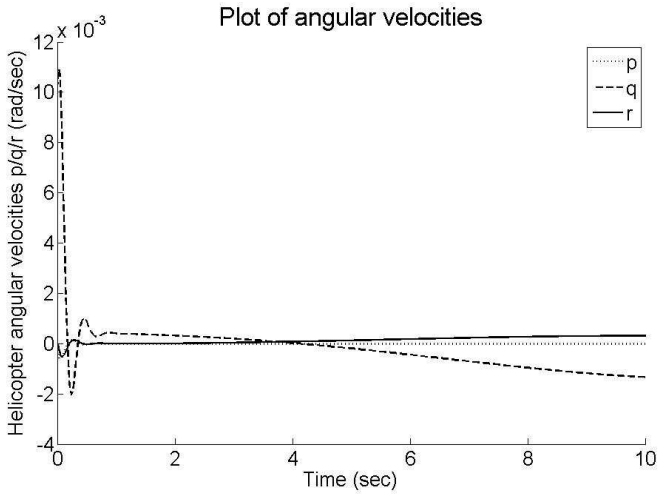

Figure 4.34: Angular rates for disturbed hover trim condition

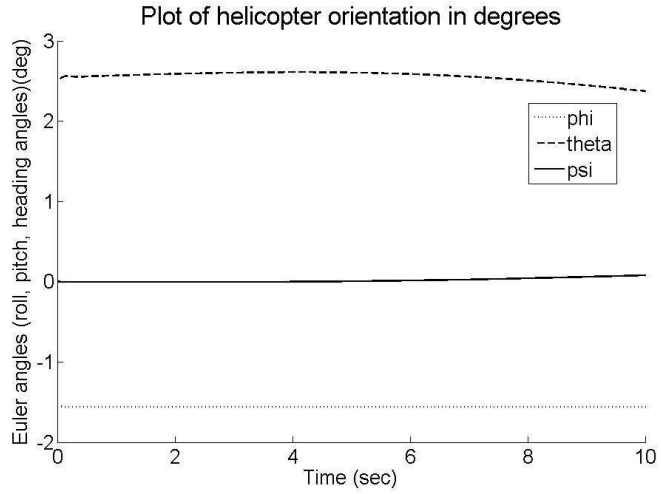

Figure 4.35: Helicopter orientation for disturbed hover trim condition

As it is observed from the graphs by the help of inner loop control model helicopter model is stabilized although a disturbance is given to the helicopter trim states.

4.3.3.3 Response to initial yaw rate

In 100 ft hover trim condition an initial yaw angular rate of 0.01 rad/sec is introduced to the simulation. Trim state plots for this condition are given below:

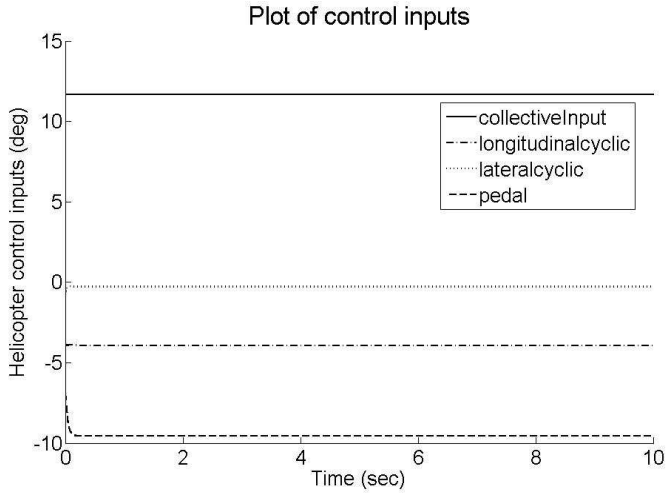

Figure 4.36: Control inputs for disturbed hover trim condition

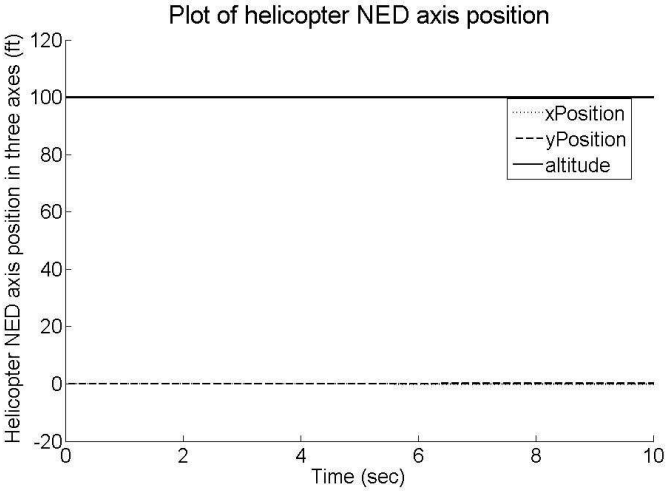

Figure 4.37: Control inputs for disturbed hover trim condition

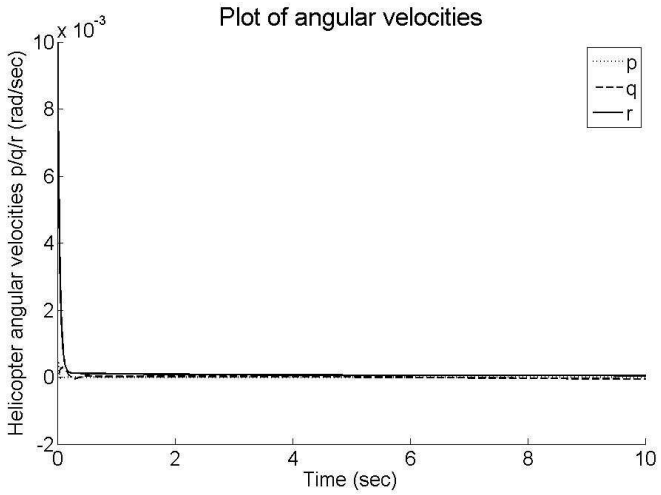

Figure 4.38: Angular rates for disturbed hover trim condition

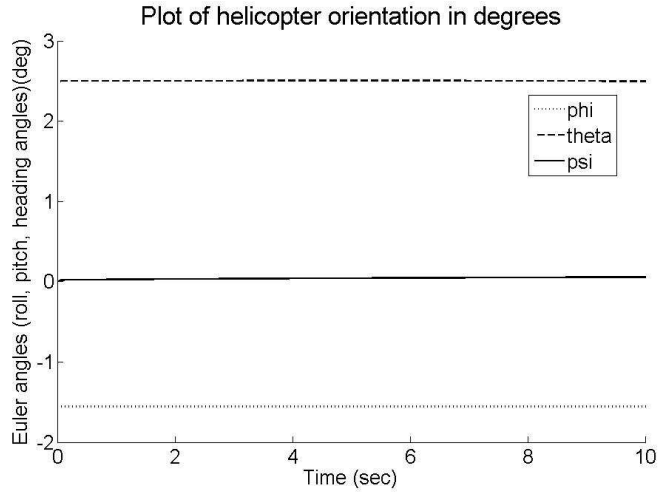

Figure 4.39: Helicopter orientation for disturbed hover trim condition

As it is observed from the graphs by the help of inner loop control model helicopter model is stabilized although a disturbance is given to the helicopter trim states.

4.3.4 Outer loop controller design

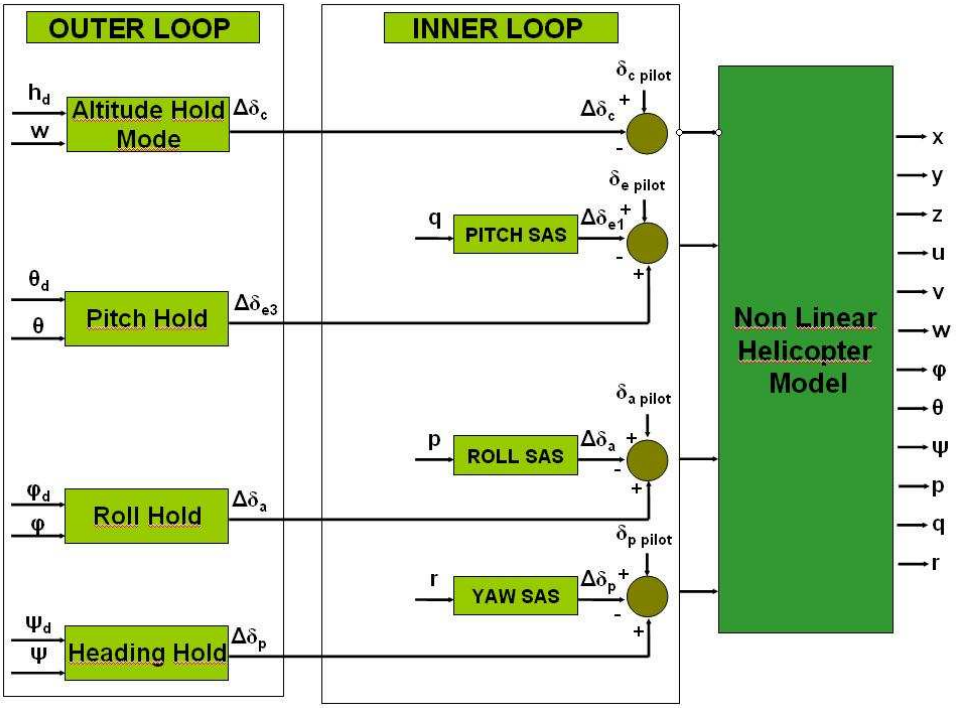

Figure 4.40: Helicopter model with outer loop controller

As it is mentioned before sequential loop closing method is used in order to design a linear controller for the helicopter. After the implementation of inner loop controller, new state space representation is obtained by linearizing the new model. In this part states include heading angle because related transfer function for the heading hold mode is needed. Therefore helicopter states are increased to nine and because of heading angle state there will be a zero valued pole caused by rigid body mode of the heading.

New eigenvalues of the helicopter model with inner loop feedback using classical control method:

$$\lambda_1 = 0 \tag{4.29}$$

$$\lambda_2 = -170.3472$$

$$\lambda_3 = -24.3099$$

$$\lambda_4 = -7.2624$$

$$\lambda_5 = -0.3890$$

$$\lambda_{6,7} = 0.0021 \pm 0.1819i$$

$$\lambda_8 = 0.0222$$

$$\lambda_9 = -0.0213$$

4.3.4.1 Pitch hold mode

The aim of pitch hold mode is adding a commanded input to the pilot control input that will help helicopter to repose to the desired pitch attitude from the actual pitch attitude value. First related transfer function of pitch attitude vs longitudinal cyclic control input is obtained.

$$\frac{\theta}{\delta_e} = \frac{numerator}{denominator} \tag{4.30}$$

$$numerator = 0.0037s^7 + 4.334s^6 + 707.3s^5 +$$

$$1.492e004s^4 + 5686s^3 - 6.649s^2 - 2.383s - 0.0005242$$

$$denominator = s^8 + 198s^7 + 5493s^6 + 3.138e004s^5 + 1.142e004s^4$$

$$+982s^3 + 374.9s^2 - 0.5743s - 0.1655$$

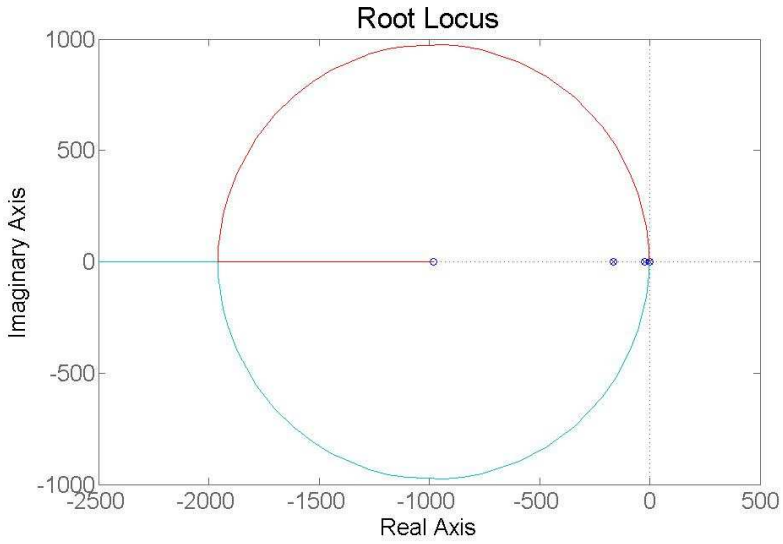

Figure 4.41: Root locus plot of pitch attitude

Then a feedback gain is selected from the root locus plot.

Block diagram of pitch hold mode:

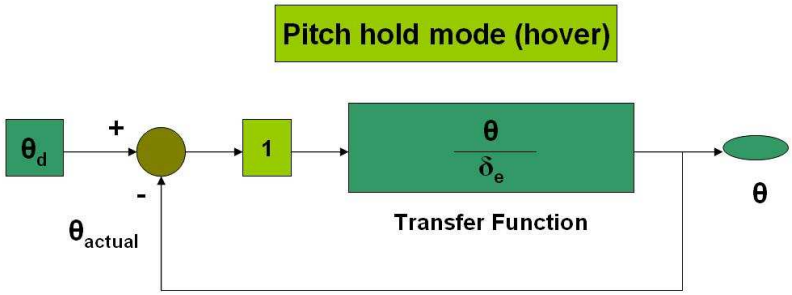

Figure 4.42: Pitch hold mode block diagram

4.3.4.2 Roll hold mode

Related transfer function of roll attitude vs lateral cyclic control input is obtained such as:

$$\frac{\phi}{\delta_a} = \frac{numerator}{denominator} \tag{4.31}$$

$$numerator = 0.021s^7 + 17.24s^6 + 534.3s^5 + 3134s^4 +$$

$$1142s^3 + 99.73s^2 + 37.98s - 0.003519$$

$$denominator = s^8 + 198s^7 + 5493s^6 + 3.138e004s^5 +$$

$$1.142e004s^4 + 982s^3 + 374.9s^2 - 0.5743s - 0.1655$$

Again a sample feedback is implemented to the system in order to acquire and hold desired 0 degree roll attitude.

Block diagram of roll hold mode:

4.3.4.3 Heading hold mode

The aim of heading hold mode is adding a commanded input to the pilot control input that will help helicopter to zero the helicopter heading attitude. Therefore First related transfer

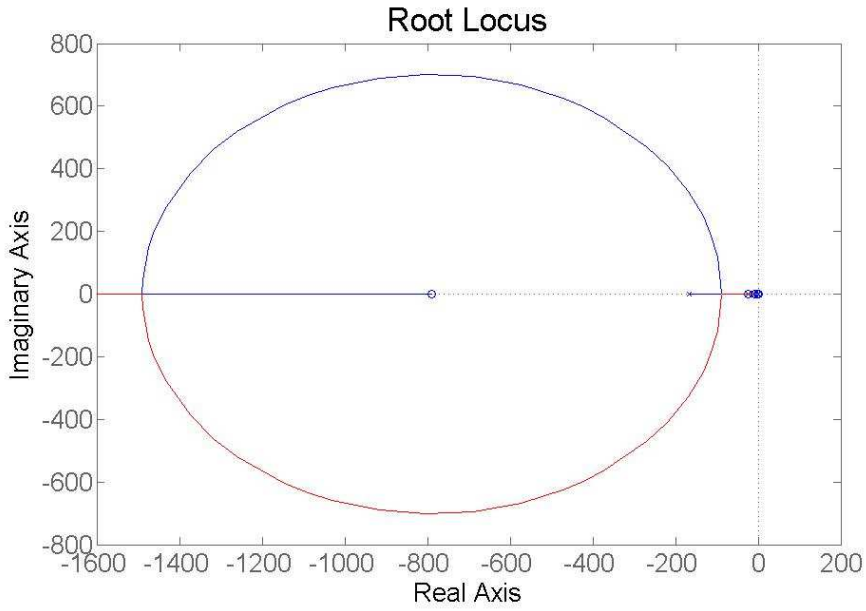

Figure 4.43: Root locus plot of roll attitude

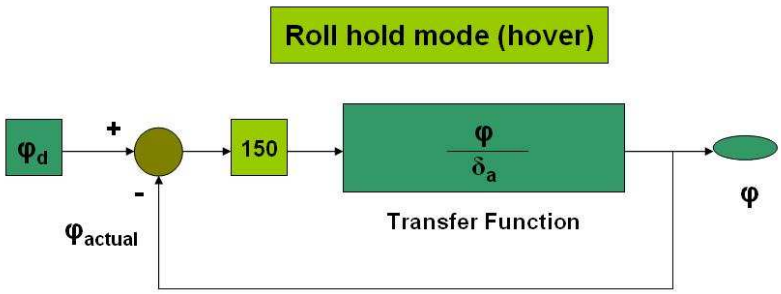

Figure 4.44: Roll hold mode block diagram

function of heading attitude vs pedal control input is obtained.

$$\frac{\psi}{\delta_p} = \frac{numerator}{denaminator} \tag{4.32}$$

$$numerator = -0.005s^8 - 5.746s^7 - 847s^6 - 6158s^5$$

$$-2266s^4 - 193.1s^3 - 74.72s^2 + 0.03943s + 0.009292$$

$$denominator = s^9 + 198s^8 + 5493s^7 + 3.138e004s^6 + 1.142e004s^5$$

$$+982s^4 + 374.9s^3 - 0.5743s^2 - 0.1655s$$

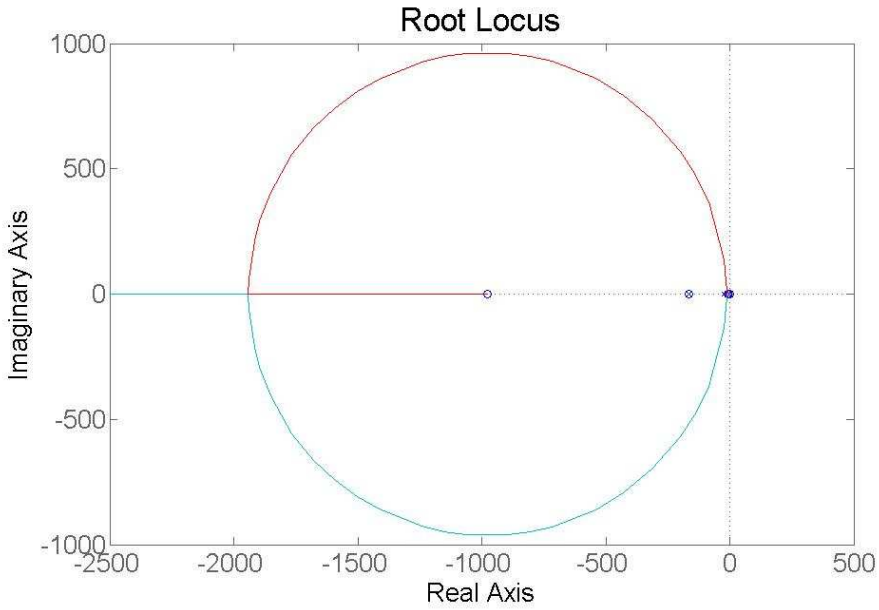

Figure 4.45: Complementary root locus plot of heading attitude

A lead compensator is designed for this mode.

Block diagram of heading hold mode:

4.3.4.4 Altitude acquire and hold mode

The aim of altitude acquire and hold mode is adding a feedback pilot control input that will help helicopter to repose to the desired altitude from the actual altitude. The related transfer function of vertical velocity vs collective control input is:

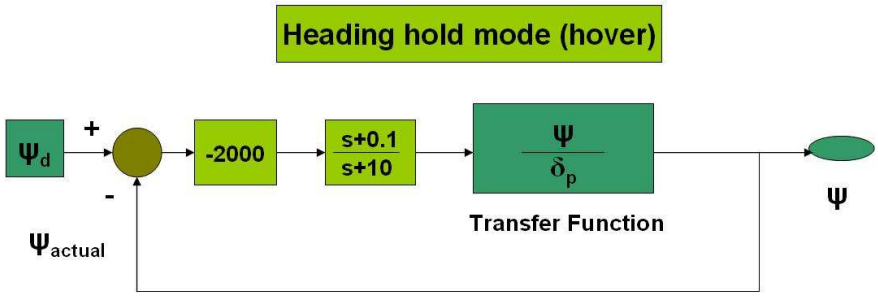

Figure 4.46: Heading hold mode block diagram

$$\frac{w}{\delta_c} = \frac{numerator}{denominator} \tag{4.33}$$

Where,

$$numerator = -356.1s^7 - 7.035e004s^6 - 1.928e006s^5 - 1.042e007s^4$$

$$-4725s^3 - 3.433e005s^2 + 179s + 182.1$$

$$denominator = s^8 + 198s^7 + 5493s^6 + 3.138e004s^5 +$$

$$1.142e004s^4 + 982s^3 + 374.9s^2 - 0.5743s - 0.1655$$

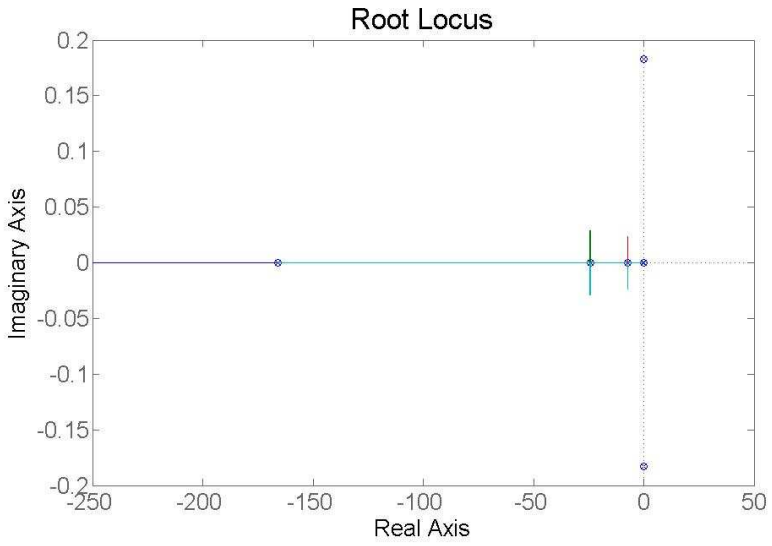

Figure 4.47: Complementary root locus plot of vertical speed

By considering the root locus plot a lead compensator is designed. Desired altitude is selected as 1000 ft and actual altitude is 100 ft.

Block diagram of altitude acquire and hold mode:

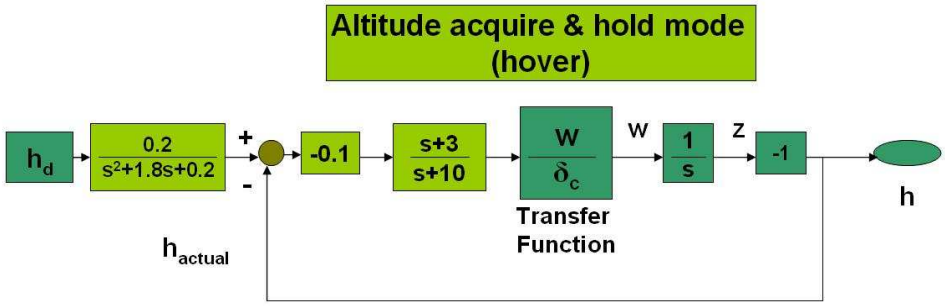

Figure 4.48: Altitude acquire and hold mode block diagram

In this mode a command shaping filter is added. First and second order filters are tested. It is found out that a second order pre-filter gives better results and hence used. By implementing altitude hold mode to the model together with pitch,roll and heading hold modes, desired altitude is acquired and hold for a long time. In these simulations desired pitch is a stepwise input equal to the trim pitch value. Roll and yaw references are set to zero degrees.

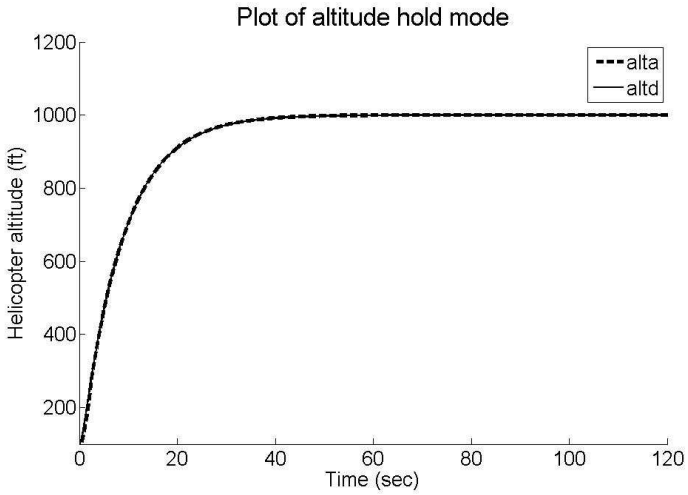

Figure 4.49: Altitude acquire and hold mode plot

Pitch hold mode, roll hold mode and heading hold modes are activated together with altitude acquire and hold mode. New eigenvalues of the helicopter model with outer loop feedback:

$$\lambda_{1,2} = -20.2179 \pm 49.9191i \tag{4.34}$$

$$\lambda_3 = -6.7304$$

$$\lambda_{4,5} = 0.3929 \pm 0.6816i$$

$$\lambda_6 = -0.0796$$

$$\lambda_7 = -0.7767$$

$$\lambda_{7,8} = -0.4480 \pm 0.0125i$$

When the eigenvalues of the new system with outer loop feedback is considered it is observed that there is a positive complex conjugate couple. This complex conjugate couple belongs to the uncontrolled helicopter states such as linear velocities.

Plot of pitch attitude is given below:

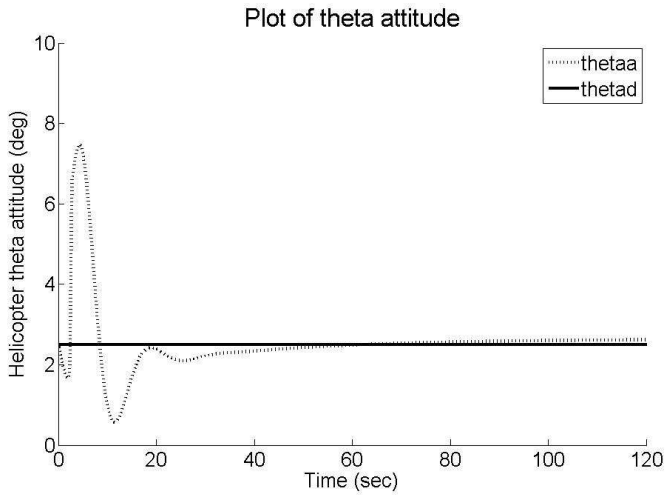

Figure 4.50: Actual and desired pitch attitude during Pitch attitude hold mode engaged

Plot of roll attitude is given below:

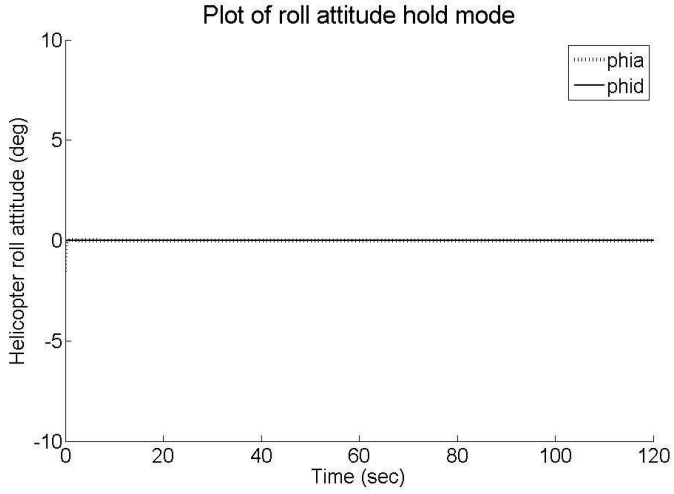

Figure 4.51: Actual and desired roll attitude during Roll attitude hold mode engaged

Plot of heading attitude is given below:

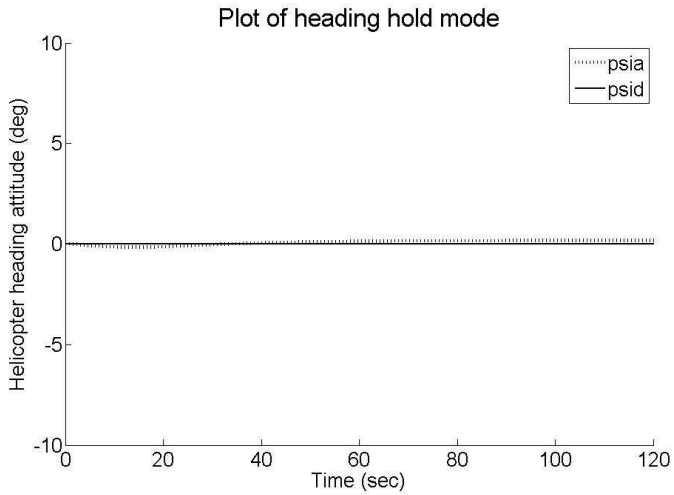

Figure 4.52: Actual and desired heading attitude during Heading attitude hold mode engaged

The controls during these flight simulations are given in figure 4.53. As it may be observed from these figures outer loop controls are quite effective.

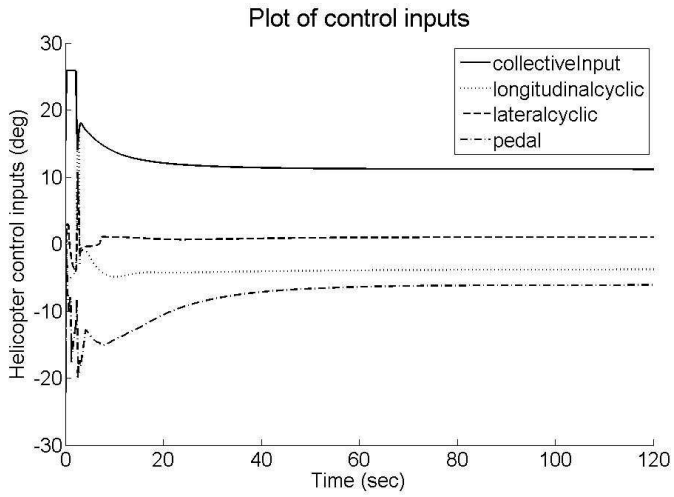

Figure 4.53: Control inputs

4.3.5 Response with outer loop control at 100 ft hover trim

In this part simulation results to out of trim initial conditions will be examined. In these simulations both inner and outer loop controls are active. This procedure is performed in order to check if the outer loop control model will stabilize the nonlinear helicopter model.

4.3.5.1 Response to initial roll angle during altitude acquire and hold mode

In 100 ft hover condition initial trim value for roll Euler angle is -1.55 degree but with 1 degree in roll attitude the simulation is initiated from -0.55 degree. By the given response to the roll Euler angle, it will be checked if helicopter stability is maintained and the desired altitude is acquired and hold. From the plots given below helicopter simulation results will be observed:

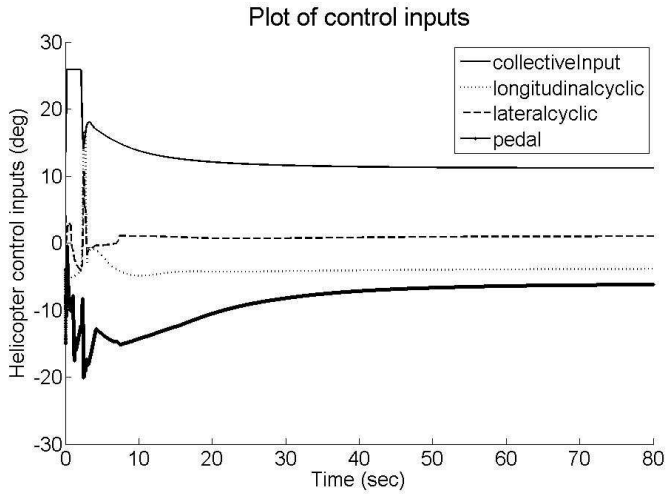

Figure 4.54: Helicopter control inputs for disturbed hover trim condition

As it is observed from the plots, outer loop control model stabilizes the helicopter and acquires the desired altitude even the simulation is initiated from disturbed trim states. The peak observed in pitch Euler angle is not related to the given disturbance. Outer loop control is active and pitch Euler attitude tends to change while helicopter acquires the desired altitude. Peaks observed in control inputs is related with commanded inputs to the controls caused by outer loop controls.

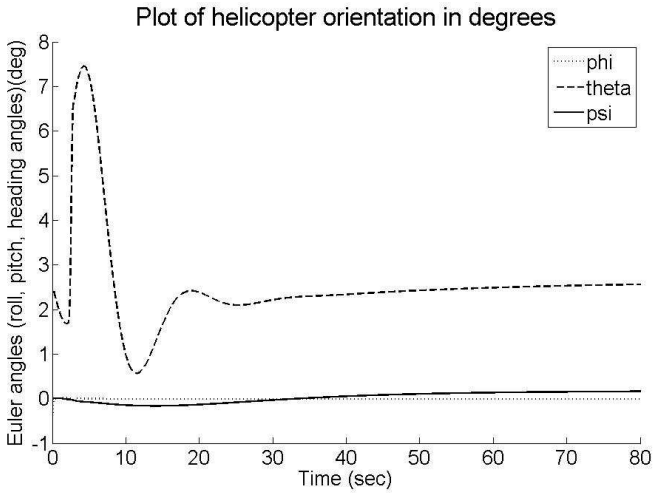

Figure 4.55: Helicopter orientation for disturbed hover trim condition

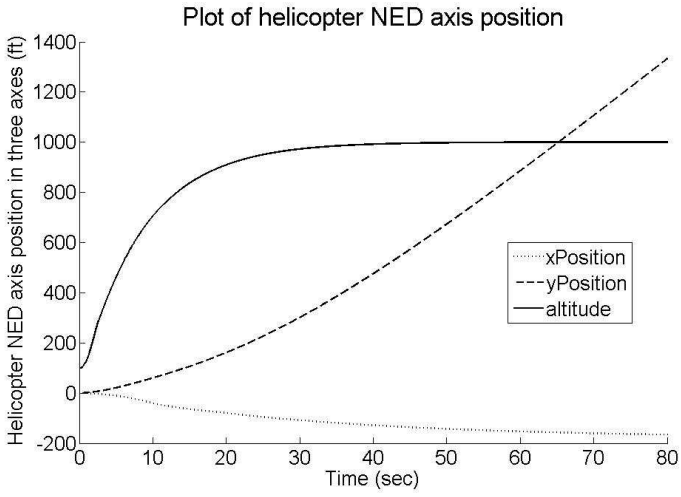

Figure 4.56: Helicopter position with respect to NED axis for disturbed hover trim condition

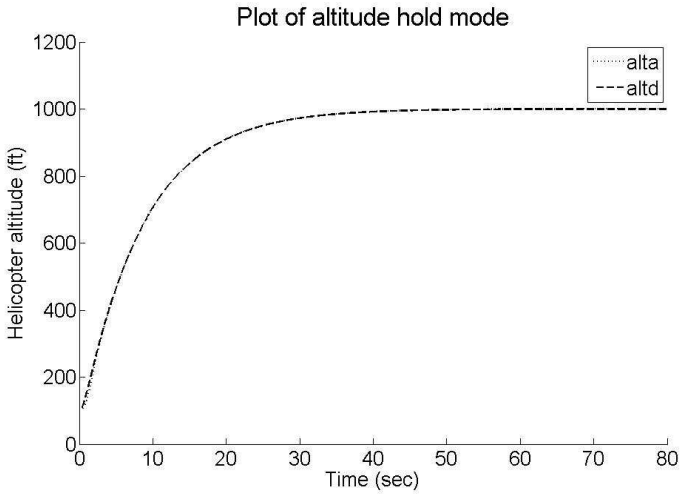

Figure 4.57: Altitude when the simulation is started from the disturbed hover trim condition

4.3.5.2 Response to initial pitch angle during altitude acquire and hold mode

In 100 ft hover condition initial trim value for pitch Euler angle is 2.5 degree but 1 degree pitch error is given to the trim flight conditions and the pitch attitude is started at 3.5 degree. From the plots given below helicopter simulation results will be observed:

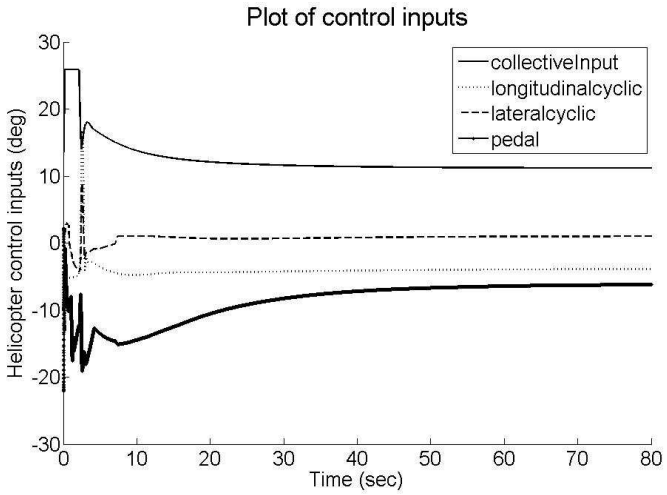

Figure 4.58: Helicopter control inputs for disturbed hover trim condition

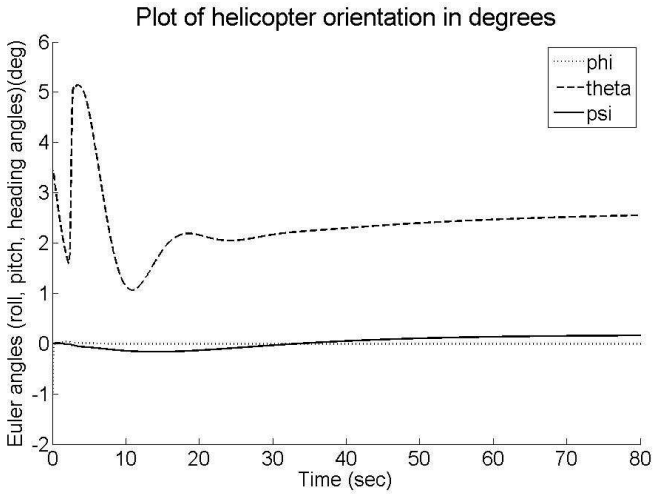

Figure 4.59: Helicopter orientation for disturbed hover trim condition

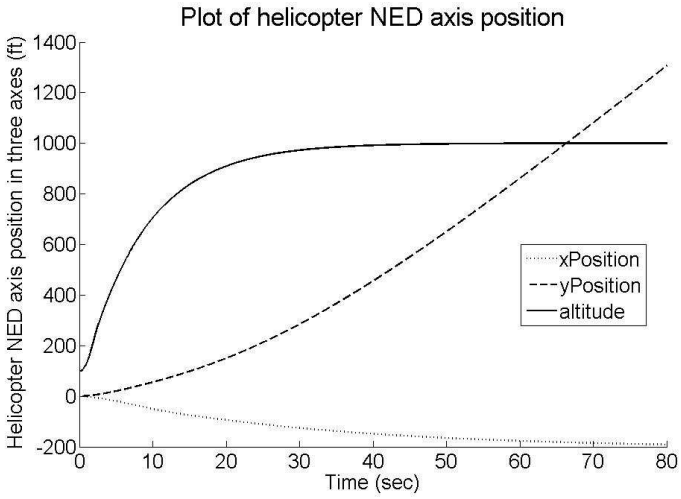

Figure 4.60: Helicopter position with respect to NED axis for disturbed hover trim condition

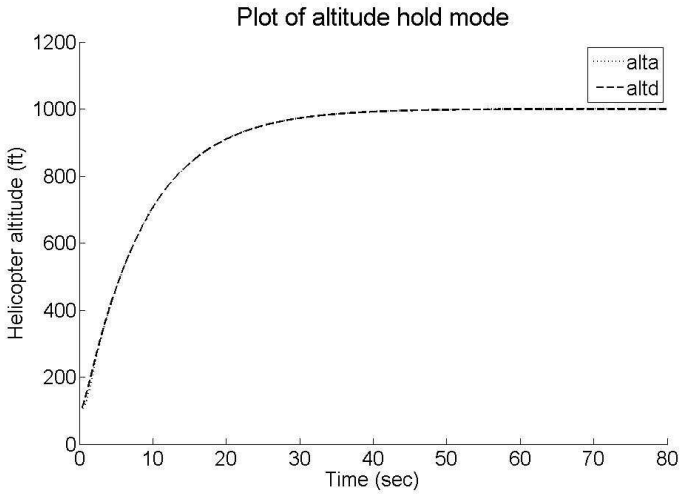

Figure 4.61: Altitude hold mode for disturbed hover trim condition

As it is observed from the plots, outer loop control model stabilizes the helicopter and acquires the desired altitude even the simulation is initiated from disturbed trim states. The peak observed in pitch Euler angle is not related to the given disturbance. Outer loop control is active and pitch Euler attitude tends to change while helicopter acquires the desired altitude. Peaks observed in control inputs is related with commanded inputs to the controls caused by outer loop controls.

4.4 AFCS design for forward flight

In this section first trim simulations will be given. Then, inner loop feedback system is designed and simulations are presented. Finally flight director modes are designed.

4.4.1 Helicopter simulation results for 100 ft 60 knot forward flight condition in trim mode

In this part trim flight simulation results at 100 ft altitude 60 knot forward speed are given. Thus, all the inputs and initial states are taken from the trim calculations. Normally helicopter shall stay at this condition. However, due to the instability inherent in the system the simulation starts to diverge as will be seen in the following plots.

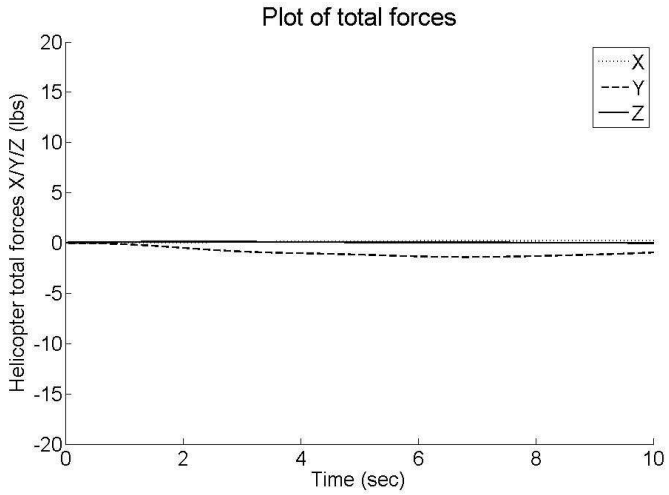

Figure 4.62: Total forces on helicopter during trim flight condition at 100 ft altitude 60 knots forward flight

In trim condition total forces and moments acting on the helicopter should be zero. As it is observed from the graphs, total forces and moments in three axis are almost zero. However Y axis force and yawing moment (N) starts to diverge after a while. This divergence will cause instability if the helicopter stays in trim without any AFCS control for a longer time. By the help of AFCS model these instability problems will be solved.

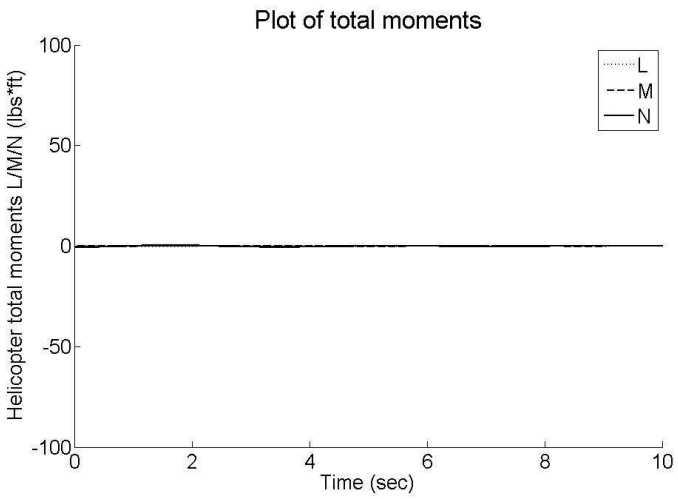

Figure 4.63: Total moments on helicopter during trim flight condition at 100 ft altitude 60 knots forward flight

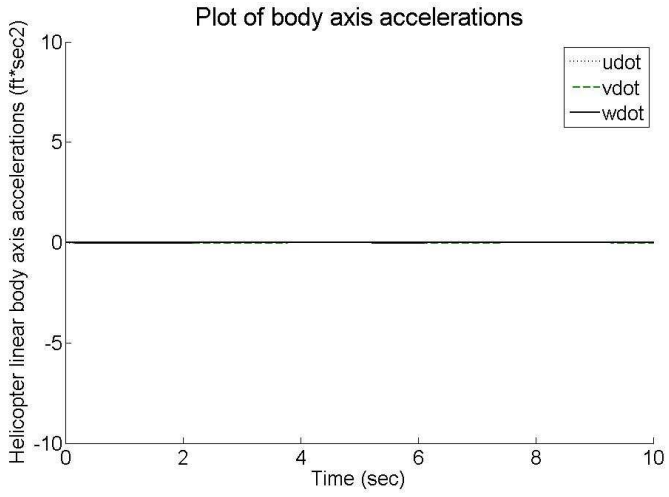

Figure 4.64: Body axis accelerations during trim flight condition at 100 ft altitude 60 knots forward flight

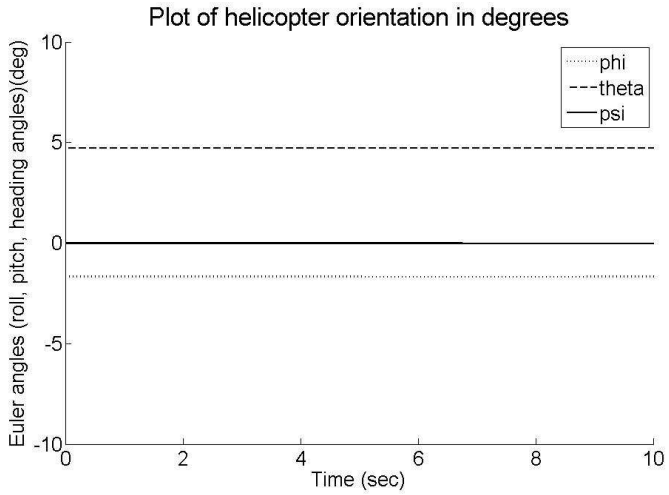

Figure 4.65: Euler angles during trim flight condition at 100 ft altitude 60 knots forward flight

4.4.2 Inner loop linear controller design for 100 ft 60 knots forward flight condition

In this section inner loop control model designs with classical control method and truncated system state feedback control method. First linearization results of uncontrolled model will be given. Then for each different design method new system will be linearized in order to analyze the stability of the new system.

4.4.2.1 Uncontrolled helicopter model linearization results

State matrix is obtained by considering positions, Euler angles, body axis velocities and body angular velocities. However position and heading angle states are neglected in order to remove rigid body modes of the system. State and control vectors are:

$$x = \begin{bmatrix} u & w & q & \theta & v & p & \phi & r \end{bmatrix}^T \tag{4.35}$$

$$u = \begin{bmatrix} \delta_e & \delta_c & \delta_a & \delta_p \end{bmatrix}^T \tag{4.36}$$

The state and input matrices are:

$$A = \begin{bmatrix} -0.0160 & 0.0915 & -0.0206 & -32.0900 & 0.0007 & 0.0000 & 0.0001 & -0.0010 \\ 0.0039 & -0.8922 & 100.7663 & -2.6529 & -0.0061 & 0.0010 & 0.9307 & 0.0006 \\ 0.0003 & -0.0367 & -0.1684 & 0.0001 & -0.0000 & 0.0004 & -0.0000 & 0.0000 \\ 0.0000 & -0.0000 & 0.9994 & 0 & 0.0000 & 0.0000 & 0.0000 & 0.0290 \\ -0.0104 & -0.0073 & -0.0005 & 0.0774 & -0.0533 & -0.0177 & 32.0751 & -100.1482 \\ 0.0046 & -0.0039 & -0.0023 & -0.0001 & -0.0201 & -0.0174 & -0.0006 & 0.4203 \\ 0.0000 & -0.0000 & -0.0024 & -0.0000 & -0.0000 & 1.0000 & -0.0000 & 0.0831 \\ 0.0063 & 0.0117 & 0.0008 & -0.0002 & 0.0255 & 0.0232 & 0.0008 & -0.5337 \end{bmatrix} \tag{4.37}$$

$$B = \begin{bmatrix} 0.0482 & 45.2161 & -0.0000 & 0.0000 \\ 0.5502 & -421.0382 & -0.0008 & -0.0000 \\ 3.6573 & -2.1475 & -0.0077 & 0.0000 \\ 0.0037 & -0.0022 & -0.0000 & -0.0001 \\ 0.0021 & 9.7798 & 5.7529 & 8.1212 \\ -0.0393 & 3.3956 & 20.8735 & 2.2974 \\ -0.0000 & 0.0033 & 0.0208 & 0.0020 \\ -0.0075 & -0.9866 & -0.6131 & -4.1237 \end{bmatrix} \tag{4.38}$$

Eigenvalues of the linearized A matrix are:

$$\lambda_{1,2} = -0.5423 \pm 1.8917i \tag{4.39}$$

$$\lambda_{3,4} = -0.1864 \pm 1.5693i$$

$$\lambda_{5,6} = 0.0538 \pm 0.0777i$$

$$\lambda_7 = -0.2063$$

$$\lambda_8 = -0.1150$$

From the above list an unstable complex conjugate pair is observed.

Longitudinal state and control vectors are:

$$x = \begin{bmatrix} u & w & q & \theta \end{bmatrix}^T \tag{4.40}$$

$$u = \begin{bmatrix} \delta_c & \delta_e \end{bmatrix}^T \tag{4.41}$$

Neglecting the coupling between the longitudinal and lateral states, longitudinal eigenvalues becomes:

$$\lambda_{1,2} = -0.5421 \pm 1.8917i \tag{4.42}$$

$$\lambda_{3,4} = 0.0038 \pm 0.0252i$$

It is observed that there is an unstable complex conjugate couple in the longitudinal eigenvalues. To stabilize the longitudinal models a proportional feedback control or a lead compensator over pitch rate may be considered. Related transfer function and root locus plot is:

$$\frac{q}{\delta_e} = \frac{3.657s^3 + 3.301s^2 + 0.05093s - 9.286e - 006}{s^4 + 1.077s^3 + 3.865s^2 - 0.02902s + 0.002508} \tag{4.43}$$

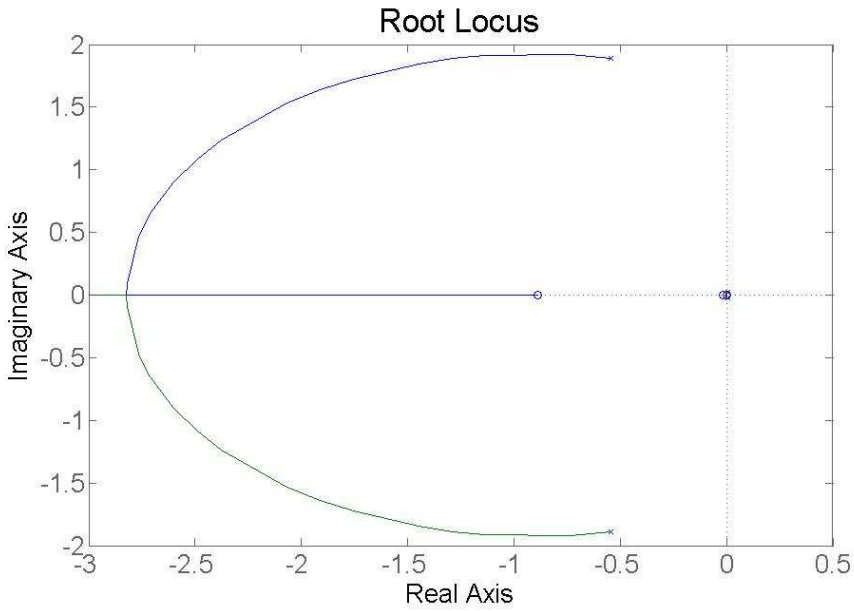

Figure 4.66: Pitch rate root locus plot

Lateral state and control vectors are:

$$x = \begin{bmatrix} v & p & \phi & r \end{bmatrix}^T \tag{4.44}$$

$$u = \begin{bmatrix} \delta_a & \delta_p \end{bmatrix}^T \tag{4.45}$$

Eigenvalues of the linearized lateral state matrix are:

$$\lambda_{1,2} = -0.1872 \pm 1.5689i \tag{4.46}$$

$$\lambda_3 = -0.2296$$

$$\lambda_4 = -0.0005$$

It is observed that lateral modes of the system are already stable. In order to further improve the stability of the lateral modes a proportional feedback control can be considered however, for large gains system may be unstable. Therefore lead compensator may be designed to stabilize the system.

Related transfer functions and root locus plots are:

Roll Angular rate:

$$\frac{p}{\delta_a} = \frac{20.87s^3 + 11.88s^2 + 52.64s - 1.386}{s^4 + 0.6044s^3 + 2.583s^2 + 0.5745s + 0.0002931} \tag{4.47}$$

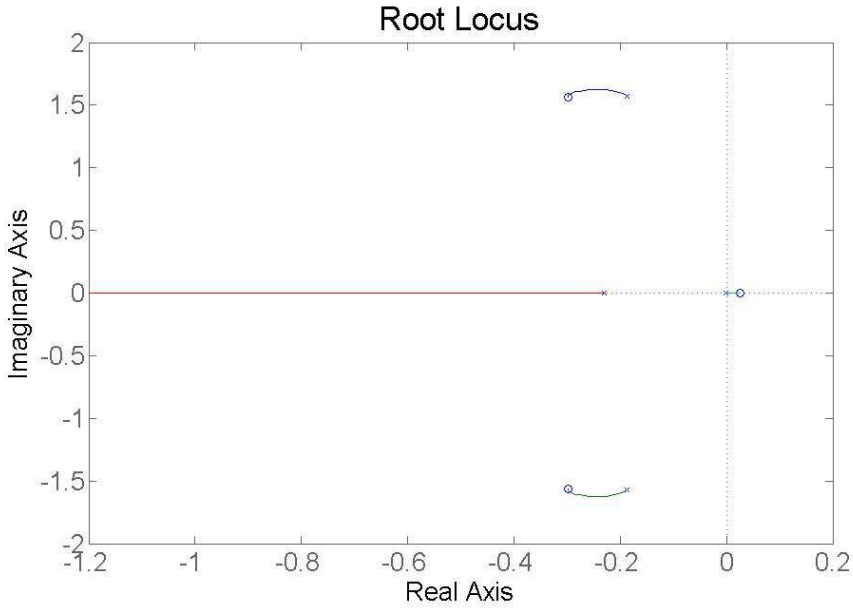

Figure 4.67: Roll rate root locus plot

Yaw angular rate:

$$\frac{r}{\delta_p} = \frac{-4.124s^3 - 0.03115s^2 + 0.0002625s - 0.7796}{s^4 + 0.6044s^3 + 2.583s^2 + 0.5745s + 0.0002931} \tag{4.48}$$

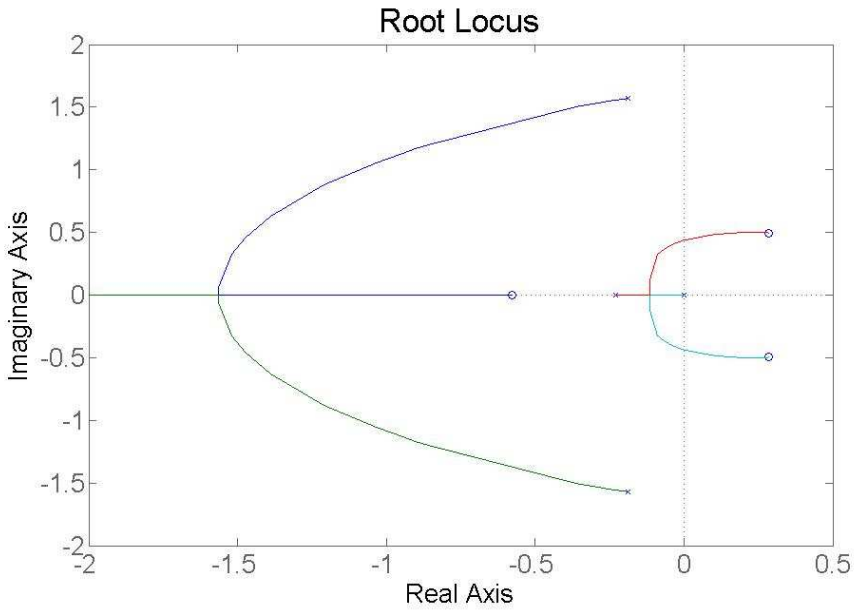

Figure 4.68: Yaw rate complementary root locus plot

4.4.2.2 Inner loop controller design using classical control method

Helicopter inner loop AFCS is designed using root locus method. By considering the longitudinal and lateral eigenvalues together with root locus plots necessary gains and lead compensator parameters are selected. The aim is moving the unstable roots to the left half s-plane and increase the stability of the system.

Pitch SAS, Roll SAS and Yaw SAS are given in figures 4.69, 4.70, 4.71.

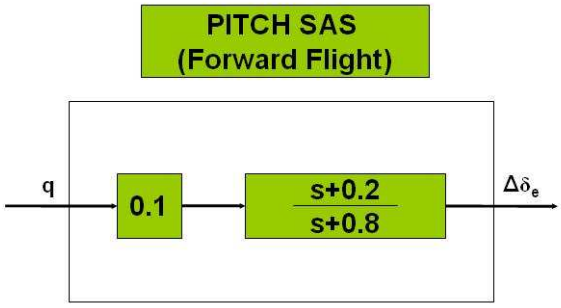

Figure 4.69: Pitch SAS

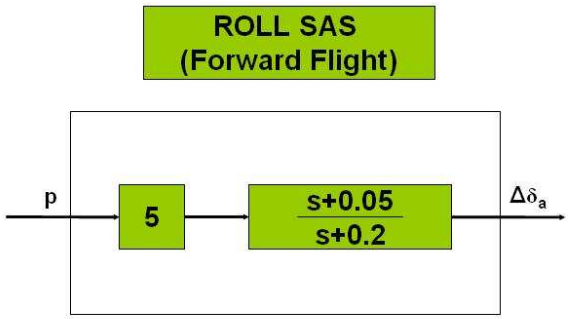

Figure 4.70: Roll SAS

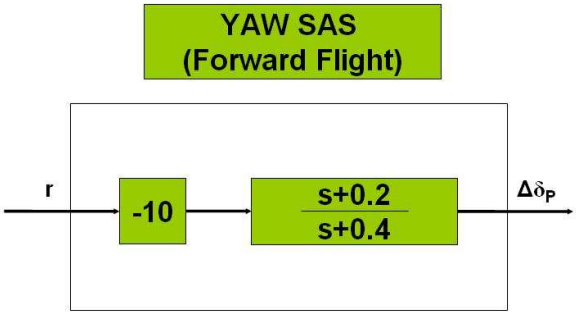

Figure 4.71: Yaw SAS

System matrix is obtained again by numerical linearization:

$$A = \begin{bmatrix} -0.0160 & 0.0915 & -0.0254 & -32.0900 & 0.0007 & -0.0000 & 0.0001 & -0.0009 \\ 0.0039 & -0.8922 & 100.7112 & -2.6529 & -0.0061 & 0.0048 & 0.9307 & 0.0002 \\ 0.0003 & -0.0367 & -0.5338 & 0.0001 & -0.0000 & 0.0351 & -0.0000 & 0.0008 \\ 0.0000 & -0.0000 & 0.9990 & 0.0000 & 0.0000 & 0.0001 & 0.0000 & 0.0278 \\ -0.0100 & -0.0063 & -0.0008 & 0.0775 & -0.0508 & -25.7162 & 32.0751 & -22.8117 \\ 0.0043 & -0.0033 & 0.0015 & -0.0001 & -0.0176 & -93.9626 & -0.0006 & 20.1792 \\ 0.0000 & -0.0000 & -0.0024 & -0.0000 & -0.0000 & 0.9012 & -0.0000 & 0.1011 \\ 0.0061 & 0.0112 & 0.0015 & -0.0002 & 0.0244 & 2.6656 & 0.0008 & -40.0090 \end{bmatrix} \tag{4.49}$$

Eigenvalues of the new system matrix are:

$$\lambda_1 = -94.9486 \tag{4.50}$$

$$\lambda_2 = -39.0104$$

$$\lambda_{3,4} = -0.7240 \pm 1.9179i$$

$$\lambda_{5,6} = -0.0515 \pm 0.0273i$$

$$\lambda_{7,8} = 0.0228 \pm 0.0295i$$

When the eigenvalues of the new system matrix is considered, it is observed that system is more stable than the uncontrolled system. The unstable complex conjugate couple belongs to the slower states of the helicopter such as linear velocities u,v and w.

4.4.2.3 Inner loop controller design using truncated system state feedback control method

In order to design a control model using truncated system state feedback control method the number of states should be equal to the number of controls. Therefore state matrix containing vertical velocity and body angular rates and control matrix containing collective control, longitudinal cyclic, lateral cyclic and pedal controls are chosen.

$$x = \begin{bmatrix} w & q & p & r \end{bmatrix}^T \tag{4.51}$$

$$u = \begin{bmatrix} \delta_c & \delta_e & \delta_a & \delta_p \end{bmatrix}^T \tag{4.52}$$

Then the truncated system, input and output measurement matrices are:

$$A = \begin{bmatrix} -0.8922 & 100.7663 & 0.0010 & 0.0006 \\ -0.0367 & -0.1684 & 0.0004 & 0 \\ -0.0039 & -0.0023 & -0.0174 & 0.4203 \\ 0.0117 & -0.0008 & 0.0232 & -0.5337 \end{bmatrix} \tag{4.53}$$

$$B = \begin{bmatrix} -421.0382 & 0.5502 & -0.0008 & 0 \\ -2.1475 & 3.6573 & -0.0077 & 0 \\ 3.3956 & -0.0393 & 20.8735 & 2.2974 \\ -0.9866 & -0.0075 & -0.6131 & -4.1237 \end{bmatrix} \tag{4.54}$$

$$C = \begin{bmatrix} 1 & 0 & 0 & 0 \\ 0 & 1 & 0 & 0 \\ 0 & 0 & 1 & 0 \\ 0 & 0 & 0 & 1 \end{bmatrix} \tag{4.55}$$

The truncated system has the following eigenvalues:

$$\lambda_{1,2} = -0.5303 \pm 1.8887i \tag{4.56}$$

$$\lambda_3 = -0.5520$$

$$\lambda_4 = 0.0009$$

Desired state matrix is selected such as:

$$A_{desired} = \begin{bmatrix} -15 & 3 & -3 & 3 \\ 3 & -8 & -3 & 1 \\ -3 & -3 & -12 & 0 \\ 3 & 1 & 0 & -3 \end{bmatrix} \tag{4.57}$$

Then the state feedback gain matrix is calculated as:

$$K = \begin{bmatrix} -0.0346 & -0.2296 & -0.0061 & 0.0068 \\ -0.8505 & 2.0069 & 0.8181 & -0.2693 \\ 0.0678 & 0.1550 & 0.5868 & 0.0859 \\ 0.7244 & 0.2705 & -0.0929 & -0.6120 \end{bmatrix} \tag{4.58}$$

The new eigenvalues of the truncated state matrix are obtained such as:

$$\lambda_1 = -17.4443 \tag{4.59}$$

$$\lambda_2 = -13.2479$$

$$\lambda_3 = -1.4757$$

$$\lambda_4 = -5.8321$$

The new eigenvalues of the full state matrix are obtained such as:

$$\lambda_1 = -17.4706 \tag{4.60}$$

$$\lambda_2 = -13.2704$$

$$\lambda_3 = -5.6954$$

$$\lambda_{4,5} = -0.7152 \pm 0.4519i$$

$$\lambda_6 = -0.2675$$

$$\lambda_{7,8} = 0.0325 \pm 0.1066i$$

From the above eigenvalues, it may be observed that the system is still unstable because there is an unstable complex conjugate pair. However, when the eigenvalues of the new truncated system are considered, it is observed that the new system is stable. The unstable complex conjugate root observed in full state matrix belongs to the slower states of the helicopter like linear velocities u,v and w. By implementing the truncated system state feedback controller system, angular rates and vertical velocity are stabilized.

4.4.2.4 Simulation results for inner loop control model designed using classical control method

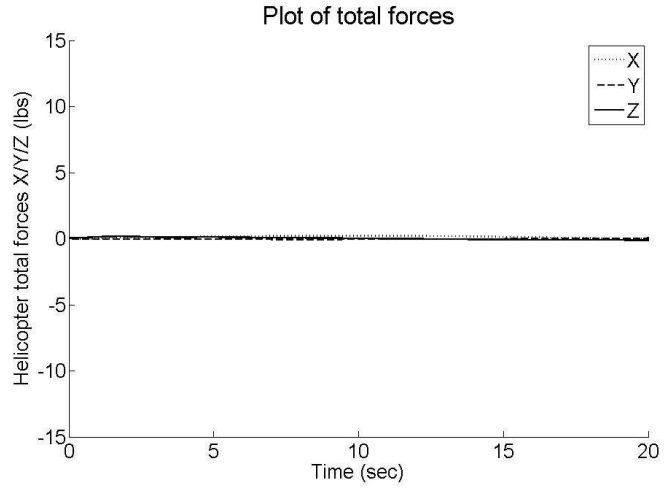

Figure 4.72: Forces for 100 ft 60 knot forward flight condition with inner loop controller

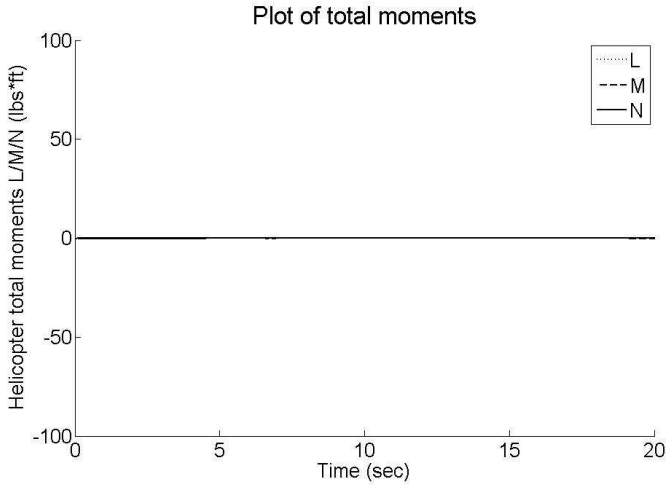

Figure 4.73: Moments for 100 ft 60 knot forward flight condition with inner loop controller

As it is observed from the plots, helicopter total forces and moments are zero that is helicopter conserves it's trim condition. Before implementing inner loop control model, forces and moments started to diverge in a small amount after a while. By the help of inner loop control model system stability is achieved and helicopter stays in trim condition for a longer duration.

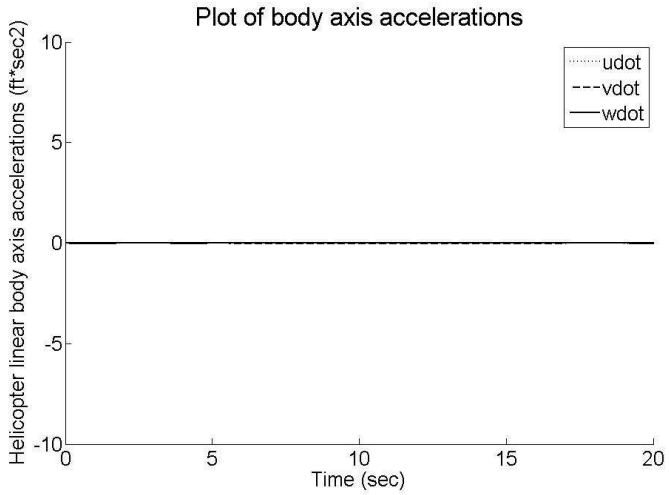

Figure 4.74: Body axis accelerations for 100 ft 60 knot forward flight with inner loop controller

Because the total forces and moments on the helicopter are zero, accelerations are zero as it should be for trim condition.

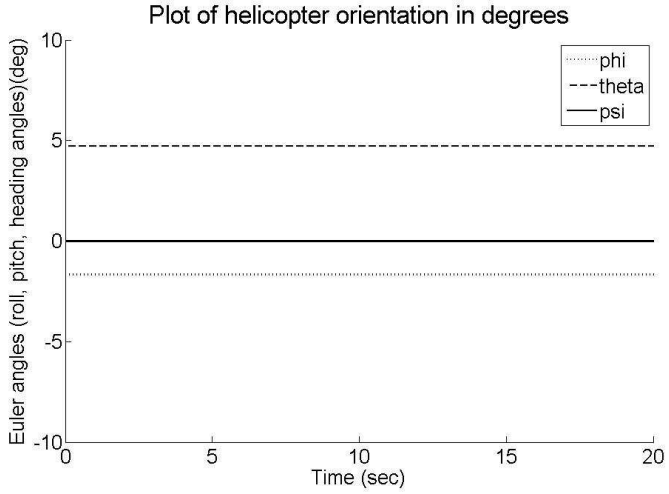

Figure 4.75: Euler angles for 100 ft 60 knot forward flight condition with inner loop controller

Helicopter orientation and NED axis positions are fixed to the trim condition for a longer duration by the help of inner loop control model.

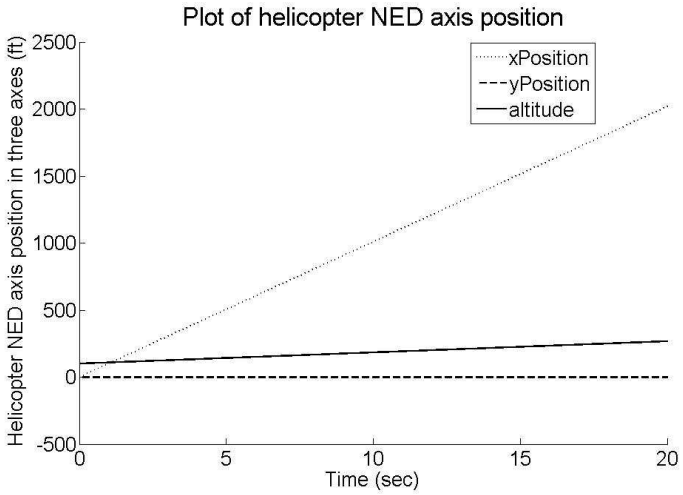

Figure 4.76: NED axis position for 100 ft 60 knot forward flight condition with inner loop controller

4.4.3 Outer loop controller design and simulation

As it is mentioned before sequential loop closing method is used to design a linear controller for the helicopter. After the implementation of inner loop controller, new state space representation is obtained by linearizing the new model. In this part states will include the heading angle because related transfer function for the heading hold mode is needed. Full system matrix will be considered, that is, longitudinal and lateral modes will not be analyzed separately as it is done in previous steps.

New eigenvalues of the helicopter model with inner loop control: Eigenvalues of the new state matrix are:

$$\lambda_1 = 0 \tag{4.61}$$

$$\lambda_2 = -94.9486$$

$$\lambda_3 = -39.0104$$

$$\lambda_{4,5} = -0.7240 \pm 1.9179i$$

$$\lambda_{6,7} = -0.0515 \pm 0.0273i$$

$$\lambda_{8,9} = 0.0228 \pm 0.0295i$$

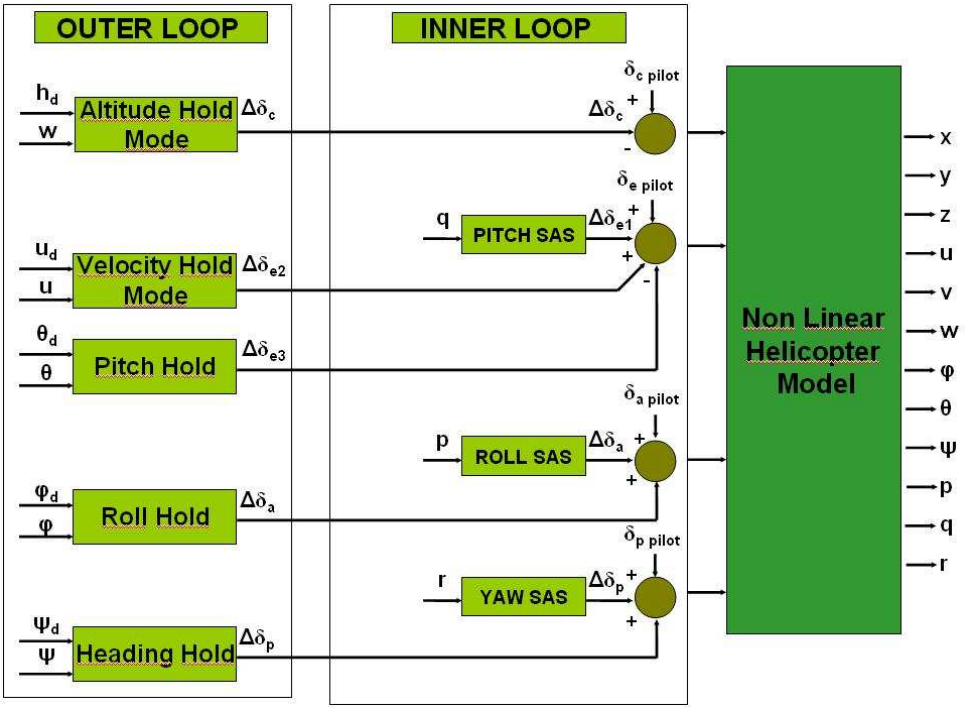

Figure 4.77: Helicopter model with outer loop controller

4.4.3.1 Pitch hold mode

The aim of pitch hold mode is adding a feedback to the pilot control input that will hold it's attitude at the desired value. First related transfer function of pitch attitude vs longitudinal cyclic control input is obtained.

$$\frac{\theta}{\delta_e} = \frac{numerator}{denominator} \tag{4.62}$$

$$numerator = 0.0037s^7 + 4.153s^6 + 507.2s^5$$

$$+1.402e004s^4 + 1.317e004s^3 + 960.4s^2 + 8.029s - 0.06014$$

$$denominator = s^8 + 135.5s^7 + 3910s^6 + 6150s^5$$

$$+1.591e004s^4 + 893.8s^3 + 1.462s^2 - 0.1548s + 0.07342$$

By considering the root locus plot state feedback gain is selected and commanded input is added to the pilot longitudinal control input. Desired pitch attitude is selected as the trim value of pitch attitude at desired 1000 ft altitude.

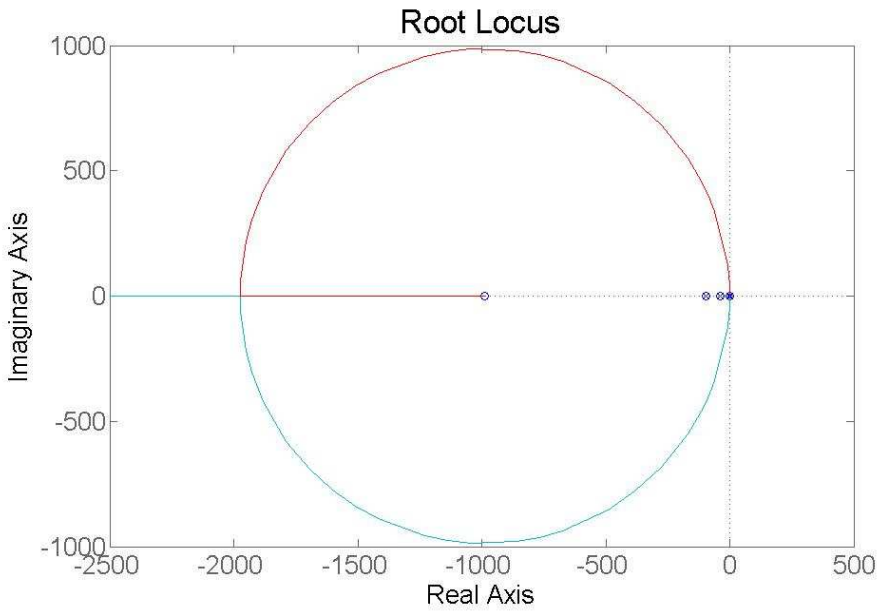

Figure 4.78: Pitch attitude root locus plot

Block diagram of pitch hold mode:

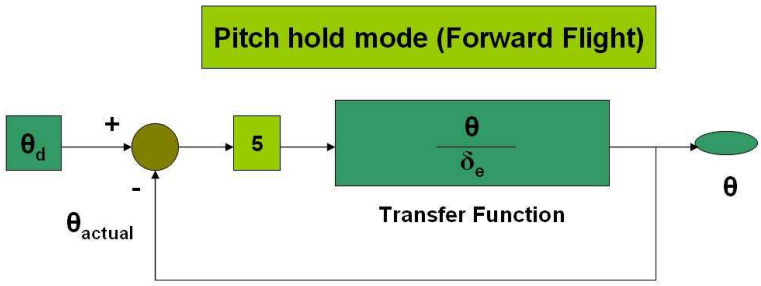

Figure 4.79: Pitch hold mode block diagram

As it is observed from the graph, desired pitch is acquired and hold. Pitch attitude is implemented to the system together with altitude acquire and hold mode. While helicopter tends to acquire desired altitude, helicopter pitch attitude changes and by activating pitch hold mode instability in pitch angle as a result of altitude hold mode is prevented.

4.4.3.2 Velocity hold mode

The aim of velocity hold mode is adding a commanded input to the pilot control input that will increase the helicopter forward speed to the desired forward speed. First related transfer function for forward speed vs longitudinal cyclic input is obtained.

$$\frac{u}{\delta_e} = \frac{numerator}{denominator} \tag{4.63}$$

$$numerator = 0.0481s^7 + 6.354s^6 + 82.62s^5 - 1.163e004s^4$$

$$-3.243e005s^3 - 4.109e005s^2 - 2.455e004s + 118.8$$

$$denominator = s^8 + 135.5s^7 + 3910s^6 + 6150s^5$$

$$+1.591e004s^4 + 893.8s^3 + 1.462s^2 - 0.1548s + 0.07342$$

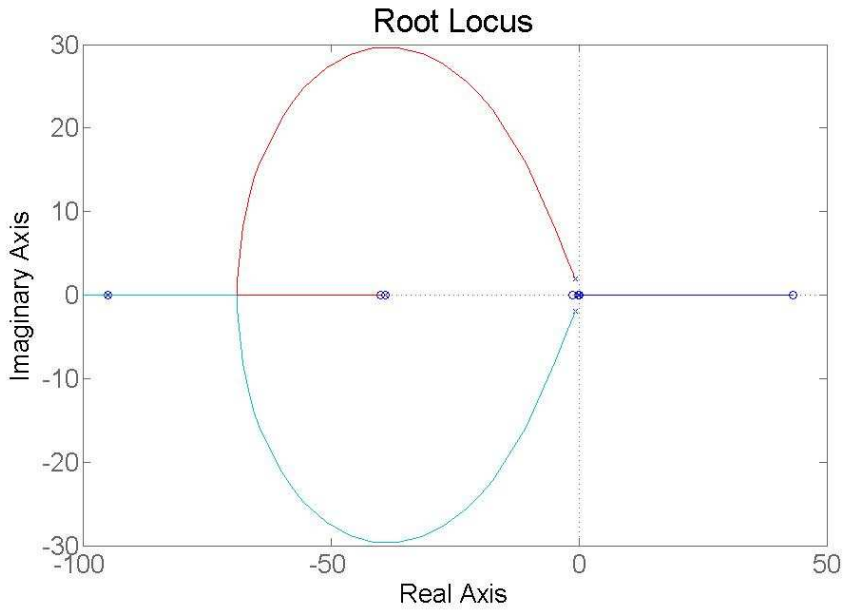

Figure 4.80: Forward speed root locus plot

By considering the root locus plot state feedback gain is selected and commanded input is added to the pilot longitudinal control input. Desired forward speed is selected as 80 knot (135.02ft/sec).

Block diagram of velocity hold mode:

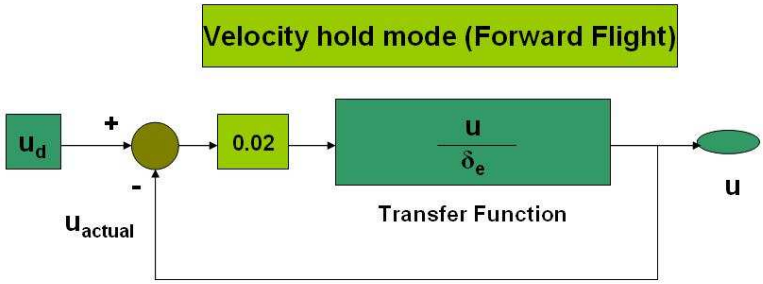

Figure 4.81: Velocity hold mode block diagram

4.4.3.3 Roll hold mode

The aim of roll hold mode is adding a commanded input to the pilot control input that will help helicopter to zero the helicopter roll attitude. First related transfer function of roll attitude vs lateral cyclic control input is obtained.

$$\frac{\phi}{\delta_a} = \frac{numerator}{denominator} \tag{4.64}$$

$$numerator = 0.0198s^7 + 19.56s^6 + 770.6s^5 + 1199s^4$$

$$+3181s^3 + 178.9s^2 + 1.26s + 0.03844$$

$$denominator = s^8 + 135.5s^7 + 3910s^6 + 6150s^5$$

$$+1.591e004s^4 + 893.8s^3 + 1.462s^2 - 0.1548s + 0.07342$$

By considering the root locus plot state feedback gain is selected and commanded input is added to the pilot lateral control input. Desired roll attitude is zero.

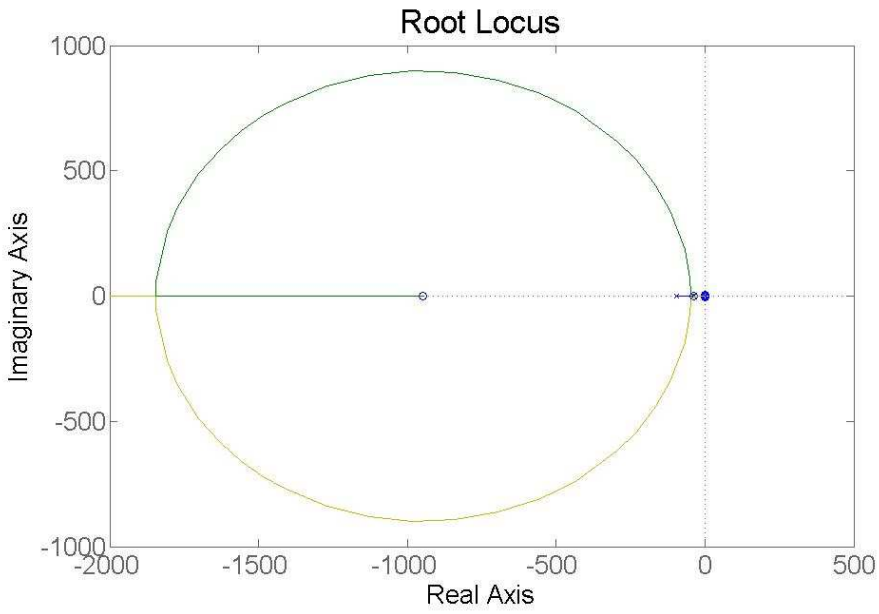

Figure 4.82: Roll attitude root locus plot

Block diagram of roll hold mode:

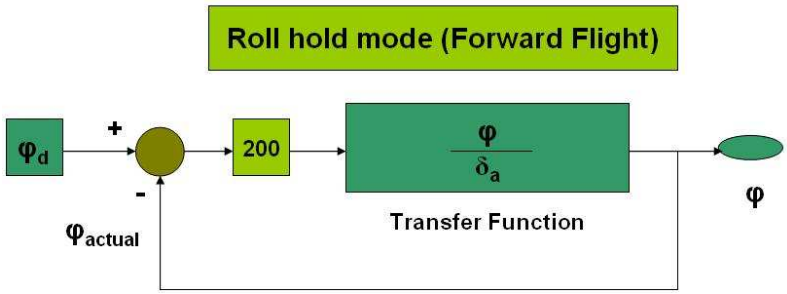

Figure 4.83: Roll hold mode block diagram

4.4.3.4 Heading hold mode

The aim of heading hold mode is adding a commanded input to the pilot control input that will help helicopter to zero the helicopter heading attitude. First related transfer function of heading attitude vs pedal control input is obtained.

$$\frac{\psi}{\delta_p} = \frac{numerator}{denominator} \tag{4.65}$$

$$numerator = -0.004s^8 - 4.337s^7 - 373.1s^6 - 548.8s^5$$

$$-1542s^4 + 1.23s^3 - 2.841s^2 + 0.04006s - 0.007454$$

$$denominator = s^9 + 135.5s^8 + 3910s^7 + 6150s^6$$

$$1.591e004s^5 + 893.8s^4 + 1.462s^3 - 0.1548s^2 + 0.07342s$$

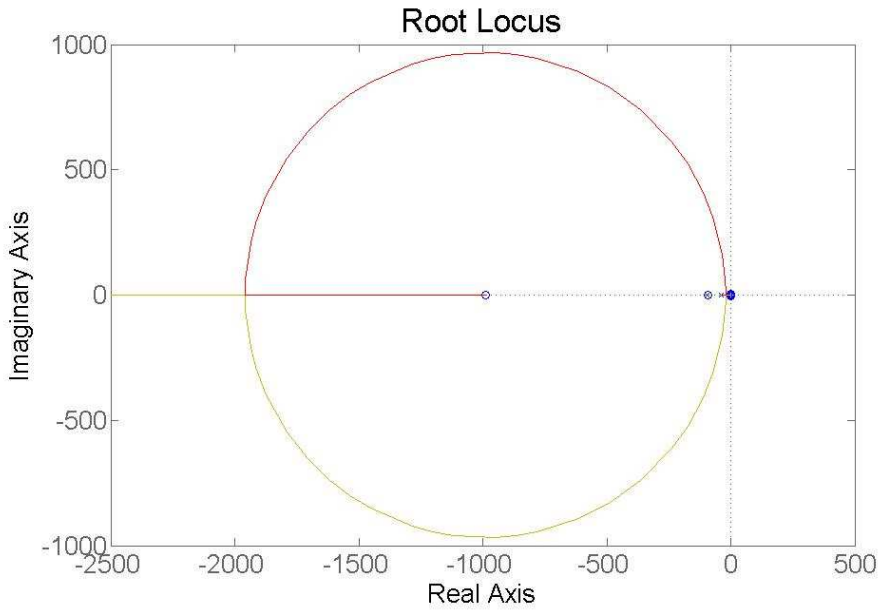

Figure 4.84: Heading attitude complementary root locus plot

By considering the root locus plot state feedback gain is selected and commanded input is added to the pilot pedal control input. Desired heading attitude is zero.

Block diagram of heading hold mode:

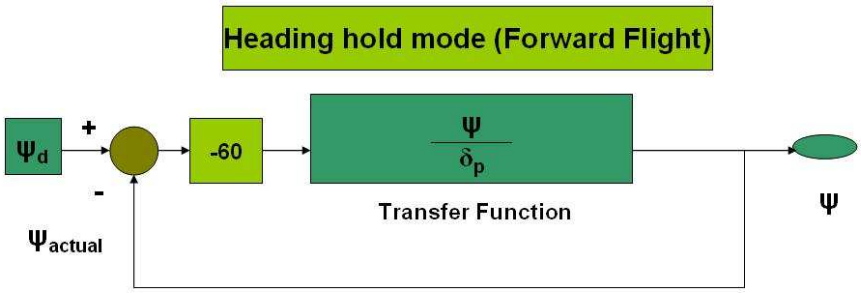

Figure 4.85: Heading hold mode block diagram

4.4.3.5 Altitude acquire and hold mode

The aim of altitude acquire and hold mode is adding an altitude feedback pilot command input to bring the helicopter to the desired altitude and keeping it there by feeding back the current altitude. Altitude acquire and hold mode is activated together with pitch hold, roll hold, heading hold and velocity hold modes. First related transfer function of vertical velocity vs collective control input is obtained.

$$\frac{w}{\delta_c} = \frac{numerator}{denominator} \tag{4.66}$$

$$numerator = -421s^7 - 5.688e004s^6 - 1.623e006s^5$$

$$-1.76e006s^4 - 1.046e005s^3 - 1.365e004s^2 - 841s - 1.147$$

$$denominator = s^8 + 135.5s^7 + 3910s^6 + 6150s^5$$

$$+1.591e004s^4 + 893.8s^3 + 1.462s^2 - 0.1548s + 0.07342$$

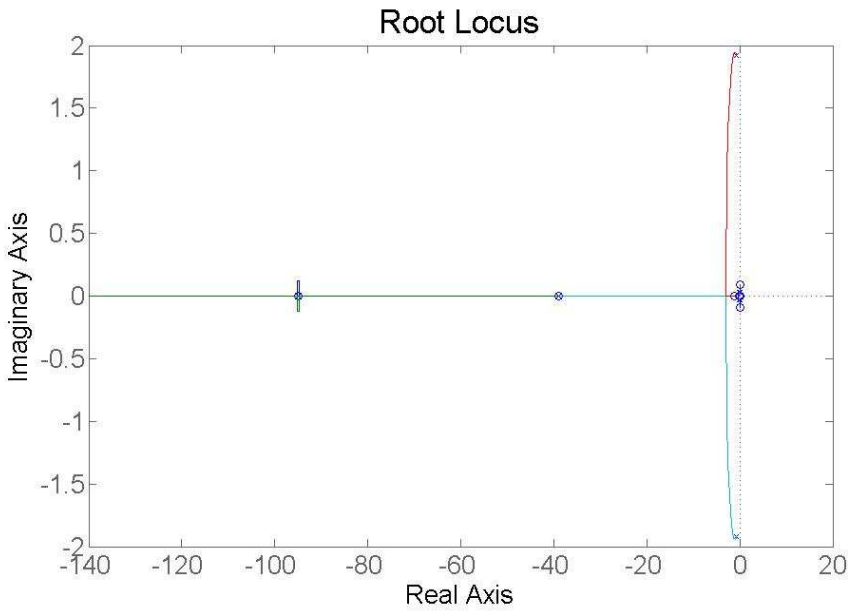

Figure 4.86: Vertical speed complementary root locus plot

Block diagram of altitude acquire and hold mode:

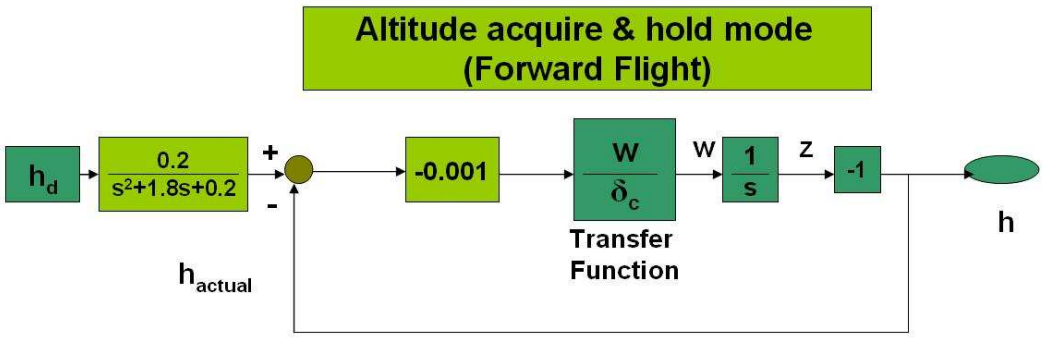

Figure 4.87: Altitude acquire and hold mode block diagram

By considering the root locus plot state feedback gain is selected and commanded input is added to the collective control input. Desired altitude is selected as 1000 ft and actual altitude is 100 ft. At the same time desired velocity is increased from 60 knots to 80 knots. By implementing altitude hold mode to the model together with pitch, roll and heading hold modes, desired altitude is acquired and hold.

New eigenvalues of the helicopter model with outer loop feedback:

$$\lambda_{1,2} = -10.9728 + 11.5494i \tag{4.67}$$

$$\lambda_{3,4} = -0.5423 \pm 1.8926i$$

$$\lambda_5 = -0.5722$$

$$\lambda_{6,7} = 0.2755 \pm 0.4849i$$

$$\lambda_{8,9} = 0.0105 \pm 0.0767i$$

The closed loop system has two pairs of complex conjugate eigenvalues with positive real parts as may be observed from the list of the eigenvalues of the new system with outer loop feedback. However, these eigenvalues belong to the slower states of the helicopter such as linear velocities. For this reason these instabilities do not show up in the simulations presented below. In figure 4.88 altitude acquire and hold simulation is given.

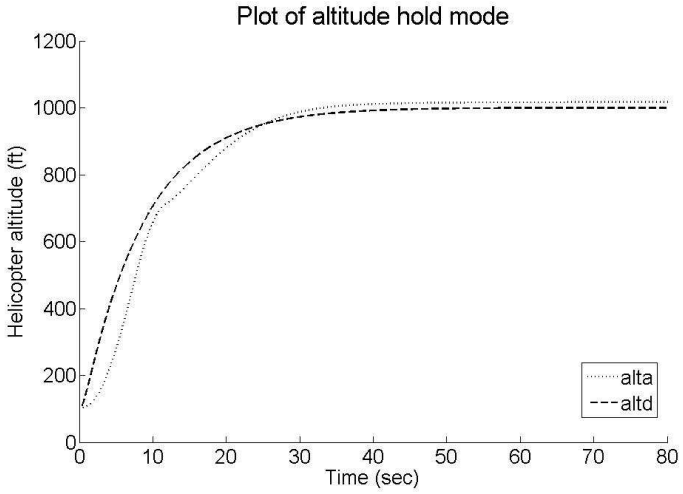

Figure 4.88: Altitude acquire and hold mode plot

In figures 4.89, 4.90, 4.91 and 4.92, velocity acquire and hold, roll hold, pitch acquire and heading hold simulations are given.

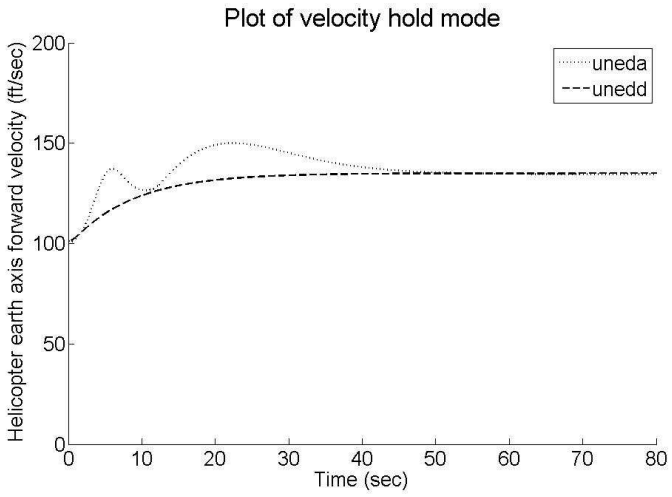

Figure 4.89: Actual and desired velocity during Velocity hold mode engaged

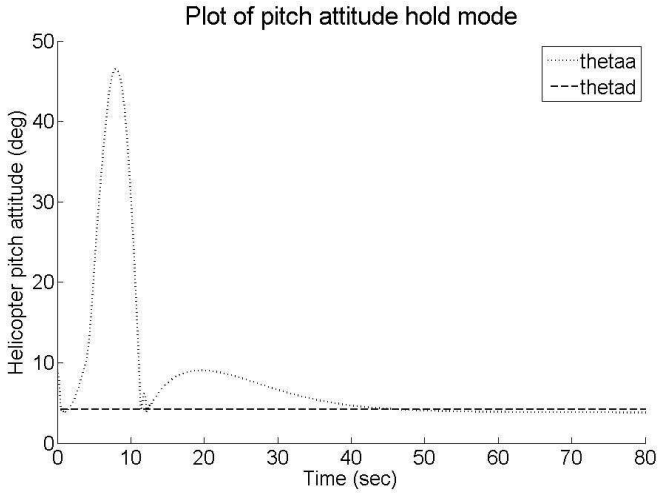

Figure 4.90: Actual and desired pitch attitude during Pitch attitude hold mode engaged

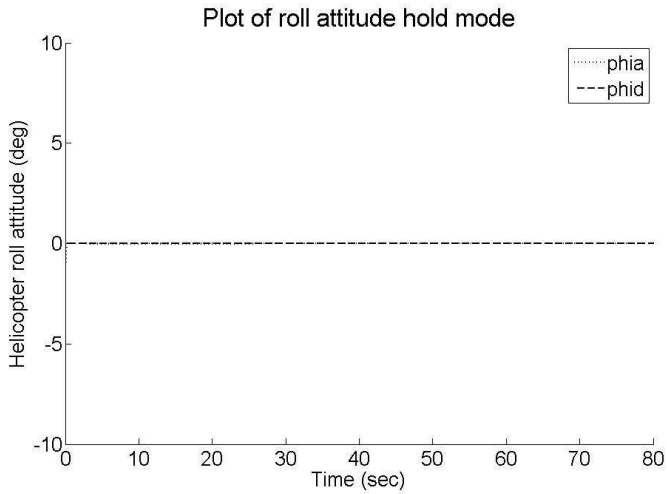

Figure 4.91: Actual and desired roll attitude during Roll attitude hold mode engaged

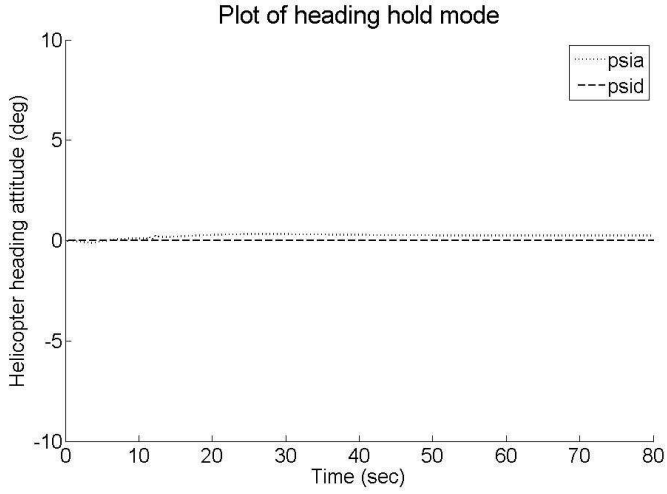

Figure 4.92: Actual and desired heading attitude during Heading attitude hold mode engaged

The controls during these flight simulations are given in figure 4.93. As it maybe observed from these figures outer loop controls are quite effective.

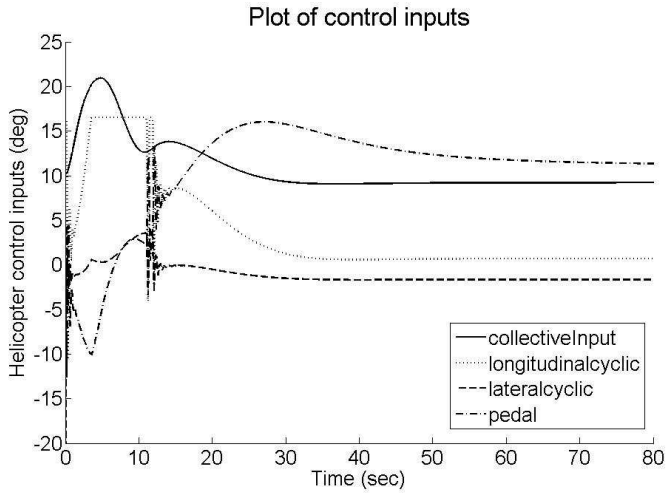

Figure 4.93: Control inputs

CHAPTER 5

CONCLUSION

The purpose of this thesis was to generate a nonlinear simulation model for a utility helicopter and to design linear controllers by using classical control theories. Agusta 109 helicopter's parameters are used, for the nonlinear helicopter model.

In the first part a nonlinear simulation model is generated considering the minimum complexity approach. Helicopter control inputs and their uncoupled dynamics are implemented by using a mixing unit model. After that main parts of the helicopter are modeled. These are main rotor, fuselage, horizontal tail, vertical tail and tail rotor. Main rotor model is modeled using momentum theory and a basic inflow model in order to calculate main rotor thrust and induced velocity. Tail rotor model is designed using the same method with main rotor. Fuselage interference effect and downwash field, upwash and downwash effects of horizontal and vertical tails are modeled. Helicopter 6 degrees of freedom equations of motion are simulated in the MATLAB environment to calculate helicopter accelerations, velocities, positions and orientations in body and Earth fixed frames.

To design a linear controller , first a trim code is written. Then the nonlinear model is linearized at the trimmed input and state values numerically. Thus a linearization code that uses nonlinear simulation model is also developed .

Automatic flight control system designs are carried out mainly using classical control approaches of sequential loop closing. First, the inner loop controllers are developed in order to stabilize the helicopter. For the classical control approach, lead compensator is also used. Modern control system design approach is also used for the inner loop controller. For this purpose truncated system equations are used. Two flight conditions are used in designs: hover

and forward flight. In both flight condition classical control approach was quite successful to design inner loop controllers.

Finally outer loop controllers are designed for the helicopter flight director modes. Altitude hold, roll attitude hold, pitch attitude hold and heading hold modes are implemented for both hover and forward flight. Outer loop controllers for forward flight also includes velocity acquire-hold mode as well.

The success of these controllers are demonstrated through simulations. It may be concluded that linear controllers are effective in controlling helicopters. In future gain scheduling approaches shall be implemented to inner and outer loop controllers to help helicopter fly anywhere within it's flight envelope.

REFERENCES

[1] Lai,G., M., Y. "*Modeling and Control of Small-Scale Helicopter on a Test Platform*", Waterloo, Ontario, Canada, 2008

[2] Van Hoydonck, W. R. M., Pavel, M. D. "*Development of a Modular, Generic Helicopter Flight Dynamics Model for Real-Time Simulations* ", AIAA Modeling and Simulation Technologies Conference and Exhibit, Hilton Head, South Carolina, August 2007

[3] De Marco, A., Duke, E. L., Berndt, J. S. "*A General Solution to the Aircraft Trim Problem*", AIAA Modeling and Simulation Technologies Conference and Exhibit, Hilton Head, South Carolina, August 2007

[4] Bhandari, S., Chen, B. H., Colgren, R., Chen, X. W. "*Application of Support Vector Machines to the Modeling and Control of a UAV Helicopter*", AIAA Modeling and Simulation Technologies Conference and Exhibit, Hilton Head, South Carolina, August 2007

[5] Cuadrado, M. G. "*A novel fixed-azimuth blade-element real-time rotor simulation model: fabes*",AIAA Modeling and Simulation Technologies Conference and Exhibit, Hilton Head, South Carolina, August 2007

[6] Weingartner, M., Lenz, J., Sachs, G. "*Object Oriented Trim of Complex High-Fidelity Simulation Models*",AIAA Modeling and Simulation Technologies Conference and Exhibit, Hilton Head, South Carolina, August 2007

[7] Coiro, D. P., De Marco, A., Nicolosi, F. "*A 6DOF Flight Simulation Environment for General Aviation Aircraft with Control Loading Reproduction*",AIAA Modeling and Simulation Technologies Conference and Exhibit, Hilton Head, South Carolina, August 2007

[8] Popinchalk, S., Glass, J., Shenoy, R., Aberg, R. "*Working in Teams: Modeling and Control Design within a Single Software Environment*",AIAA Modeling and Simulation Technologies Conference and Exhibit, Hilton Head, South Carolina, August 2007

[9] Frank, A., McGrew, J. S., Valenti, M., Levine, D., How, J. P. "*Hover, Transition, and Level Flight Control Design for a Single-Propeller Indoor Airplane*",AIAA Modeling and Simulation Technologies Conference and Exhibit, Hilton Head, South Carolina, August 2007

[10] Restrepo, C., Valasek, J. "*Structured Adaptive Model Inversion Controller for Mars Atmospheric Flight*",AIAA Modeling and Simulation Technologies Conference and Exhibit, Hilton Head, South Carolina, August 2007

[11] T. M. Fletcher, R. E. Brown "*Modeling the interaction of helicopter main rotor and tail rotor wakes*",Royal Aeronautical Journal Volume 111, Number 1124, 2007

[12] O. Tarimci, I. Yavrucuk "*Simulation Evaluation of a Flight Control System for an Autonomous Fullsize Helicopter*",4. Ankara International Aerospace Conference, 10-12 September, 2007 - METU, Ankara Paper No: AIAC-2007-062

[13] Learmount D. "*Low-cost Simulation can Transform Helicopter Training* ",Flight International, 28 September 2007

[14] J. E. Corban, A. J. Calise, J. V. R. Prasad, G. Heynen, B. Koenig, J. Hur "*Flight Evaluation of an Adaptive Velocity Command System for Unmanned Helicopters*",AIAA Guidance, Navigation and Control Conference and Exhibit, 11-14 August 2003, Austin, Texas

[15] Padfield, G. D., Pavel, M., Casolaro , D. "*Fidelity of Helicopter Real Time Simulation Models* ", 61st Annual Forum of the American Helicopter Society, Grapevine,Texas, June 2005

[16] Manimala, B., Walker, D., Padfield, G. "*Rotorcraft Simulation Modeling and Validation for Control Design and Load Prediction*", 31st European Rotorcraft Forum, Florence, Italy, September 2005

[17] M. Pavel "*Prediction of the Necessary Degrees of Freedom for Helicopter Real-time Simulation Models*", AIAA 2005-6206, AIAA Modeling and Simulation Technologies Conference and Exhibit, San Francisco California, August 2005

[18] S.B. Jon "*JSBSim:An Open Source Flight Dynamics Model in C++* ",AIAA Modeling and Simulation Technologies Conference and Exhibit 16-19 August 2004, Providence, Rhode Island

[19] E. Russel, S. Jennie "*Helicopter trimming and tracking control using direct neural dynamic programming* ",IEEE transactions on neural networks, Vol.14, No.4, July 2003

[20] Ogata, K., "*Modern Control Engineering*", Upper Saddle River, New Jersey 07458, 2002.

[21] Anon. "*World Aircraft Accident Summary 1990-2001 Index-Cap 479* ",Civil Aviation Authority, Airclaims, 2002

[22] Leishman, J.G. "*Principles of Helicopter Aerodynamics*", Cambridge Aerospace Series, 2000

[23] J. V. R. Prasad, A. J. Calise, Y. Pei, J. E. Corban, "*Adaptive Control Synthesis and Flight Test Evaluation on an Unmanned Helicopter*", IEEE International Conference on Control Applications, 1999

[24] A. J. Calise, R. T. Rysdyk "*Nonlinear Adaptive Flight Control Using Neural Networks*",IEEE Controls Systems Magazine, 1998

[25] Wie, B., "*Space Vehicle Dynamics and Control*", AIAA Education Series, 1998.

[26] Pamadi, B. N. "*Performance, Stability, Dynamics, and Control of Airplanes*", AIAA Education Series, 1998

[27] M. Christian "*Development of a Real-Time Flight Simulator for an Experimental Model Helicopter*",Diploma Thesis, Georgia Institute of Technology School of Aerospace Engineering, Atlanta, December 1998

[28] A. J. Calise, R. T. Rysdyk "*Nonlinear Adaptive Control of Tiltrotor Aircraft Using Neural Networks*",1997 SAE/AIAA World Aviation Congress, October 14-16, 1997, Anaheim, CA.

[29] A. J. Calise, R. T. Rysdyk "*Adaptive Model Inversion Flight Control For Tiltrotor Aircraft*",AIAA Guidance,Navigation and Control Conference, Aug. 1997, Paper No: 97-3758

[30] Padfield, G. D. "*Helicopter Flight Dynamics: The Theory and Application of Flying Qualities and Simulation Modeling*", AIAA Education Series, 1996

[31] Prouty, R. W. "*Helicopter Performance, Stability, and Control*", Krieger Publishing Company, 1995

[32] Mittal M., Prasad J. V. R. "*Modeling the UH-1 Helicopter using the ARMCOP Program*", Interim Progress Report, Georgia Institute of Technology 1994

[33] D. Ledar "*Helicopter Simulation for Naval Training* ",AIAA 94-3435, Thomson Training and Simulation, Gergy-Pontoise France,1994

[34] Henry L. K. ,Cynthia A. C.,Kenneth R. Y. ,Michael B. L. "*Flight Investigation the Effect of Tail Boom Strakes on Helicopter Directional Control*", AVSCOM Technical Report 93-A-003, February 1993

[35] S. Sarathy, V. R. Murthy "*An Advanced Rotorcraft Flight Simulation: Parallel Implementation and Performance Analysis*",AIAA Guidance,AIAA-93-3550-CP, 1993

[36] McLean, D., "*Automatic Flight Control Systems*", Prentice Hall, 1990.

[37] Hefley, R. K., Mnich, M. A. "*Minimum-Complexity Helicopter Simulation Math Model*", NASA Contractor Report 177476 USAAVSCOM Technical Report 87-A-7, 1988

[38] D.T. Peter, E.T. Bruce, A.D. William, T.N.C. Robert "*A Mathematical Model of a Single Main Rotor Helicopter for Piloted Simulation* ",NASA Technical Memorandum 84281, September 1982

[39] Howlett, J. J. "*UH-60A Black Hawk Engineering Simulation Program: Volume I - Mathematical Model*", NASA Contractor Report 166309 , December 1981

[40] T.N.C. Robert "*Effects of Primary Rotor Parameters on Flapping Dynamics*",NASA Technical Paper 1431, NASA Ames Research Center, January 1980

[41] T.N.C. Robert "*A Simplified Rotor System Mathematical Model for Piloted Flight Dynamics Simulation*",NASA Technical Memorandum 78575, NASA Ames Research Center, May 1979

[42] Talbot, P. D., Corliss, L. D. "*A Mathematical Force and Moment of a UH-1H Helicopter For Flight Dynamics Simulations*", NASA TM 73-254, June 1977

[43] Talbot, P. D., Corliss, L. D. "*A Mathematical Force and Moment of a UH-1H Helicopter For Flight Dynamics Simulations*", NASA TM 73-254, June 1977

[44] T. Wilcock, C.A. Thrope "*Flight simulation of a Wessex helicopter,a validation exercise* ",Aeronautical Research Council C.P. No. 1299, Aerodynamics Department, R.A.E., Bedford, 1974

APPENDIX A

Geometric Specifications of A109 Helicopter

Table A.1: Summary of A109 Geometric Dimensions

Main Rotor		
	R	18 ft
	c	1.1 ft
	a	6
	b	4
	θ_{twist}	-0.105 rad
	RPM	385
	i_s	0.11
	I_B	212
	e	0.5
	K_1	0
	C_{Do}	0.01
Tail Rotor		
	Radius	3.1 ft
	Chord	0.70 ft
	θ_{twist}	-0.137 rad
	Solidity	0.134
	a	3
Horizontal Stabilizer		
	fs_{ht}	330 in
	$wl_{ht}4$	54 in
	Z^{ht}_{uu}	0.4 ft^2
	Z^{ht}_{uw}	-34 ft^2
	Z^{ht}_{max}	-22 ft^2
Vertical Fin		
	fs_{vt}	380 in
	y^{vt}_{uu}	3.3 ft^2
	y^{vt}_{uv}	-47 ft^2
	y^{vt}_{max}	-17 ft^2

Fuselage		
	fs_{hub}	132.4
	fs_{cg}	132.7
	fs_{fus}	132
	x_{uu}^{fus}	-10.8 ft^2
	y_{vv}^{fus}	-167 ft^2
	z_{ww}^{fus}	-85 ft^2
Mass Properties		
	W	5401 lb
	g	32.2 ft/sec2
	I_{xx}	1300 slug-ft^2
	I_{yy}	6760 slug-ft^2
	I_{zz}	6407 slug-ft^2
	I_{xz}	800 slug-ft^2